ROADWAY SAFETY INSTITUTE

Human-centered solutions to advanced roadway safety

Field Implementation of Direction Rumble Strips for Deterring Wrong-Way Entries

Huaguo Zhou
Chennan Xue

Highway Research Center
Department of Civil Engineering
Auburn University

Final Report

CTS 19-22

University of Minnesota Driven to Discover℠
The University of Akron
Illinois University of Illinois at Urbana-Champaign
Southern Illinois University Edwardsville
Western Michigan University

Technical Report Documentation Page

1. Report No.	2.	3. Recipients Accession No.
CTS 19-22		

4. Title and Subtitle	5. Report Date
Field Implementation of Direction Rumble Strips for Deterring Wrong-Way Entries	July 2019
	6.

7. Author(s)	8. Performing Organization Report No.
Huaguo Zhou and Chennan Xue	

9. Performing Organization Name and Address	10. Project/Task/Work Unit No.
Highway Research Center Department of Civil Engineering 238 Harbert Engineering Center Auburn University, Auburn, AL 36849-5337	CTS #2018071
	11. Contract (C) or Grant (G) No. DTRT13-G-UTC35

12. Sponsoring Organization Name and Address	13. Type of Report and Period Covered
Roadway Safety Institute Center for Transportation Studies University of Minnesota University Office Plaza, Suite 440 2221 University Ave SE Minneapolis, MN 55414	Final Report
	14. Sponsoring Agency Code

15. Supplementary Notes

http://www.roadwaysafety.umn.edu/publications/

16. Abstract (Limit: 250 words)

This report presents the field implementation results of three directional rumble strip (DRS) patterns designed to deter wrong-way (WW) freeway entries. Southbound off-ramps at Exits 208 and 284 on I-65 in Alabama were selected for implementation because they were ranked as high-risk locations by a network screening tool developed by Auburn University. Three patterns (D3, C, and E.1) were recommended for field implementation based on the results of a previous project. Pattern D3 was installed at the off-ramp terminal near the stop bar or yield line. Pattern C was implemented at the segment between the terminal and ramp curve. Pattern E.1 was placed on the tangent part before the ramp curve. WW incident and traffic speed data before and after the implementation were collected using cameras and magnetic sensors, respectively. Field driving tests were conducted to collect sound and vibration data at various speed categories for both RW and WW directions. Before and after studies evaluated the effectiveness of the DRS patterns in reducing wrong way driving (WWD) incidents and traffic speeds on off-ramps. Sound and vibration analyses quantified the differences between right way (RW) and WW drivers' perceptions. Results showed that the number of WWD incidents and average driving distances were significantly reduced after implementing all of the DRS. The results confirmed that WWDs can perceive elevated sound and vibrations when passing the DRS. The DRS can also reduce the 85th percentile, mean, and standard deviations of off-ramp traffic speeds. A general guideline was developed for implementing different DRS to deter WW freeway entries.

17. Document Analysis/Descriptors	18. Availability Statement
Rumble strips, Highway safety, Sound (Sb), Wrong way driving, Off ramps, Vibration, Speed, Field tests	No restrictions. Document available from: National Technical Information Services, Alexandria, Virginia 22312

19. Security Class (this report)	20. Security Class (this page)	21. No. of Pages	22. Price
Unclassified	Unclassified	130	

Field Implementation of Direction Rumble Strips for Deterring Wrong-Way Entries

FINAL REPORT

Prepared by:

Huaguo Zhou
Chennan Xue
Highway Research Center
Department of Civil Engineering
Auburn University

July 2019

Published by:

Roadway Safety Institute
Center for Transportation Studies
University of Minnesota
University Office Plaza, Suite 440
2221 University Ave SE
Minneapolis, MN 55414

ACKNOWLEDGMENTS

The funding for this project was provided by the United States Department of Transportation's Office of the Assistant Secretary for Research and Technology for the Roadway Safety Institute, the University Transportation Center for USDOT Region 5 under the Moving Ahead for Progress in the 21st Century (MAP-21) Act.

The implementation of Pattern D3 at Exits 208 and 284 on I-65 was funded by the research project "Field Implementation and Evaluation of Low-Cost Countermeasures for Wrong-Way Driving Crashes in Alabama" for the Alabama Department of Transportation (ALDOT).

The project team would like to thank district administrators from ALDOT, Tracy Fletcher and Ben Thackerson, for arranging temporary traffic control during the field implementation of DRS at Exits 208 and 284 on I-65 in Alabama. The authors would also like to thank the students at Auburn University who helped with the data collection, including Dan Xu, Qing Chang, Natcha Luechakiettisak, and Md Atiquzzaman.

TABLE OF CONTENTS

LIST OF FIGURES

LIST OF TABLES

EXECUTIVE SUMMARY

This report presents the field implementation results of three directional rumble strip (DRS) patterns designed to deter wrong-way (WW) freeway entries in Alabama. The previous project, entitled "Directional Rumble Strips for Reducing Wrong-Way-Driving (WWD) Freeway Entries," developed and tested DRS patterns (named A to E) with various configurations (e.g., 1, 2, 3…) (Zhou et al., 2018). It recommended three patterns (D3, C, and E.1) for further evaluation through field implementation.

In this project, a complementary literature review was conducted to summarize the current practices of WWD warning and detection techniques as well as other countermeasures recently adopted by transportation agencies. Two southbound off-ramps at Exits 208 and 284 on I-65 in Alabama were selected for implementing the DRS based on the results of a previous research project (Zhou & Atiquzzaman, 2019) funded by the Alabama Department of Transportation (ALDOT), which developed a network screening tool to identify high-risk off-ramps for WWD. The DRS were implemented by a professional pavement striping company in Alabama with the assistance of ALDOT regional traffic engineers for temporary traffic control. In the meantime, the research assistants at Auburn University installed magnetic sensors to collect traffic volume and speed data for 336 hours during the before period and 336 hours during each of three after periods. WWD incident data were also collected for 144 hours during the before period and 144 hours during each of three after periods and a during an additional random weekend. In addition, sound and vibration data at various speed categories (i.e., 10, 15, 20, 25, 30, 35, and 40 mph) were collected for both right way (RW) and WW directions.

Before and after studies were conducted to evaluate the effectiveness of DRS in reducing WWD incidents. In addition, the impact of DRS on driving behavior was also evaluated based on before and after speed studies and a further analysis of sound and vibrations generated by the DRS was conducted. The frequencies and travel distances of WW incidents were analyzed to evaluate the effectiveness of the implemented DRS. The analysis of WWD incidents revealed a significant reduction in WWD frequencies and travel distances after implementing all of the DRS patterns. Only one WW vehicle tried to drive all the way to the freeway mainline close to Pattern E.1. The WW driver stopped and turned around because of Pattern E.1 before entering the freeway mainline. Pattern C reduced the WWD frequencies and average traveling distances by almost half. Pattern D3 was the most effective, as it prevented a large proportion of vehicles from entering the off-ramps. After implementing Pattern D3, WWD incidents were eliminated at both locations. In conclusion, no WW vehicles were found to travel farther than the latest installed DRS pattern during all three after periods.

To evaluate impacts of the DRS on driver behavior, the descriptive statistics, *z*-, and *f*-tests were applied to examine the changes in average traffic speeds and their standard deviations before and after DRS implementation. The speed analysis results suggested that the DRS can reduce average speeds and their standard deviations (SDs) of off-ramp traffic. Pattern E.1 reduced the average vehicle speed by 6.5 mph when yellow strips were applied at Exit 208 and by 2.3 mph when all white strips were applied at Exit 284. The average speeds and speed SDs decreased by 2.7 and 0.5 mph, respectively, due to the implementation of Pattern C. Pattern D3 helped lower the speed SDs by 0.5 and 1.0 mph at the stopped and yield-controlled terminals, respectively. The results implied that drivers typically required two to three days to

adopt these new traffic control devices. After that, the average speed and SDs were stable. The daytime and nighttime speed comparisons illustrated that Pattern E.1 with one-side yellow strips decreased over 10% in speed SDs during the daytime compared to the nighttime. Pattern C was able to reduce the speed SD 5% more during the nighttime. One additional benefit for Pattern D3 is that it provided better guidance for directing RW left-turn drivers. Furthermore, it was observed that motorcyclists tended to use the center gaps of Patterns C and E.1 to avoid hitting the rumble strips.

The time series and root mean square (RMS) values were applied to compare the sound levels received by RW and WW drivers. T-tests were employed to check the statistical difference in means. The vibration analysis first denoised the data through the exponential smoothing to eliminate noises such as engine vibrations. The smoothed data were then compared with the original by two-sample Kolmogorov–Smirnov (K-S) tests to ensure that they represented the data correctly. RMS values were also used to calculate the vibration values in effect. Consequently, the spectrum analysis was employed to compare RW and WW vibrations in the frequency domain. All the DRS patterns generated enough interior sound and vibrations to alert drivers. WW drivers would perceive 12 dBA louder sound and 0.045-*g* more vibrations in effect than RW drivers at Pattern D3. Similarly, differences of 5 dBA and at least 0.011 *g* occurred at Pattern C, and 9 dBA and 0.027 *g* occurred at Pattern E.1. In addition to the vibrations in effect, WW drivers could perceive higher frequencies of vibrations. To assess the influence on the nearby residential area, the exterior sound increments suggested that Pattern C produced a maximum of 10 dBA additional noises and Pattern E.1 produced a maximum of 9 dBA. The extra noises caused by Pattern D3 were completely covered by the engine noises due to low crossing speeds.

In compliance with the *Manual on Uniform Traffic Control Devices* (MUTCD), the guidelines for implementing the DRS were developed based on the results. Pattern D3 should be installed near stop bars or yield lines at the off-ramp terminals. This pattern warned WW drivers with a louder sound and more severe vibrations and worked in collaboration with Do Not Enter (DNE) signs. It should not be directly attached to the other pavement markings such as stop bars or yield lines. Red retroreflective paint can be applied on the WW side of Pattern D3 to increase its nighttime visibility. Pattern C should be placed in the middle of the long straight segment of off-ramps. The placement of Pattern C should not be confused with other pavement markings such as WW arrows. Pattern E.1 should be installed in advance of the sharp horizontal ramp curve ahead of the advisory ramp speed sign. The distance between Pattern E.1 and the advisory ramp speed sign should be considered based on the field review and engineering judgment. The use of yellow strips on the driver's side is recommended for this pattern.

CHAPTER 1: INTRODUCTION

1.1 BACKGROUND

Wrong-way driving (WWD) on freeways has been identified as a critical traffic safety problem. Drivers who make wrong-way (WW) entries onto freeways pose a serious risk to the safety of other motorists and themselves. This study evaluated the effectiveness of three sets of directional rumble strips (DRS) based on field implementation results. A previous project (Zhou et al., 2018), "Directional Rumble Strips for Reducing Wrong-Way-Driving Freeway Entries," developed and tested five DRS designs (named A to E) with various configurations (e.g., A1, A2…). Recommendations were developed to implement three DRS design patterns in the field, which were Pattern D3 (one configuration of Pattern D), Pattern C, and Pattern E.1 (a variant of Pattern E). Southbound off-ramps at Exits 208 and 284 on I-65 in Alabama were selected for implementation based on prediction model results (Zhou and Atiquzzaman, 2019) and the number of WWD incidents observed. Before and after studies were conducted to evaluate DRS patterns regarding WW incidents, as well as drivers' speed, behavior, and adoption of the DRS. Field driving tests were also conducted to collect data of sound and vibrations at various speed categories for both RW and WW directions. Speed analysis was performed to evaluate the impacts on vehicle speeds by these patterns. Time-series and spectrum analysis were employed to analyze sound and vibrations. Based on the findings, guidelines for implementing the DRS in the field were developed to deter WWD entries at freeway off-ramps.

1.2 STUDY OBJECTIVES

The objectives of this study were to

- reveal the design and implementation details of DRS patterns;
- determine the effectiveness of DRS patterns in countering WW incidents at freeway off-ramps;
- quantify the impacts on RW drivers' speed and behavior caused by the DRS;
- evaluate RW and WW sound and vibrations generated by DRS patterns through field tests; and
- develop the implementation guidelines of DRS patterns.

CHAPTER 2: LITERATURE REVIEW

The literature review in a previous project "Directional Rumble Strips for Reducing Wrong-Way-Driving Freeway Entries" (Zhou et al. 2018) summarized WWD issues as well as current transverse rumble strips (TRS) design practices. The effectiveness of TRS in terms of the crash reduction rates and drivers' perceptions of sound and vibrations were also well summarized in the previous report. In this project, a further review of current practices of WWD detection and warning techniques has been conducted and is summarized as below.

In 2013, the first National Wrong-Way Driving Summit provided a platform for practitioners and researchers to develop the best practices to reduce WWD incidents and crashes by evaluating current countermeasures (Pour-Rouholamin et al. 2015; Zhou and Pour-Rouholamin 2014a; Zhou and Pour-Rouholamin 2014b). Attendees included members from the National Transportation Safety Board (NTSB), Federal Highway Administration (FHWA), American Traffic Safety Services Association (ATSSA), state departments of transportation (DOTs), state police, state highway patrols, tollway authorities, universities, and consulting firms. Based on the survey, discussions, and presentations at the summit, the countermeasures outlined in Table 2.1 are candidates that were either implemented or worthy of implementation for mitigating WWD incidents and crashes.

Several other strategies were adopted by transportation agencies for deterring WW entries at freeway off-ramps. In 2004, California DOT deployed in-pavement warning lights on off-ramps, which were susceptible to WW incidents (Cooner, Cothron, and Ranft 2004). The lights were activated when a vehicle entered the WW direction; however, no evaluation regarding their success was conducted.

In 2007, the Harris County Toll Road Authority in Texas installed a WW detection system on 13.2 miles of toll roads (TransCore 2008). The system consisted of radar sensors for detecting WW vehicles and audible alarm software for dispatching the closest law enforcement. Accordingly, no fatalities were reported, and 23 WW drivers had been stopped or turned around since the implementation.

In 2010, the Florida DOT tested video-detection techniques on expressway off-ramps (Rose 2011). A number of false alarms were reported due to movements of vehicles on the shoulder, dark shadows, and the reflection of headlights from the wet pavement. According to a recent study on testing and evaluating video systems in Florida, the systems performed with detection accuracies of above 94%. They were able to send an email notification to the traffic management center if a WWD was detected (Lin, Chen, and Ozkul 2018).

In January 2018, the Arizona DOT implemented the first-in-nation WW driver pilot system along I-17 in Phoenix (Cain, Riley, and McKelvey 2018). The 15-mile system of 3.7 million total cost included thermal cameras, internally illuminated signs with flashing borders, message boards, and the decision-support software. Though the system provided accurate detection, around 10 false detections per camera were caused by camera shaking due to the wind in one month.

In summary, conventional countermeasures such as signage or pavement markings have the limitation in providing sufficient information to WW drivers in time. For example, WW signs can only visually alert WW

drivers in the assumption of being seen by them. Regardless of the false alarms, new ITS techniques cost relatively more due to construction, equipment, and maintenance. Therefore, there is an urgent need to deploy low-cost but effective countermeasures that can alert WW drivers, especially those older or impaired drivers by elevated in-vehicle sounds and vibrations. The literature review results indicated that the DRS had not been implemented or studied by transportation agencies in the past. Providing guidelines for the DRS implementation to DOTs, traffic agencies, and policymakers is also in demand.

Table 2.1 Candidate countermeasures for mitigating WWD incidents and crashes (Pour-Rouholamin et al., 2015)

Signage	▪ Implementing Standard Wrong-Way Sign Package ▪ Improved Static Signs ▪ Lowering Sign Height ▪ Using Oversized Signs ▪ Mounting Multiple Signs on the Same Post ▪ Applying Red Retroreflective Strip to the Vertical Posts ▪ "Freeway Entrance" Sign for All Entrance Ramps
Pavement Marking	▪ Stop Line ▪ Wrong-Way Arrow ▪ Turn/Through Lane Only Arrow ▪ Red Raised Pavement Markers ▪ Short Dashed Lane Delineation Through Turns
Geometric Improvement	▪ Entrance/Exit Ramp Separation ▪ Raised Curb Median ▪ Longitudinal Channelizers ▪ Change in Ramp ▪ Geometrics: Obtuse Angle; Sharp Corner Radii
ITS Technologies	▪ LED Illuminated Signs ▪ Dynamic Signs: Warn Other Drivers ▪ Use Existing GPS Navigation Technologies to Provide Wrong-way Movement Alerts ▪ Provide Consistent Messages or Alerts that are Intuitive to the Driver

CHAPTER 3: FIELD IMPLEMENTATION AND DATA COLLECTION

3.1 IMPLEMENTATION LOCATIONS

To select the locations for implementing DRS, a prediction model was first applied to identify high-risk locations for WWD (Atiquzzaman and Zhou 2018). The model can estimate the probability of WWD entries at an off-ramp terminal of a partial cloverleaf and a diamond interchange based on geometric design features, usage of traffic control devices, area types, and traffic volumes. Two southbound off-ramps at Exits 208 and 284 on I-65 in Alabama were ranked as the top-two-highest probabilities for WWD entries. Exit 208 had the WW entry probability of 61%, while Exit 284 had 79%. WWD incident data were collected to verify the prediction results. A total of 10 and 17 WWD incidents were observed at Exits 208 and 284, respectively, during a typical weekend. Therefore, these two sites were selected to implement the DRS for this project.

3.1.1 Location 1: Exit 208 on I-65

Exit 208 on I-65 is a partial cloverleaf interchange located in the middle of Montgomery, AL, and Birmingham, AL. According to 2017 Alabama Traffic Data, the annual average daily traffic (AADT) on the southbound off-ramp was 1,550 vehicles per day, which included 20% heavy vehicles. The lane width of the southbound off-ramp is about 16 ft. The southbound on- and off-ramps are separated by a wide median. The off-ramp terminal is a stop-controlled unsignalized intersection.

Figure 3.1 shows an aerial photo of Exit 208 on I-65. Along the southbound off-ramp, several traffic control devices were installed to prevent drivers from entering the WW. Two DNE (Do Not Enter) signs were installed on both sides of the ramp terminal. Stop signs were mounted on the back of the DNE signs on the right side of off-ramp. A combination of signs of DNE, Stop, and One-Way signs were placed at the center of the channelization island. About 100 ft away from the ramp terminal, a pair of large WW arrows with raised reflective pavement markers (RRPMs) were installed. Two WW signs were placed on both sides of the ramp around 30 ft farther. Two single WW arrows and two lane-use arrows were installed on the ramp curve. Enhanced by RRPMs, they were 430, 500, 780, and 850 ft away from the ramp terminal, respectively. An advisory ramp speed sign of 25 mph was located near the freeway gore area, which was 890 ft away from the ramp terminal. A new channelization island was installed at the ramp terminal by ALDOT regional engineers in summer 2018.

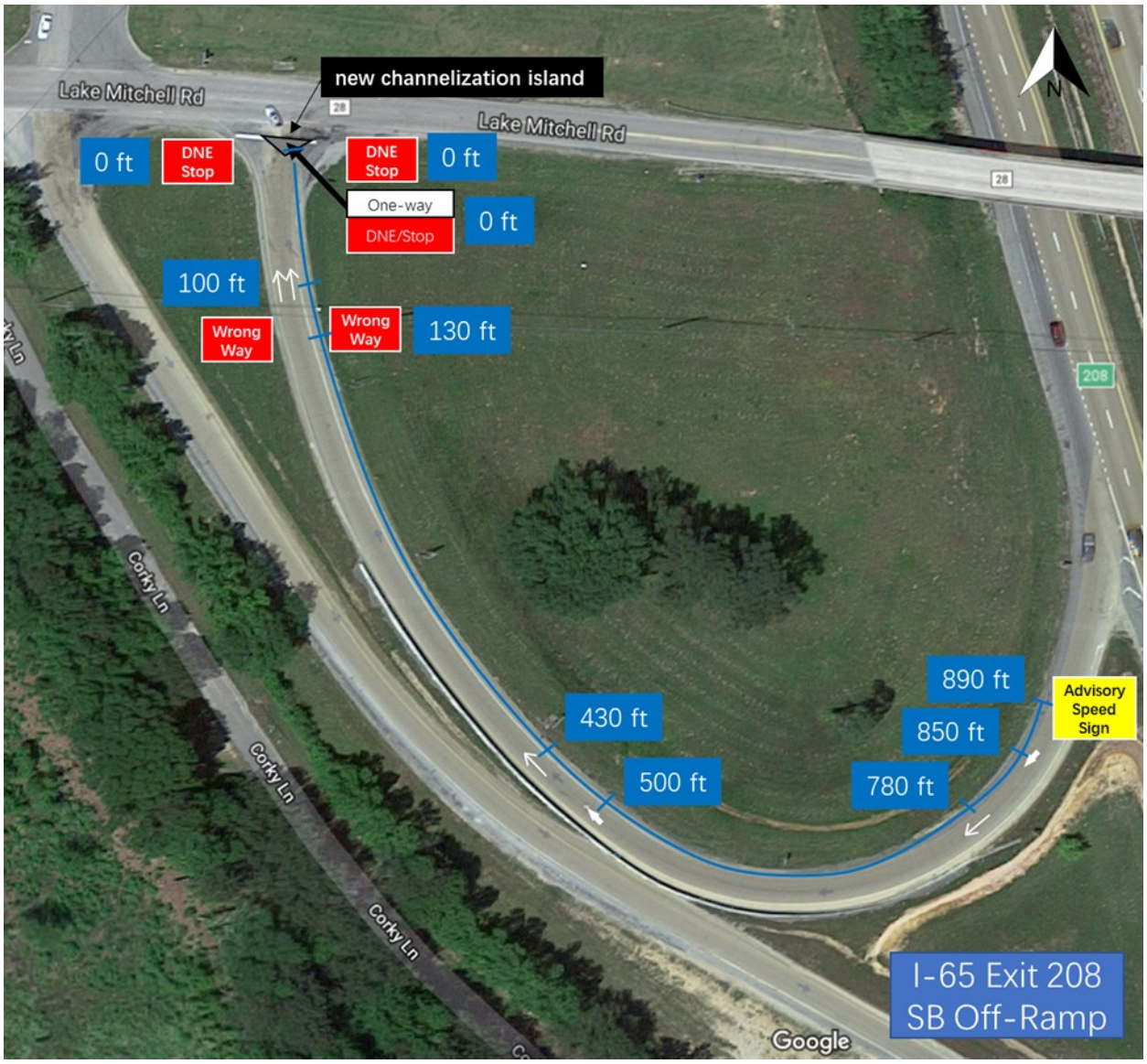

Figure 3.1 Southbound off-ramp at Exit 208 on I-65, AL

3.1.2 Location 2: Exit 284 on I-65

Exit 284 on I-65 is a partial cloverleaf interchange located 25 miles north of Birmingham, AL. According to 2017 Alabama Traffic Data, the AADT on the southbound off-ramp was 1,260 vehicles per day, which consisted of 26% heavy vehicles. The lane width of the off-ramp is about 12 ft. The southbound on- and off-ramps are separated by a concrete barrier. At the southbound off-ramp terminal, right-turn traffic is yield-controlled at the unsignalized intersection, while left-turn traffic requires a complete stop.

Figure 3.2 shows an aerial photo of Exit 284. Compared with Exit 208, fewer traffic control devices were installed on the southbound off-ramp at this site. A DNE sign was placed on the roadside of the ramp terminal to prevent drivers from entering the ramp. A yield sign was mounted on the back of the DNE sign for the right-turn vehicles. A combination of DNE, Stop, and One-Way signs was placed at the center of

the channelization pavement marking. Thirty feet away from the ramp terminal, a divided roadway sign (see R4-7 in MUTCD) with an object marker (see OM1-1 in MUTCD) was installed on the concrete barrier. Dual WW arrows enhanced by RRPMs were placed 100 ft away from the ramp terminal. It should be noted that the dual WW arrows were faded and RRPMs were damaged. Two WW signs on the right side of the off-ramp were installed sequentially, which are 100 and 215 ft away from the ramp terminal. An advisory ramp speed sign of 30 mph is located near the freeway gore area, which is 690 ft away from the ramp terminal.

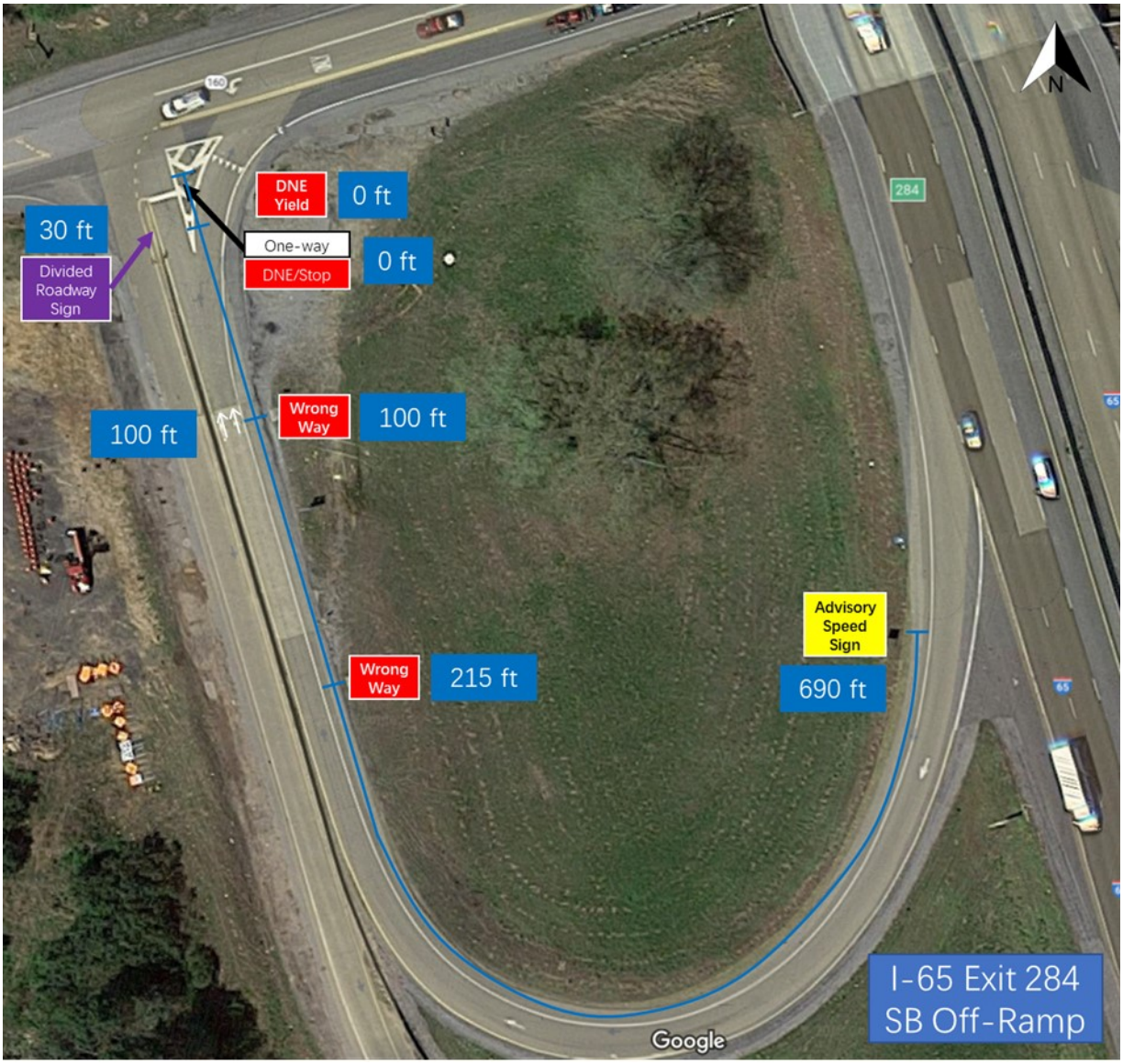

Figure 3.2 Southbound off-ramp at Exit 208 on I-65, AL

3.2 EQUIPMENT AND MEASUREMENT

Data collected included video data that captured WW incidents, speed data on the off-ramp, and in-vehicle sound and vibration data caused by the DRS and exterior sound (noise level) generated by the DRS.

In this study, portable traffic cameras (COUNTcam2) were used to monitor WW incidents and driver behavior. The speed data were collected by magnetic sensors called an NC-350 BlueStar Portable Traffic Analyzer (NC-350). Unlike speed-measurement equipment such as radar guns and tube counters, the NC-350 can provide individual vehicle data, including speed, direction, length, gap, etc. An NC-350 battery can last up to 21 days. Additionally, the sealed design of NC-350 made it robust against moisture and pressure. Protective covers were used to cover and secure the sensors. In-vehicle sound and vibration were measured by using a full-size passenger car (2018 Nissan Altima). The acoustical signature was recorded by an EXTECH HD600 Sound Level Meter, which collected 10 decibel readings every 1 s. The vibration data was recorded using a Measurement Specialists 35201A accelerometer, which recorded 100 samples per second. This device measured acceleration rates along the longitudinal, lateral, and gravitational axes. The data collection devices are shown in Figure 3.3.

(a) COUNTcam Traffic Camera

(b) NC-350 BlueStar Portable Traffic Analyzer

(c) Extech HD600

(d) Measurement Specialists 35201A

Figure 3.3 Data collection equipment: (a) video camera; (b) magnetic sensor; (c) sound level meter; (d) accelerometer

Video cameras were set at the opposite side of the crossroad at the off-ramp terminals. They were secured to extension poles, which were later locked to the sign poles on the roadside. The poles can be extended so that cameras had an approximate height of 10 ft. The cameras further had a wide, color viewing angle of 170 degrees to accommodate the entire off-ramp. The cameras can record videos with the resolution of 720P up to 72 hours after being fully charged. The sealed design made these cameras weather-proof. Figures 3.4 and 3.5 show the field setups of video cameras. All the RW and WW movements can be recorded.

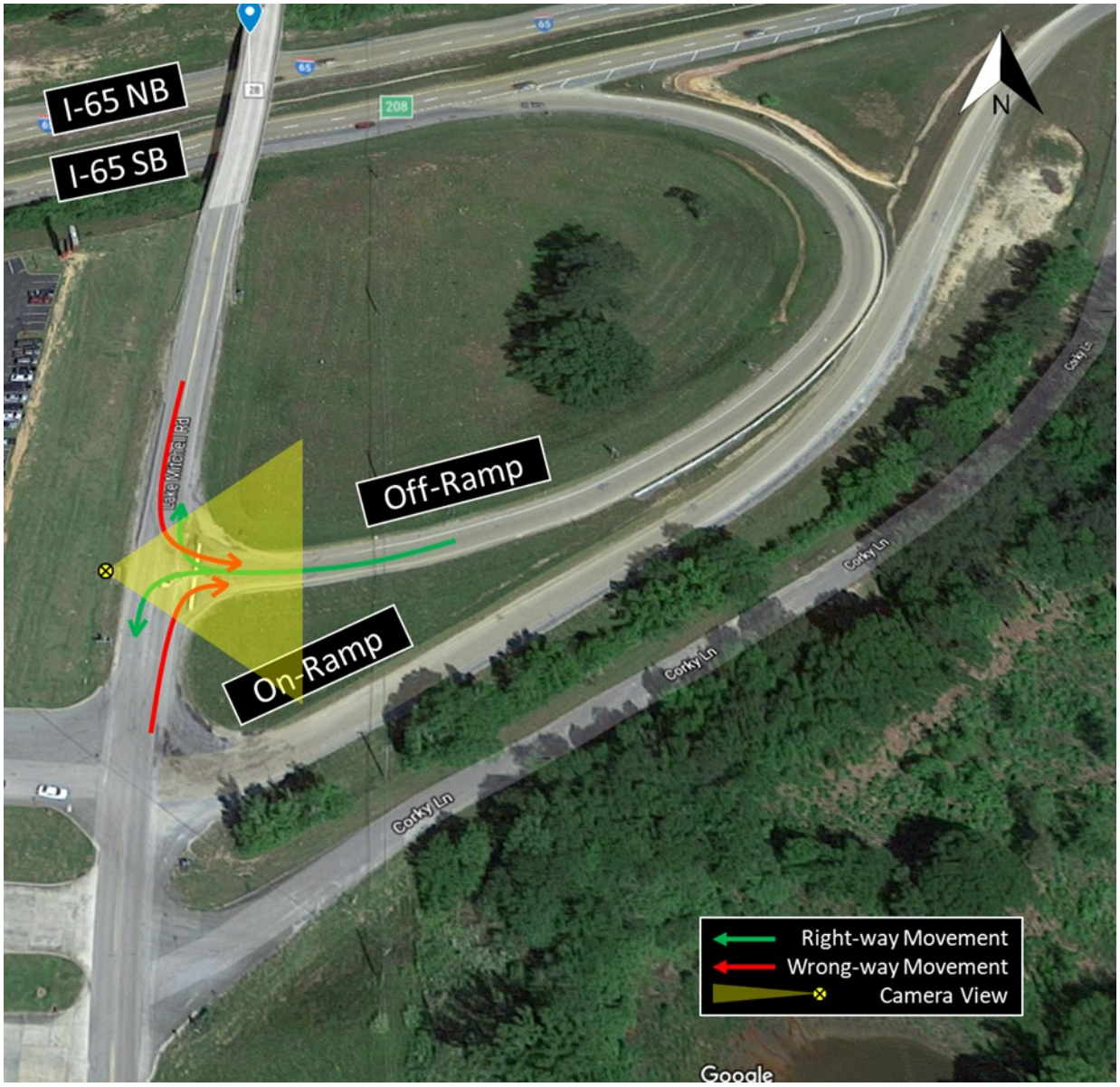

Figure 3.4 Camera deployment at Exit 208 on I-65, AL

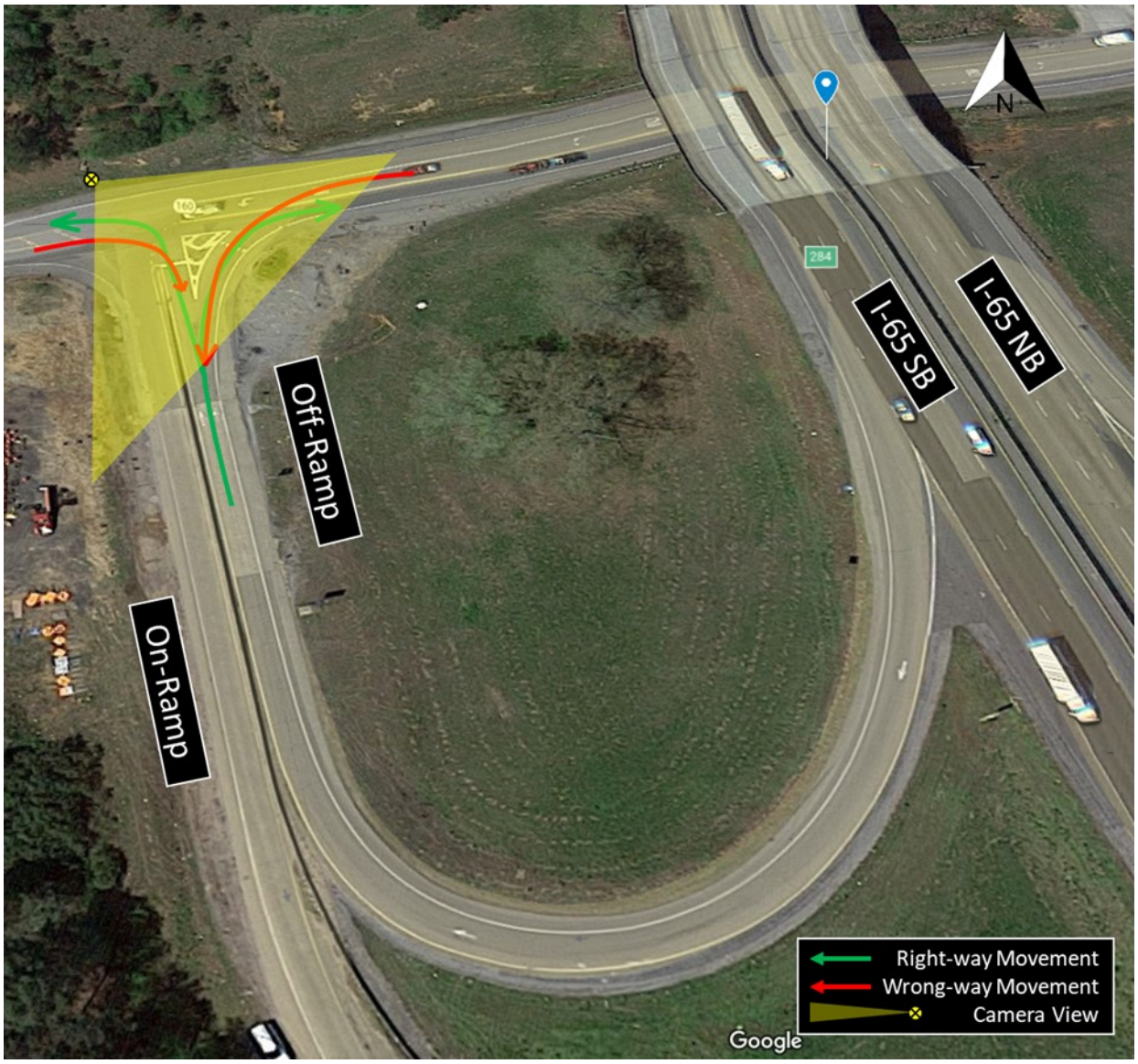

Figure 3.5 Camera deployment at Exit 284 on I-65, AL

A total of nine magnetic speed sensors (NC-350), which were labeled following their device serial numbers from #96 to #104, were used to collect speeds on off-ramps. At Exit 208 (Figure 3.6), sensors #96 and #97 were installed in front of two stop bars to record RW speeds near stop bars and WW entering speeds. Sensor #98 was positioned behind the dual WW arrows to record RW speeds, while vehicles approached the off-ramp terminal, and WW speeds near WW signs. Sensor #99 was placed near the end of the concrete barrier, about 180 ft away from #98. Sensor #100 was installed 30 ft before the advisory ramp speed sign to record RW speeds before entering the ramp curve segment and WW speeds before entering the freeway mainline.

At Exit 284 (Figure 3.7), sensor #101 was placed ahead of the yield line to collect RW speeds under the yield control and WW entering speeds. Sensor #102 was installed immediately behind the dual WW arrows to collect RW approaching speeds near the off-ramp terminal and WW speeds around the first

WW sign. Sensor #103 was placed 180 ft away from #102 to measure speeds of RW/WW vehicles exiting/entering the ramp curve. As with Exit 208, sensor #104 was also installed 30 ft before the advisory ramp speed sign to measure the RW and WW speeds close to freeway mainlines.

Protective covers were applied to hold and protect the sensors. To install covers, 3/16'' holes were predrilled; 1/4''×3-1/4'' hex washer head self-tapping masonry screws were then installed with extra 1/4'' washers. A total of eight screws were used to completely cover and secure each sensor. The installation and finished conditions are shown in Figure 3.8.

Figure 3.6 NC-350 deployments at Exit 208 on I-65, AL

Figure 3.7 NC-350 deployments at Exit 284 on I-65, AL

(a) Installing the protective cover (b) NC-350 with the protective cover

Figure 3.8 NC-350 field installation: (a) installing the protective cover and (b) NC-350 with the protective cover

During the field tests, a full-size passenger car (2018 Nissan Maxima) was used. The sound-level meter was mounted close to the driver's right ear, and an accelerometer was fixed on the driver's seat between the driver's legs. Both the sound level meter and accelerometer were controlled by a laptop computer via the equipment software and serial ports. After conditioning the sound and vibration signals, all information was logged directly into Microsoft Excel for later analysis. While the tests were conducted, the air-conditioner, stereo, and any other sound-producing sources were turned off, and the windows were rolled up to eliminate as much exterior sound as possible.

3.3 DRS IMPLEMENTATION AND INSTALLATION

According to the recommendations from the previous DRS project (Zhou et al. 2017), Pattern D3 was proposed to be installed near the stop bars of off-ramps. Pattern C was recommended to be placed in the middle of the straight long segment of an off-ramp. It was suggested that Pattern E.1 should be installed at the tangent before sharp horizontal ramp curves.

3.3.1 DRS Patterns and Field Deployments

Figure 3.9 shows Pattern D3 modified based on the advance warning markings for speed humps (see 3B-31 in the MUTCD), which has a triangle appearance, as the length of the strip gradually increases from 1 to 12 ft. Strip with lengths from 1 to 5 ft was equally 0.25 in. in thickness. The remaining strips had the same thickness of 0.5 in. Pattern D3 was designed to be positioned immediately after stop bars or yield lines in the field.

Pattern C was similar to the TRS but had various spacings. Three groups of strips with spacings of 1, 2, and 5 ft, respectively, were placed apart with 100 and 50 ft spacing, as shown in Figure 3.10. All the strips had

the same thickness of 0.25 in. Due to different lane widths, strips have unequal lengths at two sites, which were 7 ft at Exit 208 and 4.5 ft at Exit 284. A 2-ft center gap was left in the middle of the lane to allow motorcycles and emergency vehicles to bypass the strips. They can utilize the gaps to pass the DRS without additional sound and vibrations. To eliminate the effects of sound and vibrations from WW arrows, Pattern C was placed 3 ft behind the dual WW arrows at both sites.

Pattern E.1 (Figure 3.11) was designed to have double strips on the inside of the RW travel lane for increasing sound and vibrations for WW drivers. Spacing between the strips on the RW driver side was 4 ft and 2 ft on the WW driver's side. Yellow strips were applied on the RW driver's side at Exit 208, and white strips were used for both sides at Exit 284. A 2-ft center gap was also left in the middle of the lane to serve motorcycles and emergency vehicles. Pattern E.1 was installed 30 ft ahead of the advisory ramp speed sign. At that point, RW drivers were able to clearly see the advisory speed limit sign and horizontal curve ahead.

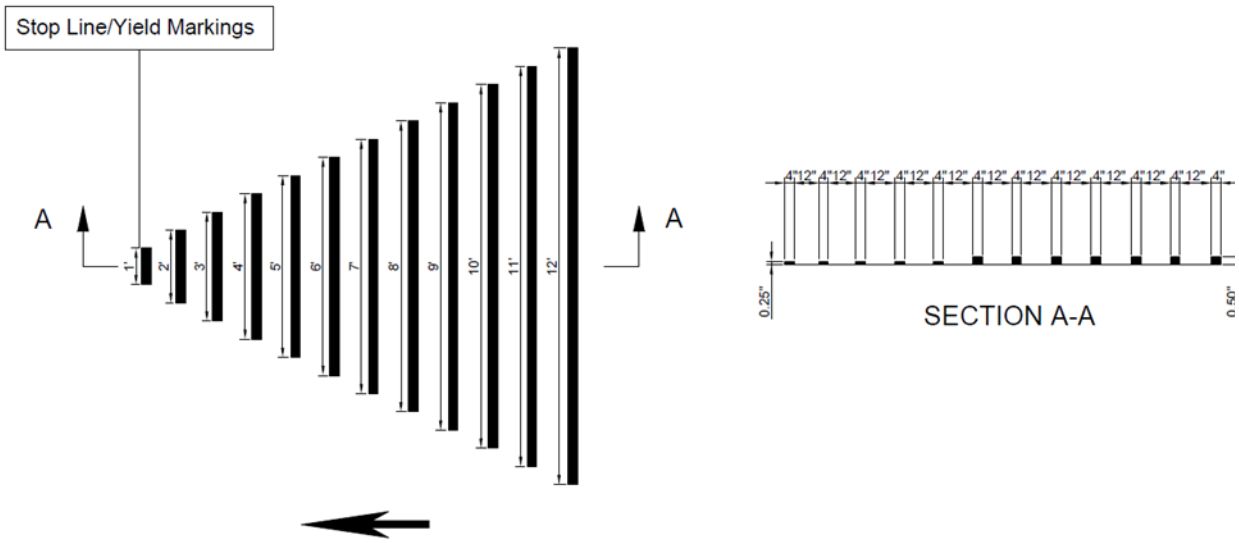

Note: 1) Not to scale;

2) ← = Traffic Flow.

Figure 3.9 DRS Pattern D3 implementation design

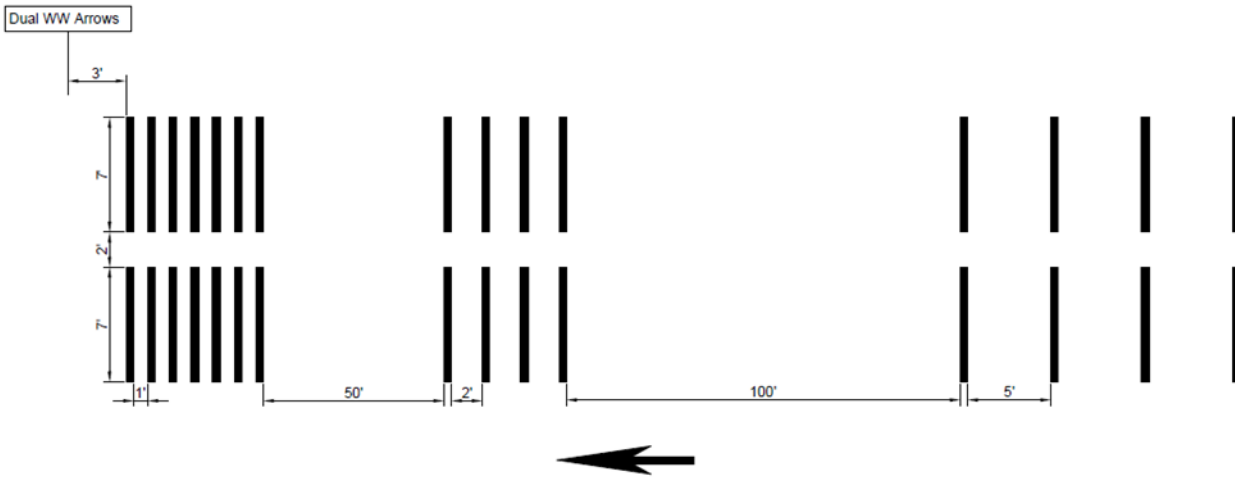

(a) Pattern C at Exit 208

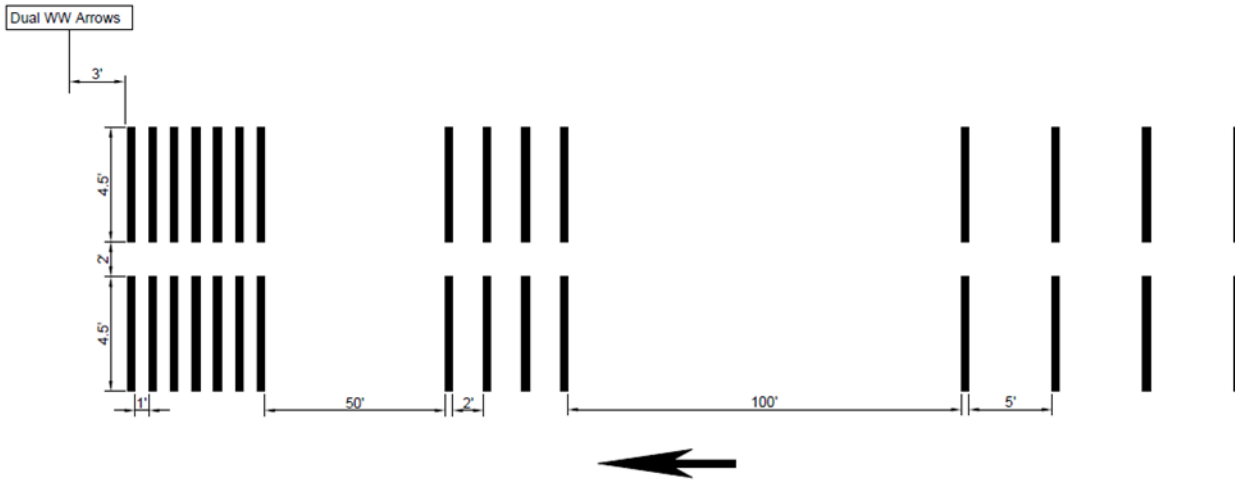

(b) Pattern C at Exit 284

Note: 1) Strips have equal thickness of 0.25'' and width of 4'';

2) Strips have different lengths at two sites (Exit 208: 7'; Exit 284: 4.5');

3) Not to scale;

4) ← = Traffic Flow.

Figure 3.10 DRS Pattern C implementation design

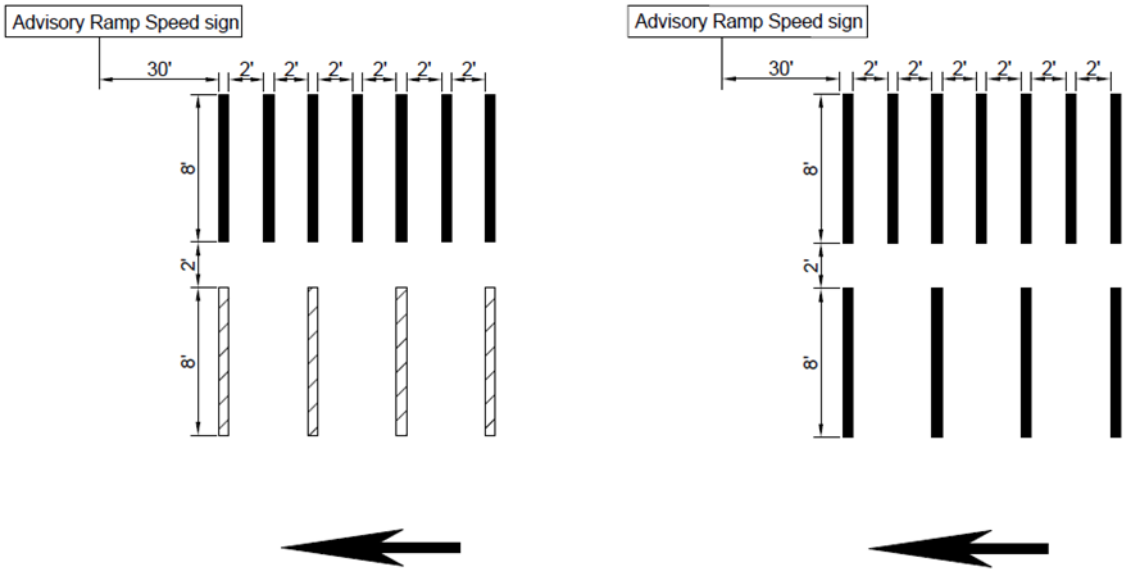

(a) Pattern E.1 at Exit 208

(b) Pattern E.1 at Exit 284

Note: 1) Strips have the equal thickness of 0.25'' and width of 4'';

2) ▨ = Yellow strips;

3) Not to scale;

4) ← = Traffic Flow.

Figure 3.11 DRS Pattern E.1 implementation design

Figures 3.12 and 3.13 illustrate the implementation configurations of the DRS in the field. In addition to alerting WW drivers directly via sound and vibrations caused by DRS patterns, they can also alert WW drivers to pay more attention to the other WW-related traffic control devices. Pattern D3 can work together with DNE and/or One-Way signs to counter initial WW entries. Pattern C can alert WW drivers of WW signs. Pattern E.1 can serve as the last countermeasure to deter WWD onto the freeway mainline. Figure 3.14 shows field photos of DRS patterns.

Figure 3.12 DRS implementation at Exit 208 on I-65, AL

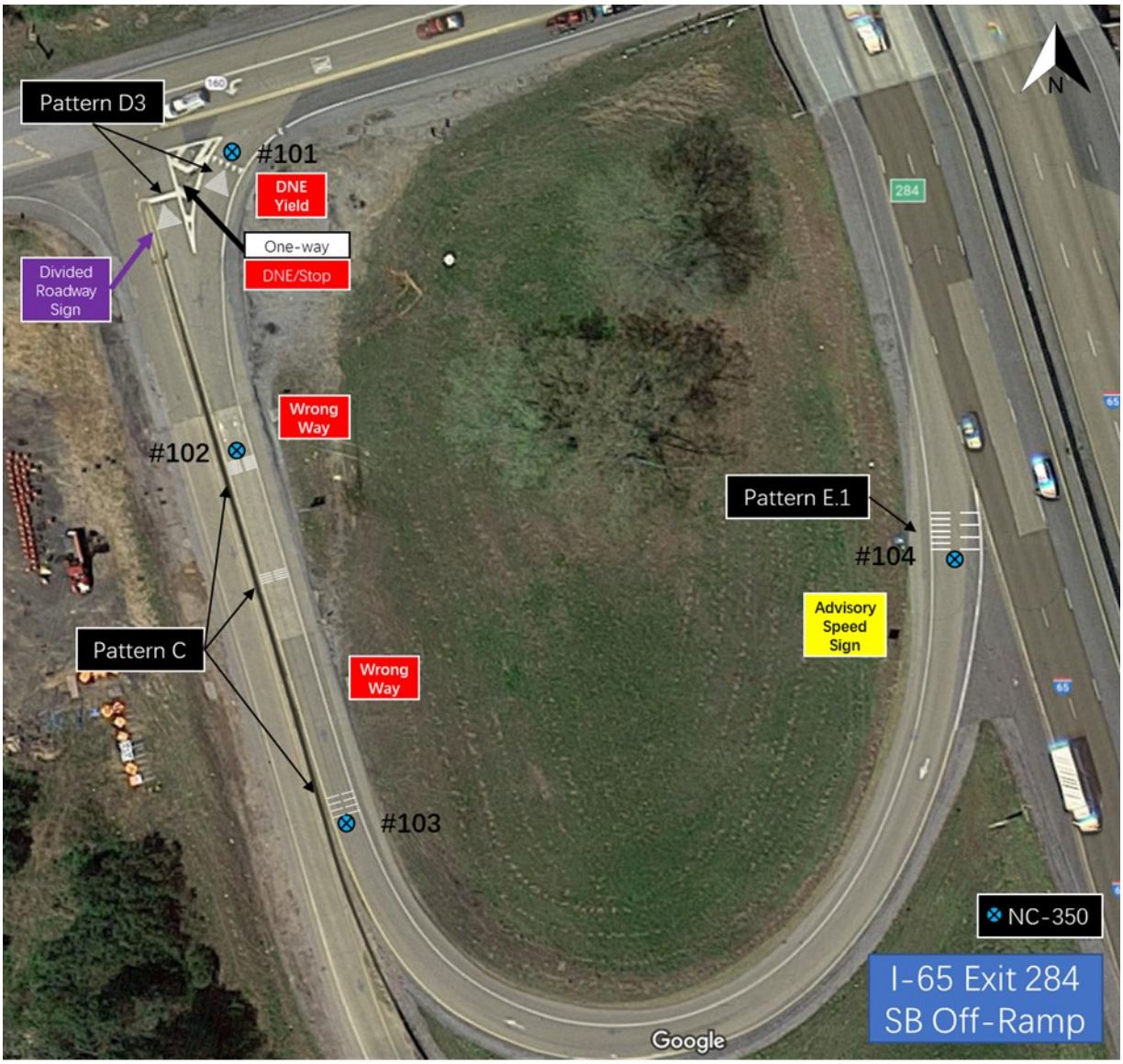

Figure 3.13 DRS implementation at Exit 284 on I-65, AL

(a) Pattern D3 at stop bars

(b) Pattern D3 at the yield line

(c) Pattern C (1-ft spacing)

(d) Pattern C (2-ft spacing)

(e) Pattern C (5-ft spacing)

(f) Pattern E.1 (yellow strips)

(g) Pattern E.1

Figure 3.14 Field photos of DRS patterns

3.3.2 DRS Installation

Installation of the DRS was conducted by a contractor (Ozark Striping, Inc) in Alabama. The material of the strips was thermoplastics. Therefore, installing the DRS required a dry pavement surface. Additionally, the surface temperature needed to be above 10°C (50°F).

Figure 3.15 summarizes the procedure for installing the DRS. First, the temporary traffic control was provided by ALDOT division maintenance crews. From the point 500 ft away from the advisory ramp speed sign, cones were placed on the right lane of freeway mainlines. The cones were used to prevent traffic from approaching and entering the off-ramp. Flashing LED message and arrow boards mounted on the trucks alerted vehicles of the closed off-ramp and making lane changes. A truck with a truck-mounted attenuator and dynamic message board was located ahead of the installation area to protect workers. Workers then started measuring distance based on parameters from the above section. Edges of strips were marked by road chalk before the surface being cleaned by the blower. Masking tape was applied to the ends of each strip. Afterward, a worker operated a hand-pushed thermoplastic screed road marking machine to install the DRS. Upon finishing the installation, glass beads were sprinkled on the strips to improve their reflection. Masking tape, as well as the excessive thermoplastics on them, was removed at the end. Lastly, installations were inspected by using a tape measure.

(a) Traffic control (ramp closed)

(b) Protection (truck-mounted attenuator and dynamic message board)

(c) Measure distance

(d) Mark and sketch

(e) Clean the surface

(f) Tape the ends of the strips

(g) Install the DRS

(h) Improve reflection and remove tapes

(i) Inspection after installation

Figure 3.15 Procedure of the DRS installation

3.4 FIELD IMPLEMENTATION SCHEDULE AND STUDY PERIODS

Table 3.1 summarizes the study periods and schedule of the DRS implementations. The week from November 2 to 8, 2018, was defined as the before week (W0), when the speed data was first collected. The after periods consisted of four weeks. Week1 (W1) started from December 12 to 18, 2018. Week2 (W2) was from December 18 to 24, 2018. Week3 (W3) was from January 6 to 12, 2019. During W0, no DRS was installed. To eliminate the potential overlapping effects of different DRS patterns, Pattern E.1 was first implemented on the first day of W1 (Dec 12). At the beginning of W2, Pattern C was installed. On the first day of W3, Pattern D3 was placed in the field. Additional video data was collected during a random weekend (named W4) from March 8 to 11, 2019. Speed data was recorded for W0 to W3. In addition, 72-hour (weekend) video data was recorded during the weekend of each study period. The installation of the DRS typically took 3 hours for one site, including transportation from one site to another. Thus, speed data collected during the DRS installations was removed. Traffic volumes counted by NC-350 are also listed in Table 3.1. The volumes were consistent through the weeks. Compared with the 2017 Alabama Traffic Data, it was found that volumes at Exit 208 were relatively lower than the reference data. Fewer RV activities during the winter could result in the reduction of traffic volumes. To evaluate the operational and safety impacts of the DRS, other modifications such as geometric changes at these off-ramps should be avoided. According to the district administers, no new construction was conducted during this project at both sites, except for regular maintenance.

Table 3.1 DRS field implementation schemes

Schedule		DRS Pattern Installed			Traffic Volume*	
Phase	**Time**	**E.1**	**C**	**D3**	**Exit 208**	**Exit 284**
Before	W0				1,347	1,127
After	W1	×			1,291	1,180
	W2	×	×		1,299	1,195
	W3	×	×	×	1,379	1,208
	W4	×	×	×	-	-

Note:

W0 = Week0 (11/02/2018-11/08/2018);

W1 = Week1 (12/12/2018-12/18/2018);

W2 = Week2 (12/18/2018-12/24/2018);

W3 = Week3 (01/06/2019-01/12/2019);

W4 = Week4 (03/08/2019-03/11/2019);

*Data from NC-350;

Reference AADT: Exit 208 = 1,550; Exit 284 = 1,260 (Source: 2017 Alabama Traffic Data).

CHAPTER 4: EFFECTIVENESS OF DRS ON WWD INCIDENTS

4.1 DESCRIPTIVE STATISTICS OF WW INCIDENTS

4.1.1 WWD Frequencies

Figure 4.1 summarizes the frequencies of WWD incidents at the two study locations at five different weekend periods (W0 to W4). WWD vehicles were classified as either passenger cars or heavy vehicles (e.g., semitrailer trucks, RVs, pickup trucks with trailers).

There was a downward trend of the number of WWD incidents. A total of 19 WWD incidents was initially recorded at the two study locations during the weekend of W0, including 10 heavy vehicles and 9 passenger cars. After implementing Pattern E.1 at W1, the number of WWD incidents (16 incidents) remained similar because most WW drivers turned around before Pattern E.1. The number of WWD incidents decreased to 12 after installing Pattern C at W2. After implementing Pattern D3, only two WW incidents occurred during the weekend of W3 and zero during another random selected after period (W4). It should be noted that no heavy vehicles made a WW entry after installation of Pattern D3 (W3 and W4). Details of each WWD incident record can be found in Appendix A.

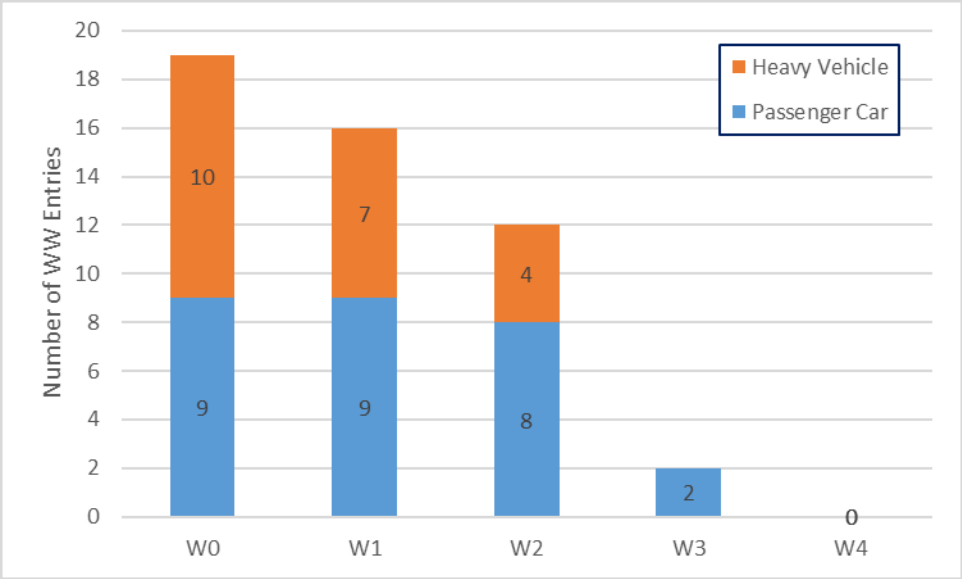

Figure 4.1 Frequencies of WW incidents at two study locations

4.1.2 Time of the Day

To identify the time frames when most WWD incidents occurred, the time when each WW incident happened from W0 to W4 was recorded. Three-hour intervals were created to summarize the frequencies of WW incidents.

As presented in Figures 4.2 and 4.3, the number of WWD incidents observed during the daytime (7:00 – 17:00) and nighttime [17:00 – 7:00 (next day)] was similar at both locations. Most WWD incidents happened during morning peak hours (6:00 – 9:00) and the late nighttime (21:00 – 24:00) at Exit 208. Nonlocal drivers, including freight trucks and RVs, may not be familiar with the geometry of the interchange. Insufficient illumination during those time periods could also contribute to the higher frequencies of WW incidents. However, the majority of WW incidents occurred around the afternoon peak hours (15:00 – 24:00) at Exit 284.

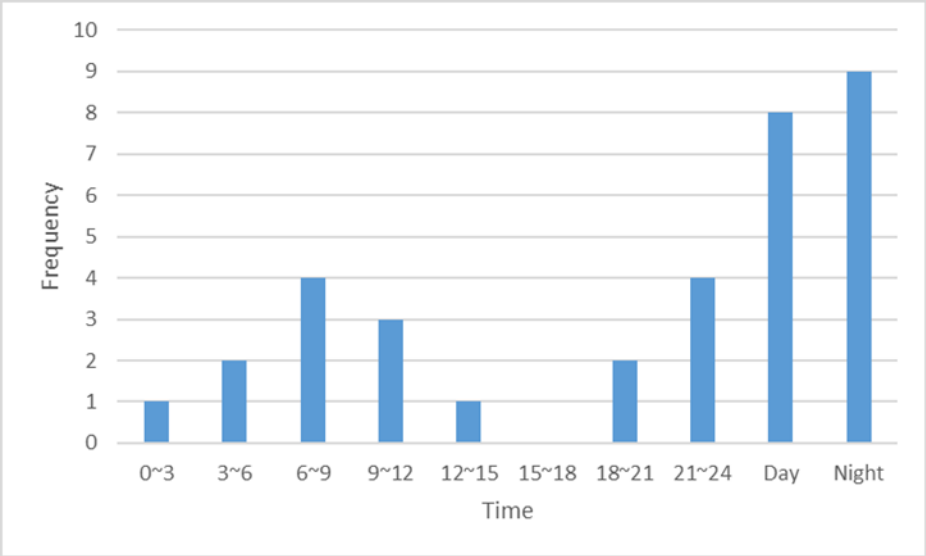

Figure 4.2 Time of the day when WW incidents occurred at Exit 208 on I-65, AL

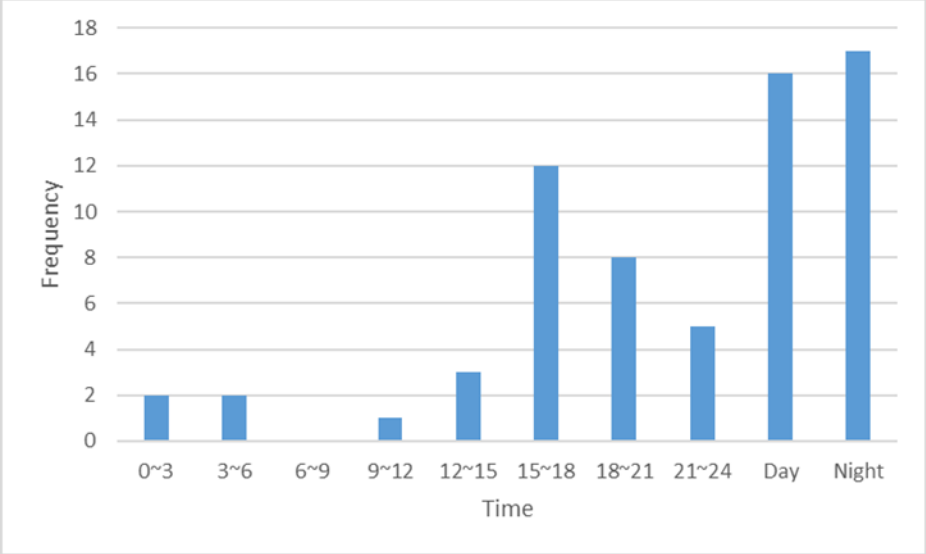

Figure 4.3 Time of the day when WW incidents occurred at Exit 284 on I-65, AL

The radar distributions in Figure 4.4 indicated the time frames when most WW incidents occurred at both sites. Initially, during W0 and W1, WW incidents tended to happen around afternoon peaks, night, and

early morning. After implementing Pattern C, the number of WW incidents from 15:00 to 21:00 significantly reduced, while increases showed during the mid-night. After installing Pattern D3, WW incidents in the early morning and late night were significantly reduced.

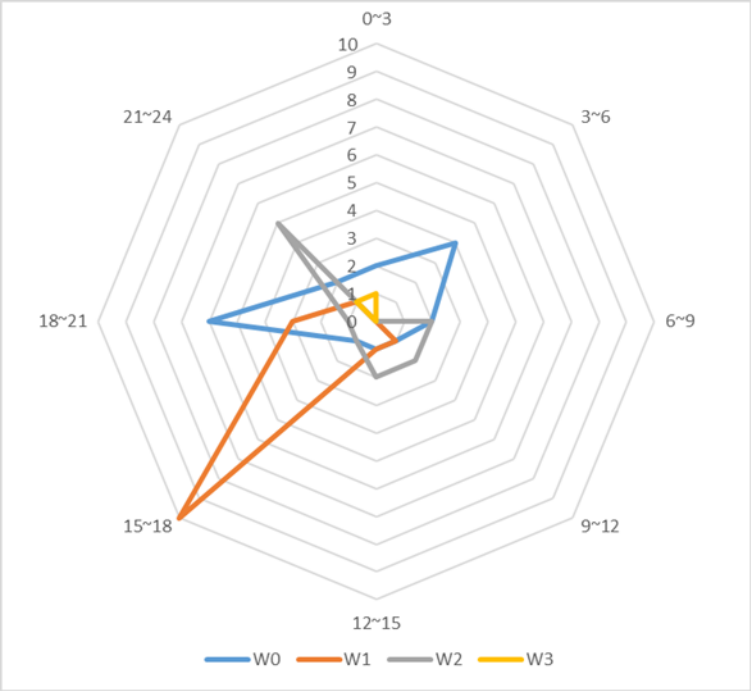

Figure 4.4 Changes in time frames of WW incidents after implementing the DRS

4.2 WWD DISTANCES

In addition to the frequency of WW incidents, the WWD distance was another criterion to evaluate the effectiveness of each DRS pattern. Two types of WWD distance were estimated. One was the cumulative WWD distance (the sum of distances traveled by all WW drivers), the other the average distance per WW entry. As shown in Figure 4.5, both the cumulative and average WWD distances present decreasing trends, especially after the installation of all the DRS (W3 and W4).

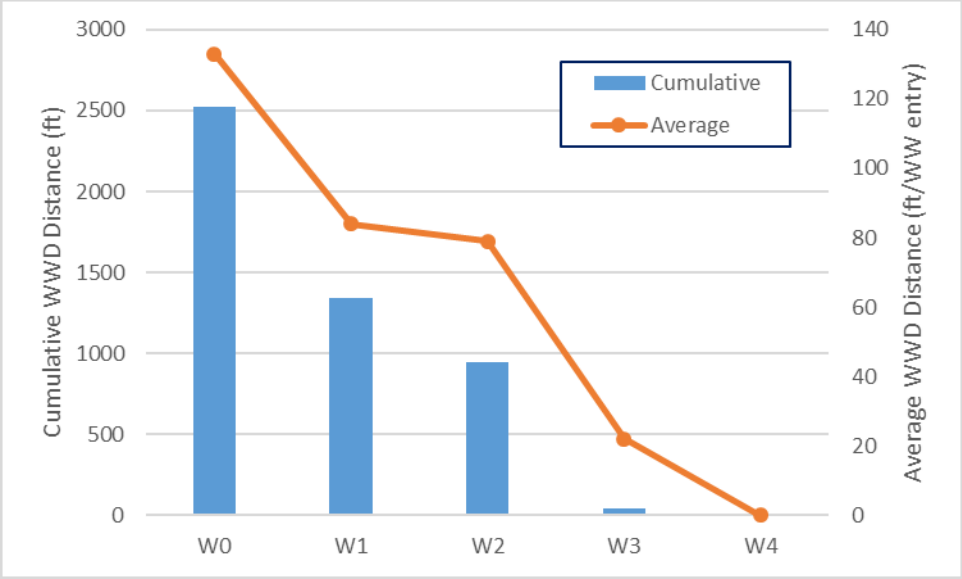

Figure 4.5 WWD distances at two study locations

4.3 EFFECTIVENESS OF DRS IN DETERING WWD

As an only countermeasure that can provide in-vehicle sound and vibrations to WW drivers, the DRS aimed at alerting WW drivers to pay attention to other WW-related traffic control devices, such as static DNE signs, WW signs, and WW arrows. This section analyzed the effectiveness of DRS based on the location where the WW driver turned around.

4.3.1 Pattern E.1

Pattern E.1 was installed at W1. During the one-week before period, only one WW driver was recorded to travel all the way to the freeway mainline and never return. No other such critical event happened in the four after periods. Only one semitrailer truck stopped and turned around at the middle of the ramp curve right before Pattern E.1 when there was no off-ramp RW traffic at Exit 208 in the W1. More data should be collected to evaluate the effectiveness of the Pattern E.1 in deterring WWD incidents.

4.3.2 Pattern C

At Exit 208, a total of five WWD incidents happened during the three after periods (W2, W3, and W4). Table 4.1 lists the details of each WWD incident. Two of them stopped and turned around at the 2-ft spacing strip group of Pattern C. WW drivers were apparently alerted by Pattern C and noticed the WW signs. Pattern C and WW signs were identified as potential effective countermeasures. The other three WW incidents were stopped and turned around by the DNE sign and dual WW arrows. At Exit 284, three out of seven WWD incidents were affected by Pattern C. The remaining four WW drivers turned around before Pattern C by RW traffic or other traffic control devices, such as a divided roadway sign or DNE sign.

To conclude, Pattern C had an impact on over 40% of WWD self-corrections at Exit 208 and Exit 284.

Table 4.1 Records of WW incidents at Exit 208 on I-65, AL after implementing Pattern C

Number	Time	Stopped	Potentially Effective Countermeasures
1	2018/12/21 11:42	before the second set of Pattern C	Pattern C; WW signs
2	2018/12/22 23:10	just passed the channelized island	DNE sign
3	2018/12/23 11:26	in front of the dual large WW arrows	dual large WW arrows
4	2018/12/24 6:44	in front of the dual large WW arrows	dual large WW arrows
5	2018/12/24 8:23	just passed the second set of Pattern C	Pattern C; WW signs

Table 4.2 Records of WW incidents at Exit 284 on I-65, AL after implementing Pattern C

Number	Time	Stopped	Potentially Effective Countermeasures
1	2018/12/21 12:09	just passed the yield line	DNE sign
2	2018/12/21 20:06	just passed the first set of Pattern C	Pattern C; WW sign
3	2018/12/22 13:32	just passed the yield line	off-ramp traffic
4	2018/12/22 21:32	at the second set of Pattern C	Pattern C; WW sign; off-ramp traffic
5	2018/12/22 22:55	at the third set of Pattern C	Pattern C; off-ramp traffic
6	2018/12/22 22:57	just passed the yield line	Divided roadway sign
7	2018/12/23 15:50	hesitated at the entrance	Divided roadway sign

4.3.3 Pattern D3

After implementing Pattern D3, only one WWD incident occurred during the W3 and W4 for a total of 144 hours at each location, respectively (Table 4.3). These two incidents were affected by Pattern D3. Both vehicles stopped and immediately turned around at Pattern D3 or immediately after D3. Pattern D3 had an impact on all the WWD self-corrections at the two study locations.

Table 4.3 Records of WW incidents at Exit 208 and 284 on I-65, AL after implementing Pattern D3

Exit 208 on I-65, AL			
Number	Time	Stopped	Potential Effective Countermeasures
1	2019/1/13 2:48	at Pattern D3	Pattern D3; DNE sign; off-ramp traffic
Exit 284 on I-65, AL			
Number	Time	Stopped	Potential Effective Countermeasures
1	2019/1/13 21:56	just passed Pattern D3	Pattern D3; WW sign

CHAPTER 5: EFFECTIVENESS OF DRS ON TRAFFIC SPEEDS

5.1 DATA PROCESSING

5.1.1 Data Filtering and Cleaning

Traffic speed data were collected for one week in each study period. To evaluate the effects of DRS on traffic speed at different locations of the off-ramp, raw speed data need to be filtered and cleaned prior to analysis. Descriptions of some variables of the raw data are listed in Table 5.1. For the purpose of analyzing the RW vehicle speed, the advice code of 2 was selected. According to *Reference.com* (Reference, 2019), the average length of passenger cars ranges from 14.4 to 16.4 ft in America. Thus, a filter was set to search records between 14 and 17 ft. To eliminate the effects of slow leading vehicles on speeds, gaps greater than 2 s were selected. The 2 s time headway was associated with the space headway of more than 90 ft. This will ensure that the average speeds on the off-ramps were estimated for the free-flow condition. Consequently, boxplots were utilized to detect potential outliers. Outliers were filtered if they were more than the upper limit or less than the lower limit. For a normal distribution (α= 0.05), 0.7% of the data (outliers) was beyond the upper and lower limits. Here, interquartile range (IQR) = upper quartile (Q3) – lower quartile (Q1), lower limit = Q1 – 1.5xIQR, and upper limit = Q3 + 1.5xIQR. Finally, approximately 70% of speed data remained for analysis after filtering and cleaning process.

Table 5.1 Variables of the raw speed data (partial)

Variable	Unit	Description
DateTime	Year/month/day/time	Date and time when a vehicle occupied the sensor
AdviceCode	-	Codes for different records. For example, 2 is the correct direction, 4 stands for the reversed direction, and 128 means that records exceeded the preset filters.
Speed	Mph	Vehicle speed when it passed the sensor
Length	Ft	Detected vehicle length
Gap	S	Time headway between recorded vehicles

5.1.2 Data Preview

An example of traffic volume and speed data from the sensor #98 during a week is illustrated in Figure 5.1. In Figure 5.1-a, daily traffic volumes of a week are presented. Morning and afternoon peaks can also be observed. Roughly, Sunday and Monday had lower traffic volumes, while Friday had the highest afternoon peak. Taking the Thursday data as an example in Figure 5.1-b, morning, midday, and afternoon peaks can be found around 8 a.m., 2 p.m., and 6 p.m. Much lower volumes were recorded during the nighttime. Figure 5.1-c shows the speed histogram of the day, which follows the normal distribution. Speeds are concentrated within 15 to 27 mph.

5.1.3 Methods

Descriptive statistics such as maximum, 85th percentile, mean, minimum, and variance (standard deviation) were first calculated. Details can be found in Appendix B.

To compare the average speeds, *z*-tests were employed. As the speed distributions were normal, both *z*- (when variances were known) and *t*-tests can be applied. *Z*-tests were used when the sample size was large (i.e., greater than 30), while *t*-tests were utilized with small sample sizes. The significance level of *z*-tests used in this study was 0.05.

Garber and Gadiraju (1989) found that crash rates increased by 0.3% with a 1 unit increase in speed variance (mph^2). In this study, *f*-tests were applied to compare the before and after speed variances. Also, the driver adoption of the DRS was investigated through changes in speed variances after the implementation.

(a)

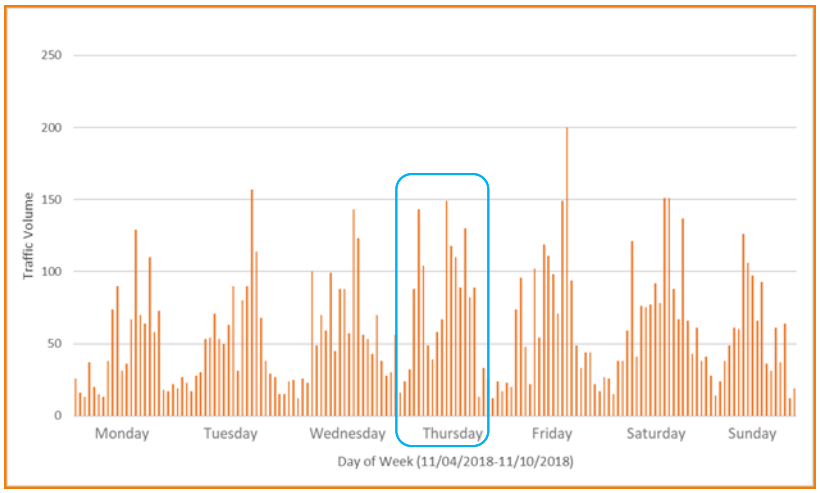

(b)

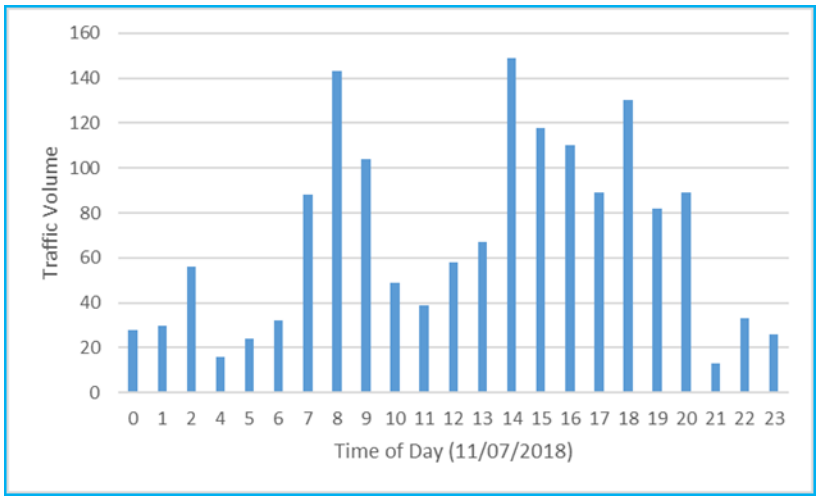

(c)

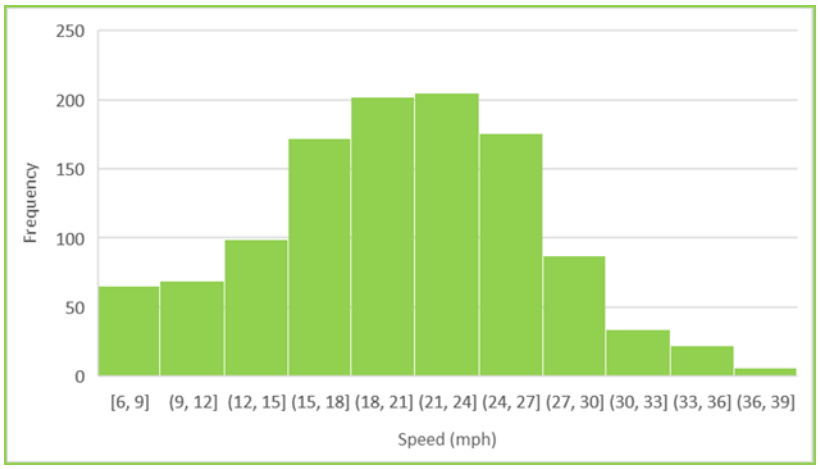

Figure 5.1 Sample traffic volume and speed data: (a) week volume; (b) Thursday volume in (a); (c) speed histogram of (b)

5.2 SPEED DISTRIBUTIONS

The speed distributions were first reviewed to have a big picture of speed changes before and after the DRS implementation. The speed data at all the locations follow the normal distribution. All speed distribution curves are contained in Appendix B.

Figures 5.2 shows the speed distributions at sensor #98 located immediately after the Pattern C at I-65 Exit 208. The most probable speeds were between 21 to 23 mph during W0 (Figure 5.2-a) and W1 (Figure 5.2-b) before Pattern C was implemented. After implementing Pattern C at W2 and W3, the speed distributions at sensor #98 shifted to the left, which reduced mode of speeds to 17-19 mph (Figures 5.2-c and 5.2-d). The similar trend was found at the second study location (I-65 Exit 284), as shown in Figure 5.4. The mode of traffic speeds concentrated around 20 mph for the first two weeks, while it shifted to near 17 mph after the implementation of the Pattern C. These results indicated Pattern C can reduce average vehicle speeds by 3-4 mph.

Figures 5.3 shows that the speed distribution at sensor #100 located immediately after the Pattern E.1 during the before period (W0) (Figure 5.3-a) is different from the three after periods (Figures 5.3-b, c, and d). After implementing the Pattern E.1 at W1, the mode of speed reduced from 36 to 30 mph. The standard deviations also had a significant reduction. Figure 5.5 shows the distribution of speed at sensor #104 located immediately after the Pattern E.1 at I-65 Exit 284. The fitted distributions show that the mean speed was reduced from over 30 mph for the first week to around 27 mph for the three after periods. However, the shapes of distributions became wider due to the increased standard deviations. The results implied that Pattern E.1 has the potential to lower vehicle speeds before the ramp curves.

Table 5.2 summarizes the means and standard deviations of the speed distribution at all locations. Speed distributions give a clear view of the data and its changes. Detailed analysis of mean, 85th percentile, and standard deviation of speeds were further discussed in the following sections.

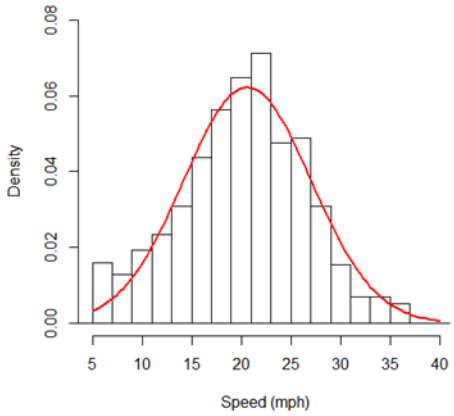

(a) W0

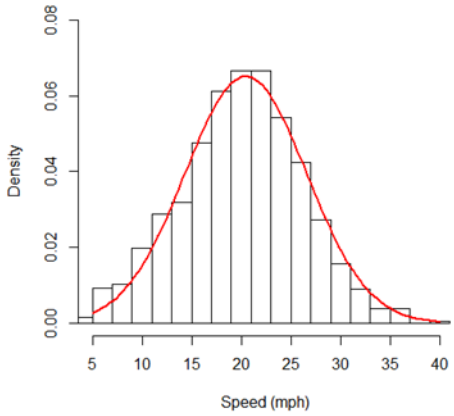

(b) W1

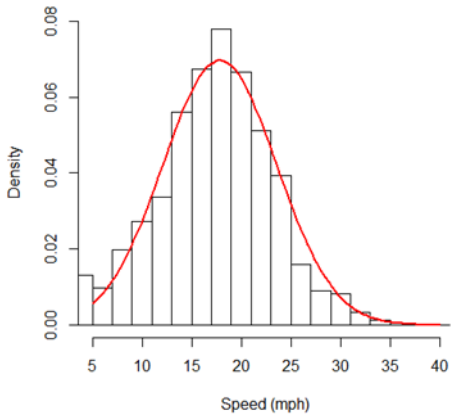

(c) W2

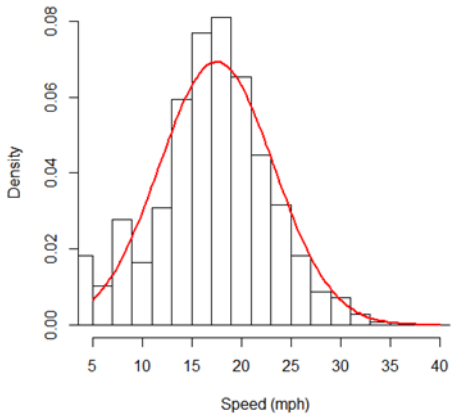

(d) W3

Note: bar - observed distribution; curve - fitted normal distribution

Figure 5.2 Speed distributions at sensor #98

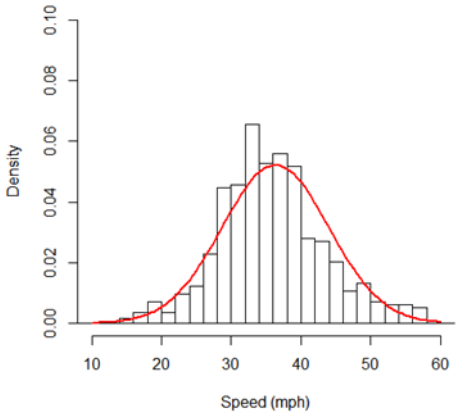

(a) W0

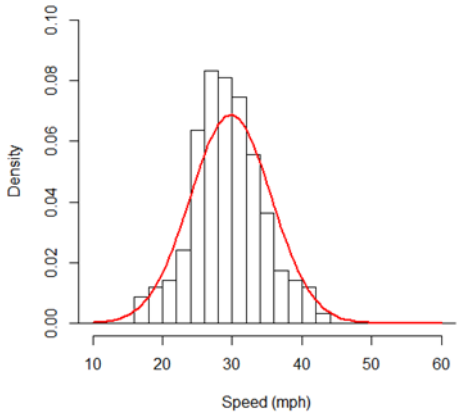

(b) W1

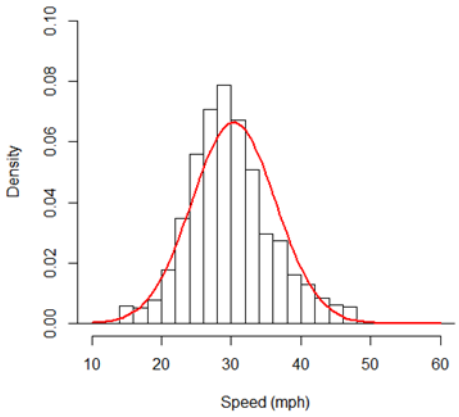

(c) W2

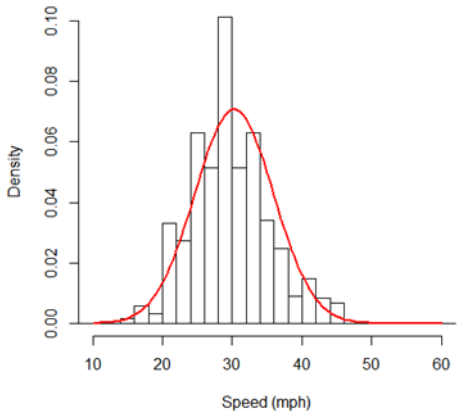

(d) W3

Note: bar - observed distribution; curve - fitted normal distribution

Figure 5.3 Speed distributions at sensor #100

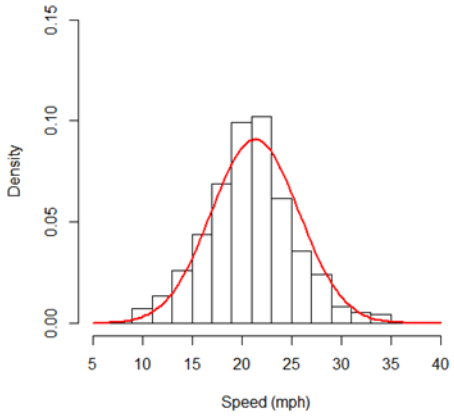

(a) W0

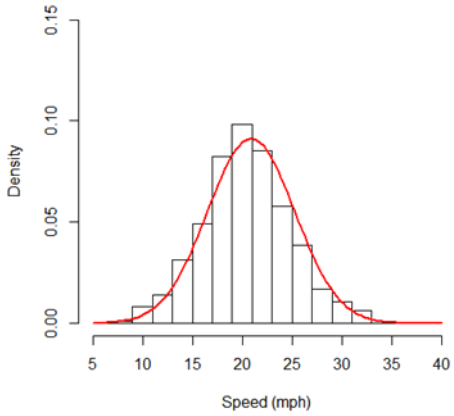

(b) W1

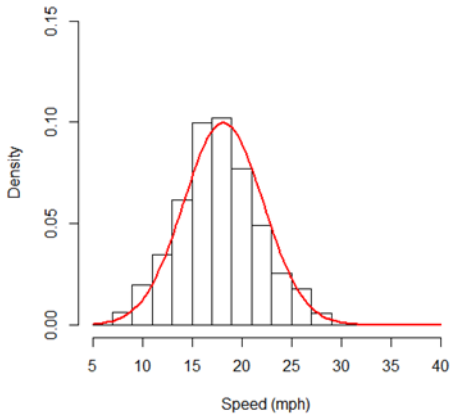

(c) W2

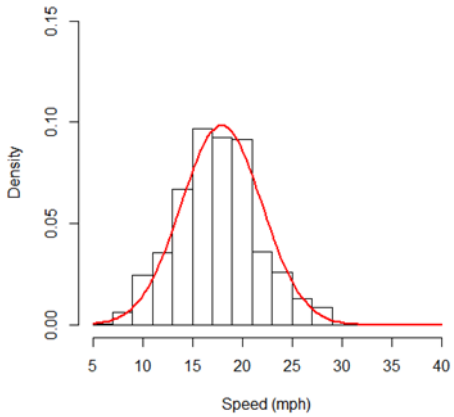

(d) W3

Note: bar - observed distribution; curve - fitted normal distribution

Figure 5.4 Speed distributions at sensor #102

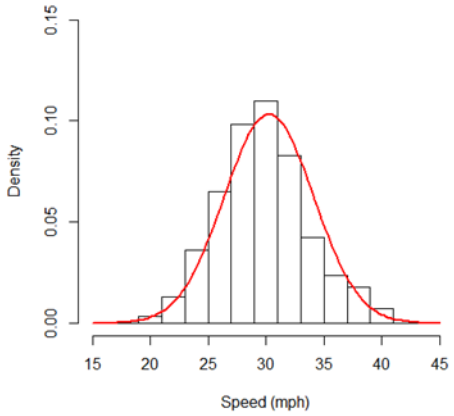

(a) W0

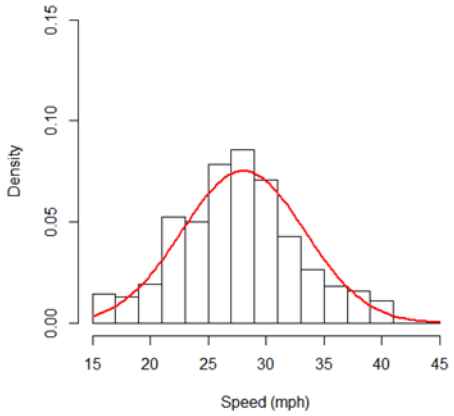

(b) W1

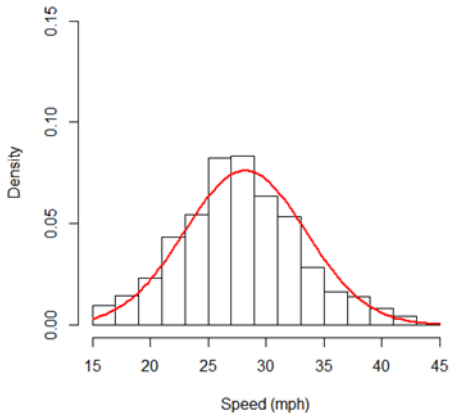

(c) W2

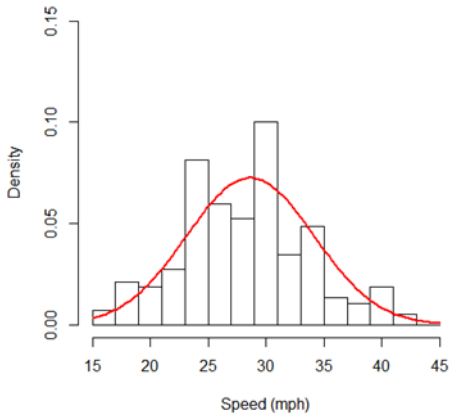

(d) W3

Note: bar - observed distribution; curve - fitted normal distribution

Figure 5.5 Speed distributions at sensor #104

Table 5.2 Characteristics of speed distributions

Time	W0	W1	W2	W3	W0	W1	W2	W3
Characteristics	Mean				Standard Deviation			
Sensor #96	8.91	9.17	8.87	8.95	2.82	2.82	2.90	2.93
Sensor #97	10.68	10.84	10.54	10.29	3.52	3.49	3.56	3.11
Sensor #98	20.62	20.48	17.85	17.52	6.41	6.13	5.73	5.76
Sensor #99	33.28	31.49	31.21	31.84	6.15	5.20	5.27	5.59
Sensor #100	36.32	29.81	30.37	30.29	7.65	5.08	6.01	5.64
Sensor #101	12.77	12.59	12.43	11.57	4.80	4.47	4.75	3.76
Sensor #102	21.35	20.90	18.17	17.94	4.39	4.37	4.00	4.05
Sensor #103	27.35	26.67	26.22	26.64	3.35	3.48	3.50	3.59
Sensor #104	30.25	28.04	28.20	28.64	3.86	5.29	5.23	5.49

Note: Significant changes in means of speed distributions

5.3 AVERAGE SPEEDS

The average speeds of RW vehicles were estimated at each location for each of four study periods (W0-W3). A comparison between the average speed before and after each DRS implementation was conducted to examine if the DRS pattern has an impact on average speed. In addition, the average speed was compared with the posted advisory speed limit (25 mph at Exit 208 and 30 mph at Exit 284). As shown in Figure 5.6-a, the average speed from sensor #100 significantly decreased by 6.5 mph (from 36.3 to 29.8 mph) at Exit 208 after the installation of Pattern E.1. While at Exit 284 (Figure 5.6-b), a significant reduction of 2.3 mph (from 30.3 to 28 mph) in the average speed from sensor #104 was observed after implementing Pattern E.1. Because the average speed in the before period was close to the speed limit, less reduction in Exit 284 was observed compared with that in Exit 208. Moreover, as shown in Table 5.3, it was found that 94% of vehicles exceeded the advisory ramp speed limit at Exit 208 in the W0 period. This percentage

was reduced to 83% by installing Pattern E.1, while the percentage of vehicles, which was over the advisory ramp speed limit, decreased from 45% to 30% at Exit 284. This finding implied that Pattern E.1 can slow down RW drivers and help them to follow the advisory speed limit when they were approaching the ramp curve. The possible reason for more reduction in Exit 208 is because the posted advisory speed limit (25 mph) at Exit 208 is much lower than the average speed of 36.3 mph in the W0 period.

After installing Pattern C, as shown in Figure 5.6, significant changes in average speeds between W1 and W2 can be observed from sensors #98 and #102 at Exits 208 and 284, respectively. The same average speed reduction of 2.7 mph occurred at both off-ramps when RW vehicles passed Pattern C.

At Exit 208 (Figure 5.6-a), the average right-turn speed slightly increased by 1.3 mph at the stop bar where sensor #97 was located after implementing Pattern D3, while there was no significant change from sensor #96 for left turns. The possible reason is that more right-turning vehicles stopped on Pattern D3 before the stop bar and then accelerated to merge the crossroad traffic. Sensor #97 was installed after the stop bar. The average speed at the yield line (sensor #101 in Figure 5.6-b) was significantly reduced by 0.8 mph at Exit 284 because most of vehicles did not make a full stop behind the yield line.

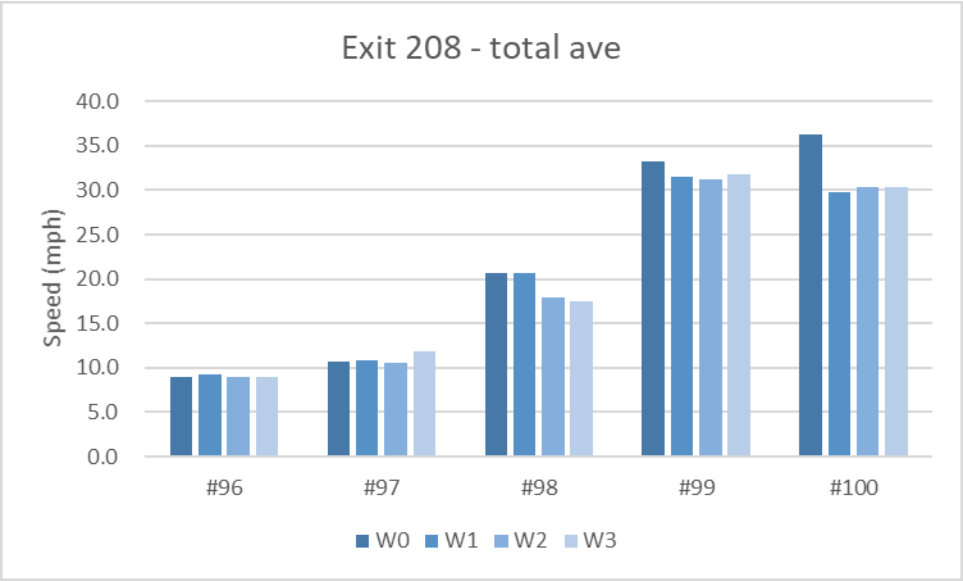

(a)

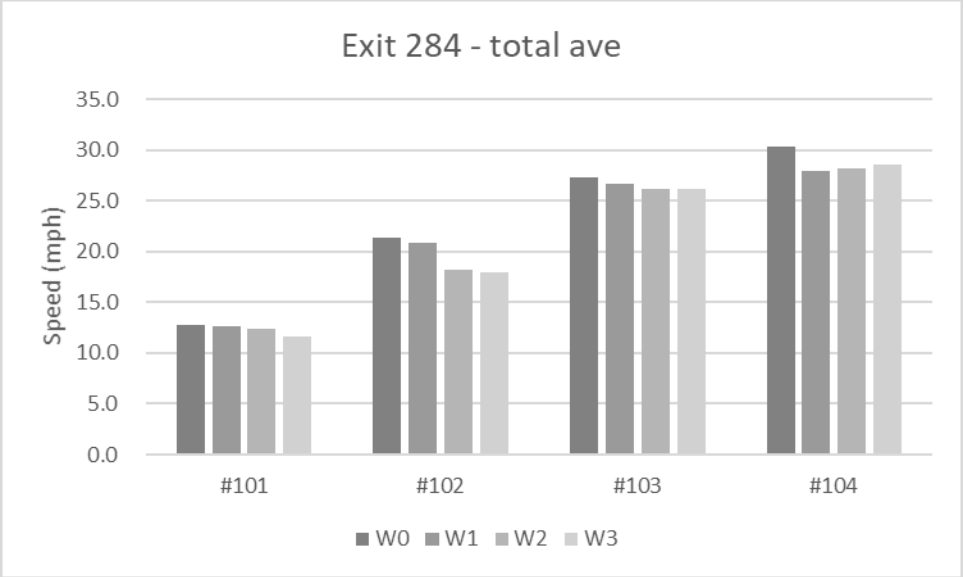

(b)

Figure 5.6 Average speeds on southbound off-ramps at Exits (a) 208 and (b) 284 on I-65, AL

Table 5.3 Pattern E.1 helped drivers follow the advisory ramp speed limit

Time	Traffic Volume		Vehicles Exceed the Advisory Ramp Speed Limit		Note
	Exit 208	Exit 284	Exit 208	Exit 284	
W0	1,347	1,127	1,266 (94%)	507 (45%)	Pattern E.1 wasn't installed
W1	1,291	1,180	1,072 (83%)	354 (30%)	Pattern E.1 was installed

The above significances were tested using *z*-tests at the significance level of 0.05. Statistical results can be found in Table 5.4. Average speeds among the four study periods, which showed no significant difference, are not listed.

Table 5.4 *Z*-tests results of changes in average speeds

Sensor	Comparison Groups		*p*-value
#97	W2	W3	0.02
#98	W1	W2	0.00
#99	W0	W1	0.00
#100	W0	W1	0.00
#101	W2	W3	0.00
#102	W1	W2	0.00
#104	W0	W1	0.00

Note: 1) *z*-tests; 2) significance level = 0.05.

5.4 85TH PERCENTILE SPEEDS

The 85th percentile speeds generally describe the speeds higher than 85 percent of drivers. The upper 15th percentile of this distribution represents aggressive driving speeds. The MUTCD recommends that the speed limit be within 5 mph of the 85th percentile speed of free-flowing traffic. Adjustments can be made if there are horizontal and vertical curves (possible limited sight distance).

As shown in Figure 5.7-a, the advisory ramp speed limit is 25 mph at Exit 208. The 85th percentile speed when vehicles approached the ramp curve (sensor #100) stabilized at around 35 from 44 mph after implementing Pattern E.1. The 85th percentile speed was reduced from 39 mph to around 35 mph at the location (sensor #99). The results indicated that the majority of drivers reduced their speed by 4 to 9 mph by Pattern E.1. Moreover, changes in upper 15th percentile speeds also implied that Pattern E.1 can help mitigate aggressive driving. As listed in Tables 5.5 and 5.6, characteristics of the upper 15th percentile speeds when vehicles approached and exited the ramp curve, including maximum, mean, minimum, and standard deviation, were reduced after implementing Pattern E.1. With *p*-values less than 0.05 from *z*- and *f*-tests at the significance level of 0.05, their mean and standard deviation proved to have significant decreases.

The advisory ramp speed limit was 30 mph at Exit 284, as presented in Figure 5.7-b. No significant difference of the 85th percentile speed was observed when vehicles entered (sensor #104) and exited (sensor #103) the ramp curve because the initial 85th speed was close to the speed limit.

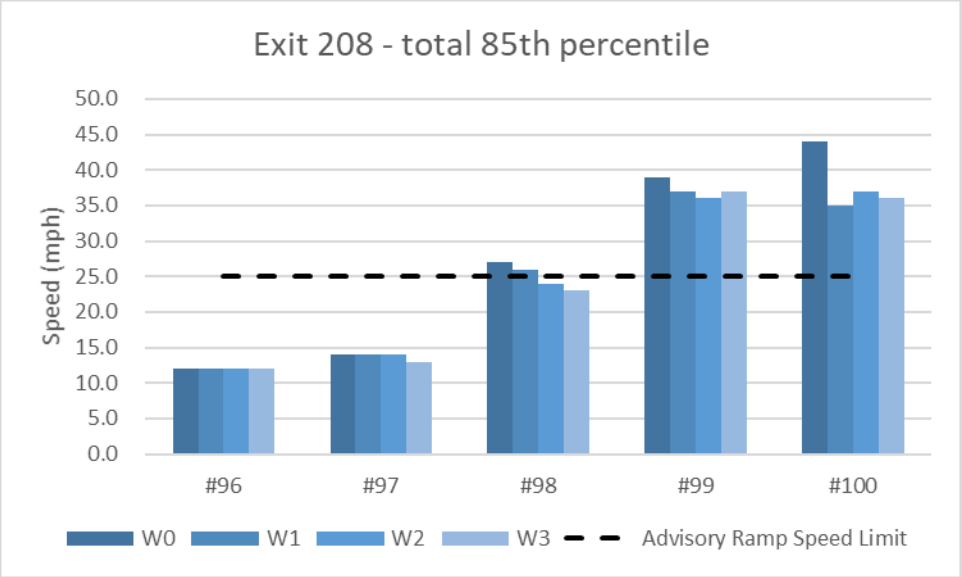

(a)

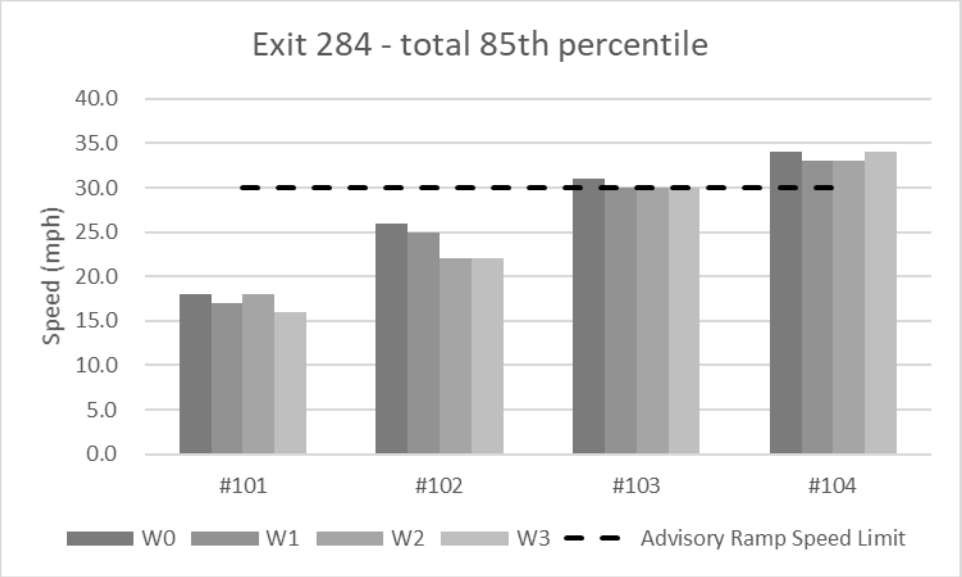

(b)

Figure 5.7 85th percentile speeds on southbound off-ramps at Exits (a) 208 and (b) 284 on I-65, AL

Table 5.5 Speed characteristics of upper 15th percentile speeds from sensor #99 at Exit 208 on I-65, AL

Characteristics (Unit: mph)	W0	W1	W2	W3
Max	51.0	45.0	45.0	48.0
Mean	43.0	40.1	39.5	40.7
Min	40.0	38.0	37.0	38.0
Standard Deviation	3.1	1.9	2.3	2.6

Table 5.6 Speed characteristics of upper 15th percentile speeds from sensor #100 at Exit 208 on I-65, AL

Characteristics (Unit: mph)	W0	W1	W2	W3
Max	58.0	44.0	47.0	46.0
Mean	49.7	38.7	41.5	40.4
Min	45.0	36.0	38.0	37.0
Standard Deviation	4.0	2.3	3.0	2.8

5.5 STANDARD DEVIATIONS OF SPEEDS

Figure 5.8 presents the standard deviations (SDs) of RW speeds along the off-ramps from W0 to W3 at the two study locations. At Exit 208, the SDs of RW speed at all five locations showed a decline trend after implementing DRS. In the W1 period after implementing Pattern E.1, SDs from sensors #100 and #99 significantly decreased by 2.5 and 1.0 mph, respectively. From W1 to W2, the SDs from sensor #98 were significantly reduced by 0.5 mph after installation of Pattern C. Further, Pattern D3 led to a decrease of 0.5 mph in SDs for right-turning speed at the stop bar (sensor #97).

At Exit 284, Pattern D3 led to a decrease of 1.0 mph in the SDs for right-turn speeds at the yield line (sensor #101). Pattern C reduced 0.4 mph in the SDs of average speed in the middle of ramp (sensor #102). However, SDs from sensor #104 significantly increased by 1.4 mph after installing Pattern E.1. Moreover, the SD from sensor #104 significantly increased by 0.9 mph in the W2 period. The possible reason is that

average speed of this location was close to the posted speed limit. Some drivers further reduced their speeds after implementing the DRS.

Speed variances were tested using *f*-tests at the significance level of 0.05. The results are shown in Table 5.7. Speed variances between adjacent weeks, which show no significant difference, are not listed.

Table 5.7 *F*-test results of changes in speed variances

Sensor	Comparison Groups		*p*-value
#97	W2	W3	0.00
#98	W1	W2	0.03
#99	W0	W1	0.00
#100	W0	W1	0.00
	W1	W2	0.00
#101	W2	W3	0.00
#102	W1	W2	0.00
#104	W0	W1	0.00

Note: 1) *f*-tests; 2) significance level = 0.05

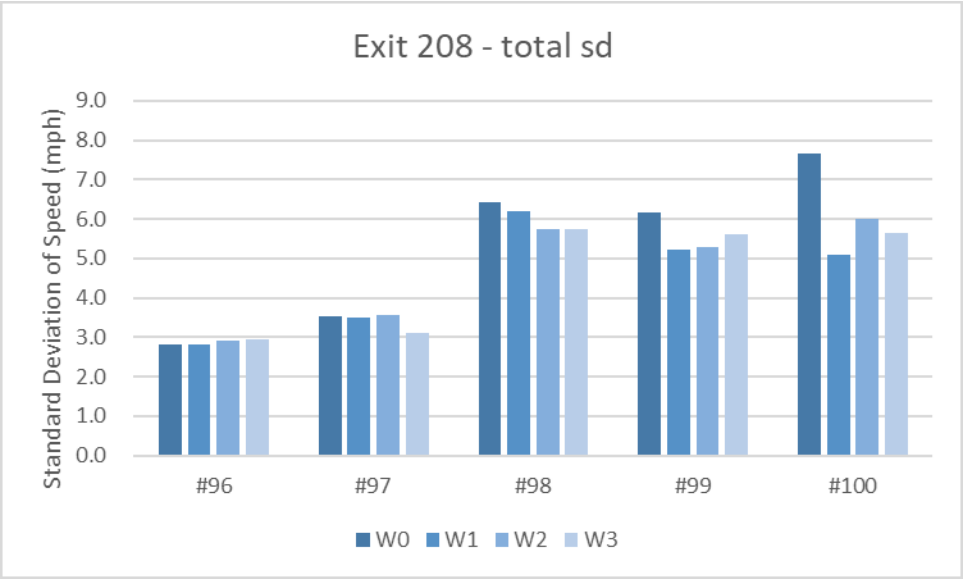

(a)

(b)

Figure 5.8 Standard deviations of speeds on southbound off-ramps at Exits (a) 208 and (b) 284 on I-65, AL

5.6 DRIVER ADOPTION OF THE DRS

Considering that the DRS were new traffic control devices, drivers may require time to get used to them. The trends of daily changes in speed SDs were used to evaluate the driver adoption of a certain DRS pattern. The following sections describe the driver adoption process of each DRS pattern as time goes by. Speed SDs at each location were recorded for each day from W0 to W3. The simple moving average method (Interval = 2 days) was applied to track the trend.

5.6.1 Driver Adoption of Pattern E.1

As illustrated in the previous sections, significant changes of speed SDs were identified before vehicles entering the off-ramp curves at both locations after installing Pattern E.1. Figure 5.9 presents the trends of the driver adoption process.

At Exit 208 (Figure 5.9-a), an immediate drop of the speed SD was observed on the first day of W1 when Pattern E.1 was installed. It roughly took two days for the speed SD to become stable around 5 mph. After another week, it had the trend that the speed SD there had increased by 1 mph. Hence, Pattern E.1 was not eventually in effect until the third day. Once drivers got used to it, the speed SD could slightly increase.

In contrast, an increasing trend can be found from Day 1 (D1) to Day 3 (D3) during W1 at Exit 284 (Figure 5.9-b), which was related to the installation of Pattern E.1. The speed SD then stabilized between 5 and 6 mph. Therefore, speed differences gradually increased within three days, as drivers became increasingly familiar with the Pattern E.1.

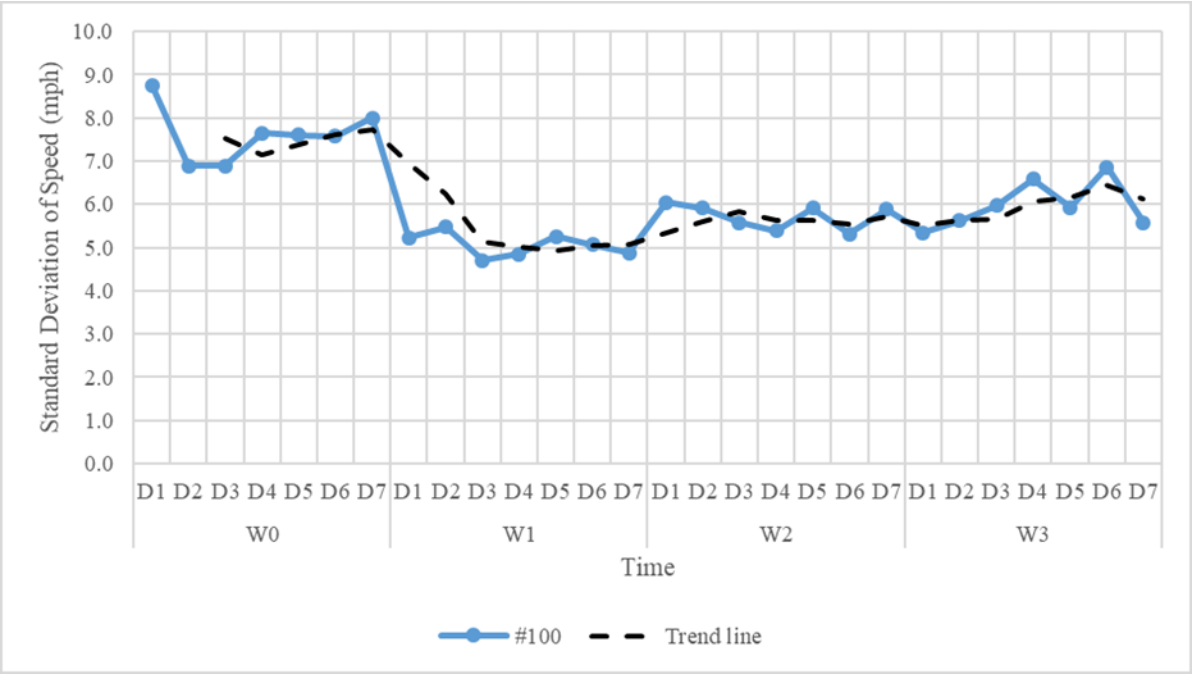

(a)

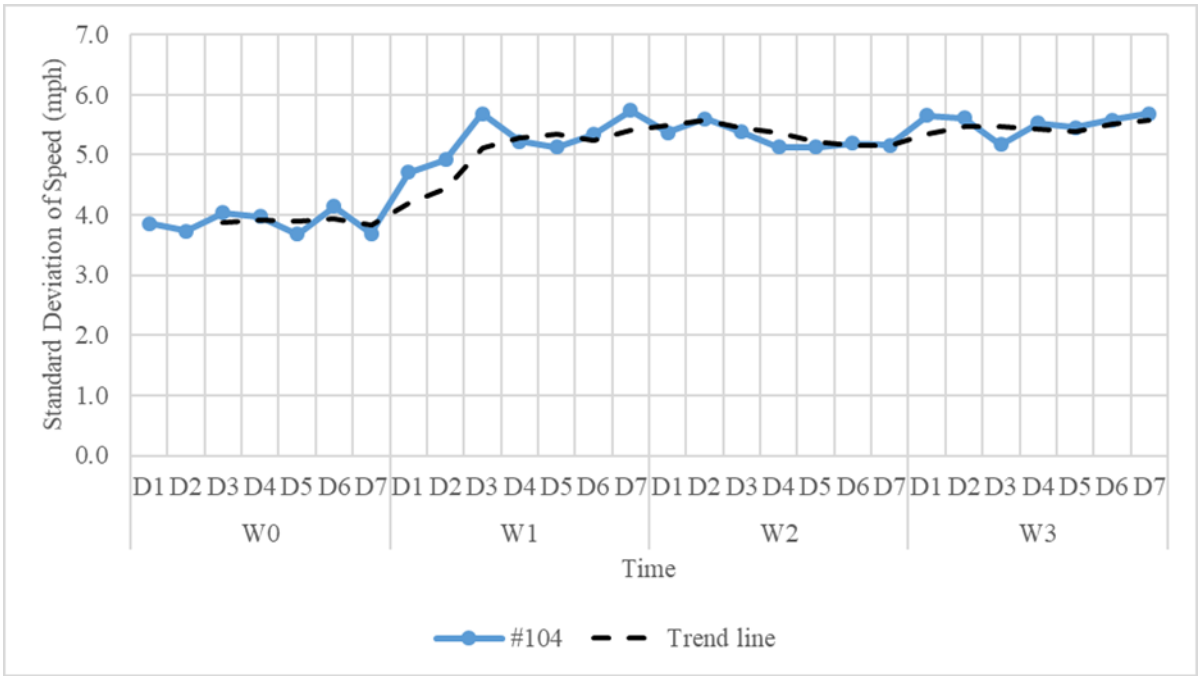

(b)

Figure 5.9 Driver adoption of Pattern E.1 at Exits (a) 208 and (b) 284 on I-65, AL

5.6.2 Driver Adoption of Pattern C

Significant reductions in speed SD at the segment between the ramp curve and terminal were also found after installation of Pattern C.

As presented in Figure 5.10, the speed SDs gradually decreased after Day 1 (D1) at W2 until becoming stable. The first drop of speed SDs occurred on the second day of W2. Because Pattern C and TRS were alike, drivers easily became accustomed to this DRS pattern.

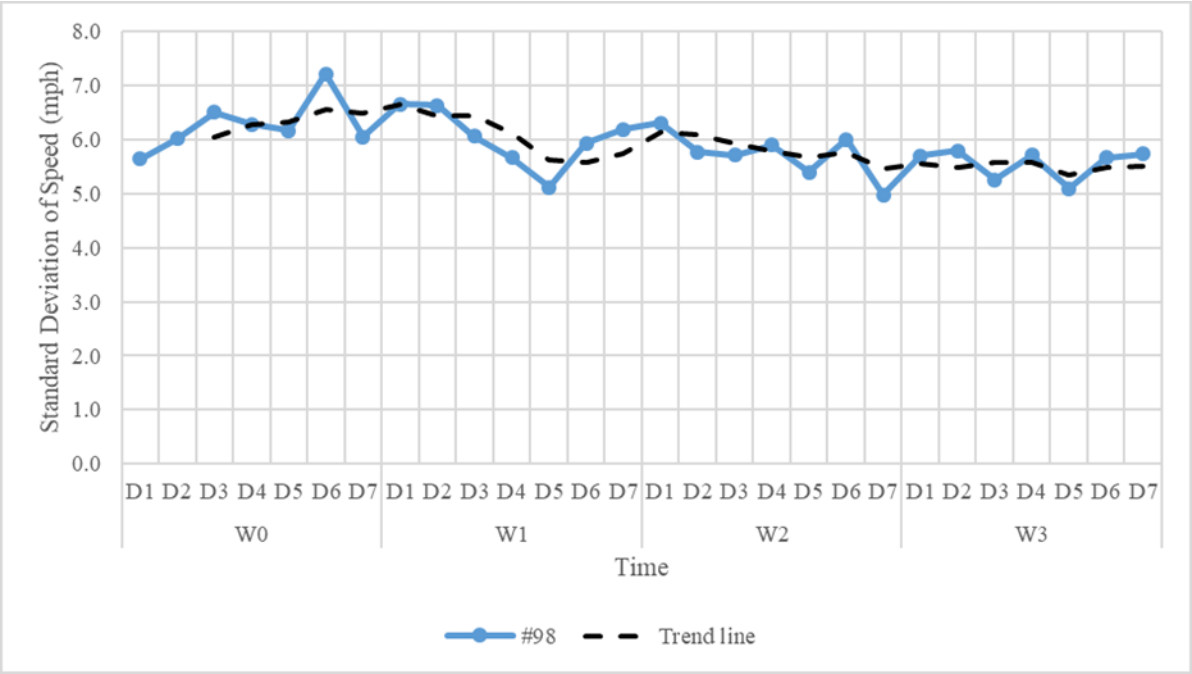

(a)

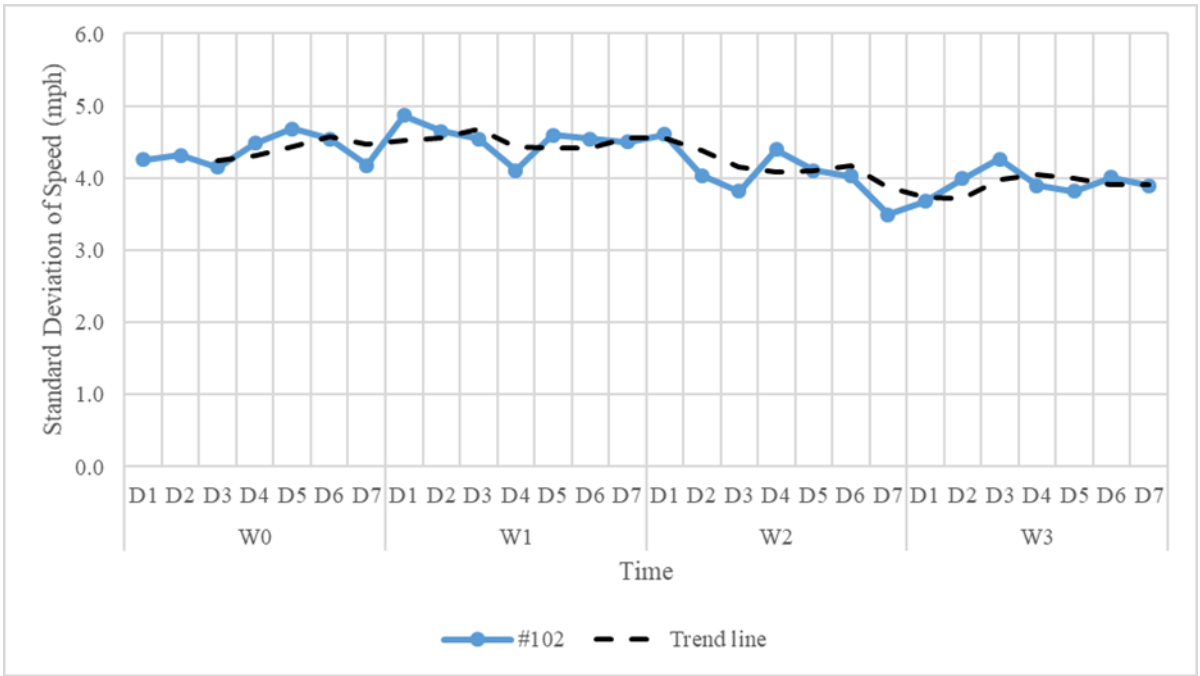

(b)

Figure 5.10 Driver adoption of Pattern C at Exits (a) 208 and (b) 284 on I-65, AL

5.6.3 Driver Adoption of Pattern D3

Pattern D3 helped reduce the speed SDs at both stop and yield-controlled ramp terminals. As presented in Figure 5.11-a, the decreasing trend of the speed SD for right-turn vehicles slowed after three days at Exit 208. It indicated that an increased proportion of drivers made complete stops, which resulted in smaller speed differences. The downhill trend also indicated that Pattern D3 could help more drivers make complete stops at the stop bar, even if there is no vehicle on the crossroad. While at the yield-controlled terminal, as shown in Figure 5.11-b, it took two days for RW drivers to further lower the speed SDs. Pattern D3 eventually reduced the average speed SD below 5 mph, which may make it safer to merge onto the crossroad by taking more time to choose a gap.

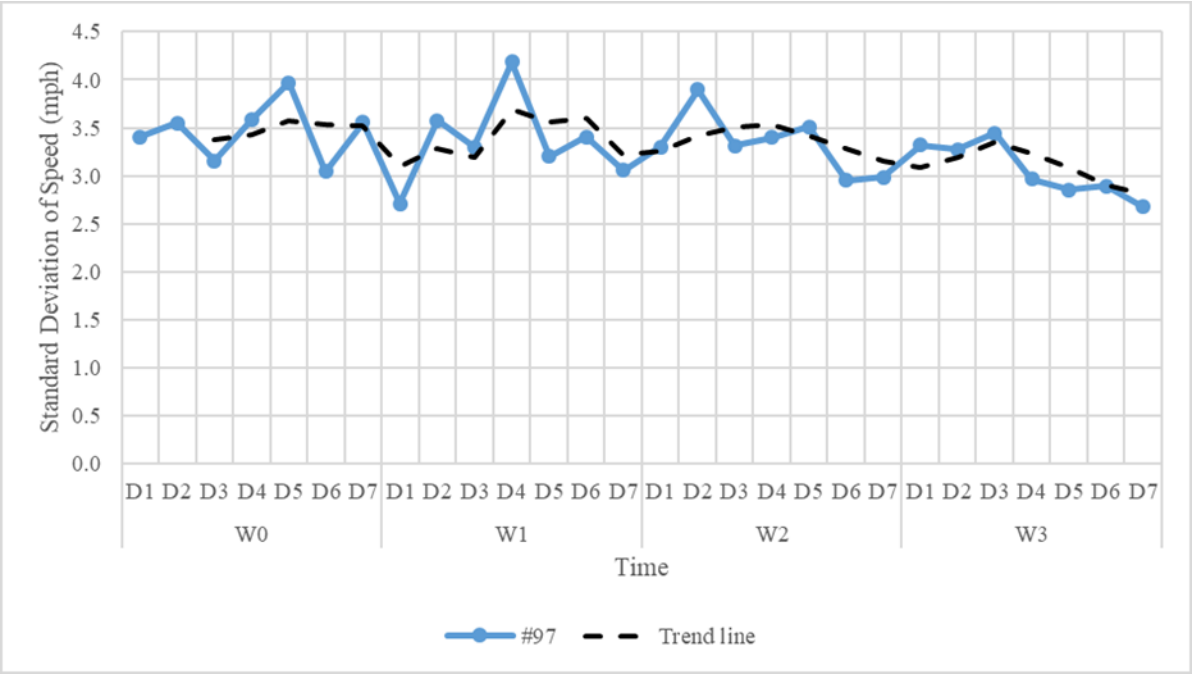

(a)

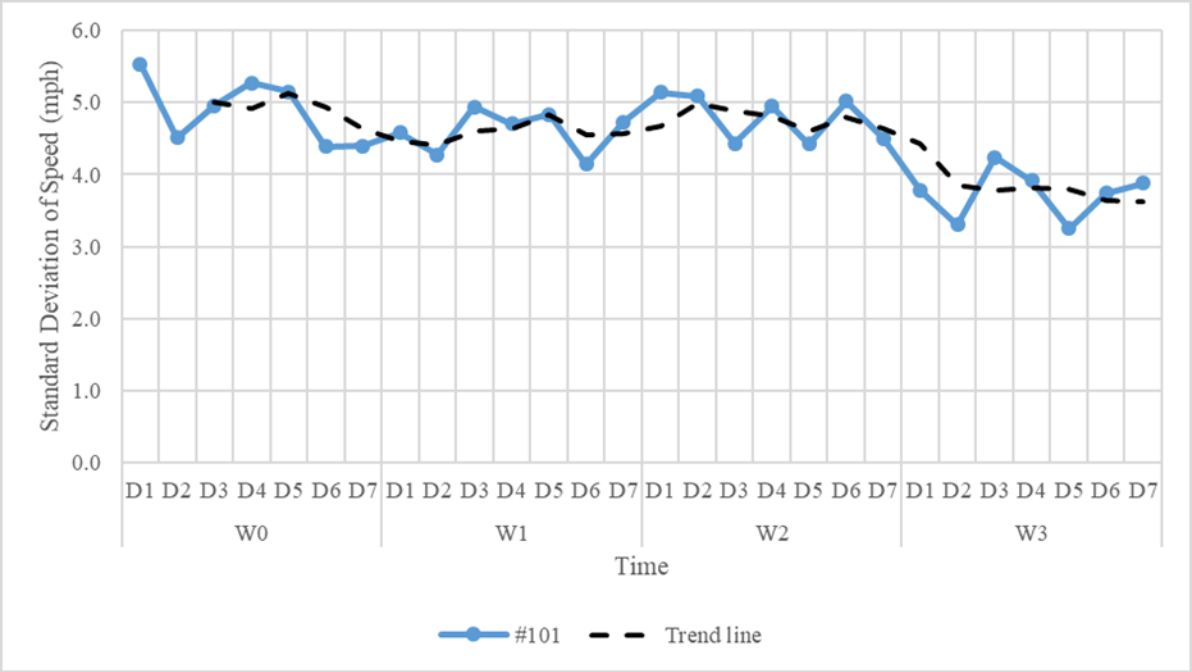

(b)

Figure 5.11 Driver adoption of Pattern D3 at Exits (a) 208 and (b) 284 on I-65, AL

5.7 COMPARISONS BETWEEN DAYTIME AND NIGHTTIME

Daytime was considered from 7 a.m. to 5 p.m. when it was not completely dark based on videos. About 60% of traffic volume occurred during the daytime. Findings of comparisons of average speed and its SD between daytime and nighttime are summarized as follows.

5.7.1 After Implementing Pattern E.1

As previously discussed, Pattern E.1 was able to reduce average speeds when RW vehicles approached the off-ramp curve. As shown in Table 5.8, vehicles traveled faster during the daytime than the nighttime before entering the ramp curve according to data from sensors #100 and #104. Also, average speeds decreased more at Exit 208 than Exit 284, according to the speed reductions and their percentages. Pattern E.1, with all white strips, can reduce average speed by 1.8 mph at Exit 284 during the daytime. However, the *z*-test result indicated that it wasn't significant at the 95% confidence level because the *p*-value exceeded 0.05. During the nighttime, the average speed at Exit 284 significantly reduced by 2.6 mph, which was more than the reduction during the daytime. Pattern E.1, with one-side yellow strips, at Exit 208 can significantly reduce average speeds by 6.9 and 6.5 mph during daytime and nighttime, respectively.

Table 5.8 Comparisons of daytime and nighttime average speeds after implementing Pattern E.1

Time	Location	Average Speed (mph)		Speed Reduction (mph)	Reduction %	*p*-value*
		W0	W1			
Daytime	Exit 208	37.0	30.1	6.9	19%	0.00
	Exit 284	30.8	29.0	1.8	6%	0.06
Nighttime	Exit 208	35.6	29.1	6.5	18%	0.00
	Exit 284	29.6	27.0	2.6	9%	0.02

*Note: 1) *z*-tests; 2) significance level = 0.05.

The SD comparisons listed in Table 5.9 show that speed SDs at Exit 284 decreased 10% more during daytime than nighttime. However, there was no difference between daytime and nighttime at Exit 208, given the SD reductions over 30%.

Table 5.9 Comparisons of daytime and nighttime speed standard deviations after implementing Pattern E.1

Time	Location	Speed SD (mph)		SD Reduction (mph)	Reduction%	*p*-value*
		W1	W2			
Daytime	Exit 208	7.7	5.1	2.6	34%	0.00
	Exit 284	3.8	5.4	-1.6	-42%	0.00
Nighttime	Exit 208	7.6	5.1	2.5	33%	0.00
	Exit 284	3.8	5.0	-1.2	-32%	0.00

*Note: 1) *f*-tests; 2) significance level = 0.05.

5.7.2 After Implementing Pattern C

At the straight long segment between the ramp terminal and curve, the average speed reductions by Pattern C between daytime and nighttime were similar at both locations based on data from sensors #98 and #102, as shown in Table 5.10. Compared with the daytime, an extra 3% reduction was observed at Exit 284 during the nighttime. Moreover, the average speed during the nighttime was higher than that during the daytime before installing Pattern C at Exit 284 (W1). After implementing Pattern C (W2), the average speed was reduced from 21 to around 18 mph throughout the day.

Besides slowing down RW vehicles, Pattern C also reduced speed SDs (Table 5.11). In general, larger SD reductions were found at both locations during the nighttime, which were more than 10% of the SDs during W1.

Table 5.10 Comparisons of daytime and nighttime average speeds after implementing Pattern C

Time	Location	Average Speed (mph)		Speed Reduction (mph)	Reduction%	*p*-value*
		W1	W2			
Daytime	Exit 208	21.3	18.4	2.9	14%	0.00
	Exit 284	20.7	18.3	2.4	12%	0.00
Nighttime	Exit 208	19.7	16.9	2.8	14%	0.00
	Exit 284	21.1	18.0	3.1	15%	0.00

*Note: 1) *z*-tests; 2) significance level = 0.05.

Table 5.11 Comparisons of daytime and nighttime speed standard deviations after implementing Pattern C

Time	Location	Speed SD (mph)		SD Reduction (mph)	Reduction%	*p*-value*
		W1	W2			
Daytime	Exit 208	6.1	5.8	0.3	5%	0.03
	Exit 284	4.4	4.1	0.3	7%	0.02
Nighttime	Exit 208	5.9	5.3	0.6	10%	0.01
	Exit 284	4.4	3.9	0.5	11%	0.02

*Note: 1) *f*-tests; 2) significance level = 0.05.

5.7.3 After Implementing Pattern D3

The average speeds and speed SDs at the off-ramp terminals did not show any differences between daytime and nighttime after implementing Pattern D3 (Tables 5.12 and 5.13). The reduction percentage of the average speeds and speed SDs were close in regard to data from sensors #97 and #101.

Table 5.12 Comparisons of daytime and nighttime average speeds after implementing Pattern D3

Time	Location	Average Speed (mph)		Speed Reduction (mph)	Reduction%	*p*-value*
		W2	W3			
Daytime	Exit 208	10.7	10.5	0.2	2%	0.00
	Exit 284	12.5	11.6	0.9	7%	0.00
Nighttime	Exit 208	10.3	10.1	0.2	2%	0.00
	Exit 284	12.3	11.6	0.7	6%	0.00

*Note: 1) *z*-tests; 2) significance level = 0.05.

Table 5.13 Comparisons of daytime and nighttime speed standard deviations after implementing Pattern D3

Time	Location	Speed SD (mph)		SD Reduction (mph)	Reduction%	*p*-value
		W2	W3			
Daytime	Exit 208	3.7	3.3	0.4	11%	0.00
	Exit 284	4.8	3.8	1.0	21%	0.00
Nighttime	Exit 208	3.3	2.9	0.4	12%	0.00
	Exit 284	4.6	3.6	1.0	22%	0.00

*Note: 1) *f*-tests; 2) significance level = 0.05.

CHAPTER 6: ANALYSIS OF SOUND AND VIBRATIONS

This chapter summarizes the data description, methods, and findings of interior sound and vibrations as well as the exterior sound levels generated by the DRS.

6.1 INTERIOR SOUND

This section analyzes the interior sound generated by the DRS in order to gain a further understanding of different sound levels among ambient, RW, and WW driving conditions.

6.1.1 Data Description

Interior sound data were collected through field driving tests. Due to the limitations of temporary ramp closures, the field driving tests were only conducted at Exit 208 on I-65. Both RW and WW interior sound data were acquired under seven speed categories, including 10, 15, 20, 25, 30, 35, and 40 mph. To gather the RW sound data, one researcher drove a full-size passenger car from the deceleration lane to the off-ramp terminal on the closed ramp. Driving in the reversed direction obtained the WW sound data. Figure 6.1 presented the sample RW sound data along the off-ramp at a constant speed of 20 mph. Initially, from 0 to 5 s, some noises resulted from the vehicle acceleration. At 7 s, the first peak was generated by passing Pattern E.1. A second peak was created by passing the WW arrow at 14 s. However, the first lane-use arrow was not hit. Then, the vehicle passed the following WW and lane-use arrows at 22 and 26 s. Afterward, passing Pattern C generated three sound peaks. The dual WW arrows led to a consequential peak. The last peak was produced by passing Pattern D3.

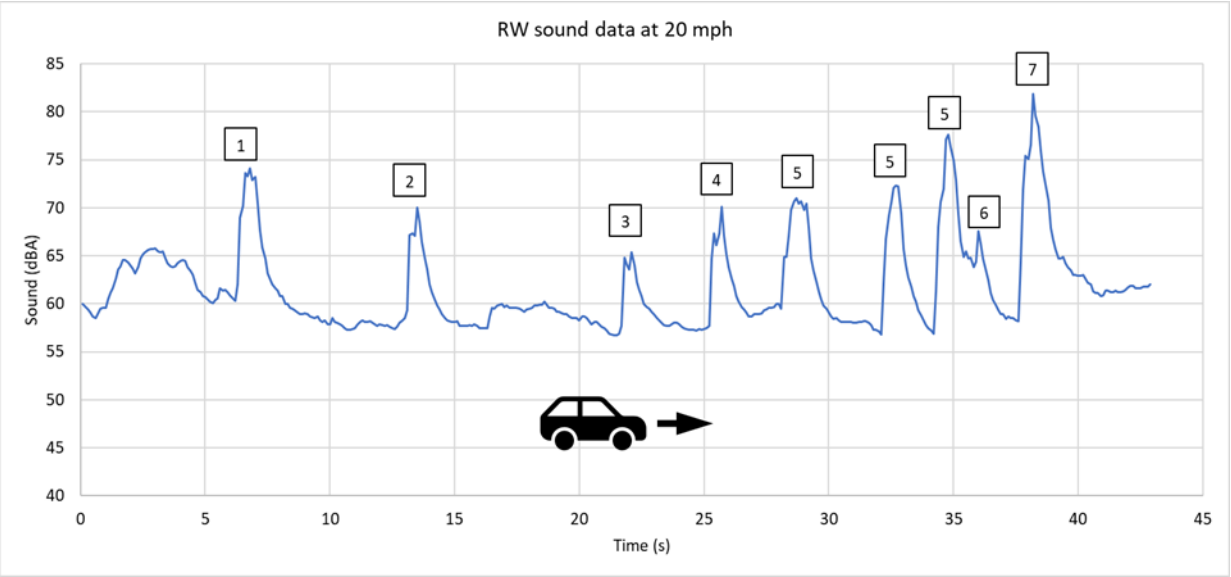

Note: 1 = Pattern E.1; 2 = WW arrow; 3 = WW arrow; 4 = lane-use arrow; 5 = Pattern C; 6 = dual WW arrows; 7 = Pattern D3.

Figure 6.1 Sample RW sound data along the off-ramp at 20 mph

6.1.2 Methods

The time-series technique was used to visualize the sound data. It was applied to obtain an understanding of sound data taken over time, including the peaks when vehicles pass the DRS.

To present an effective value of the varying sound waveforms, root mean square (RMS) value was employed to show the equivalent constant value, which gave the same effect. In other words, it determined the average power output (energy) of the sound.

T-tests at the significance level of 0.05 were also used to discern significant differences between the average RW and WW sound levels.

6.1.3 Findings

6.1.3.1 Pattern E.1

According to the NC-350 speed data, the average RW speed was 30 mph and WW 35 mph. Figure 6.2 presents the RW and WW sound of Pattern E.1. This DRS pattern created a 15 dBA louder sound for RW drivers and 20 dBA more for WW drivers than in the ambient conditions. The effective value of WW sound was 71.74 dBA, which was almost 5 dBA higher than the RW effective value (66.94 dBA). The *p*-value of the *t*-test (significance level = 0.05) was 0.012, which indicated that RW and WW sound levels were significantly different in means.

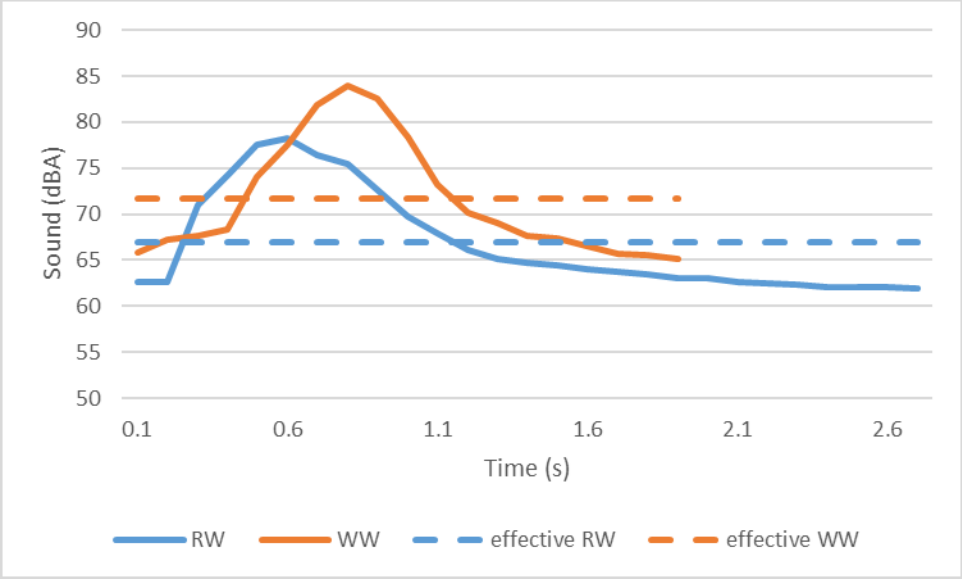

Figure 6.2 RW and WW sound of Pattern E.1

6.1.3.2 Pattern C

Figure 6.3 shows the RW and WW sound of Pattern C. As shown in Figure 6.3-a, based on the speed data collected by NC-350, the average RW speed was 30 mph and WW 35 mph when vehicles passed the strips of 5-ft spacings. RW drivers were able to perceive a maximum of 10 dBA louder sound than in ambient conditions, while WW 17 dBA. Moreover, RW drivers can hear a sound that is equivalent to 65.33 dBA and WW 69.34 dBA. WW drivers can obtain 4 dBA more sound in effect. A *p*-value of 0.03 implied that a significant difference existed between the average RW and WW sound levels.

Figure 6.3-b presents the RW and WW sound generated by 2-ft-spacing strips of Pattern C. The RW drivers drove at 25 mph and WW 35 mph on average. When against ambient conditions, strips produced 15 dBA louder sound for RW drivers and 17 dBA more for WW drivers at most. The effective values also signified that WW drivers (72.49 dBA) would get a 5 dBA louder sound in effect than RW drivers (67.36 dBA). The *t*-test result revealed the average WW sound level was significantly different from the RW one with a *p*-value of 0.03.

The RW and WW sound produced by 1-ft-spacing strips of Pattern C is shown in Figure 6.3-c. The speed sensor recorded an average speed of 20 mph for RW drivers and captured the WW speed of 35 mph. In comparison with the ambient status, a maximum of 17 dBA louder sound was caused by strips for RW drivers and 20 dBA for WW drivers. Effective values also suggested that WW drivers (70.73 dBA) would receive an increased 5-dBA sound as opposed to RW drivers (65.93 dBA). A *p*-value of 0.02 manifested the significant difference between the average RW and WW sound levels.

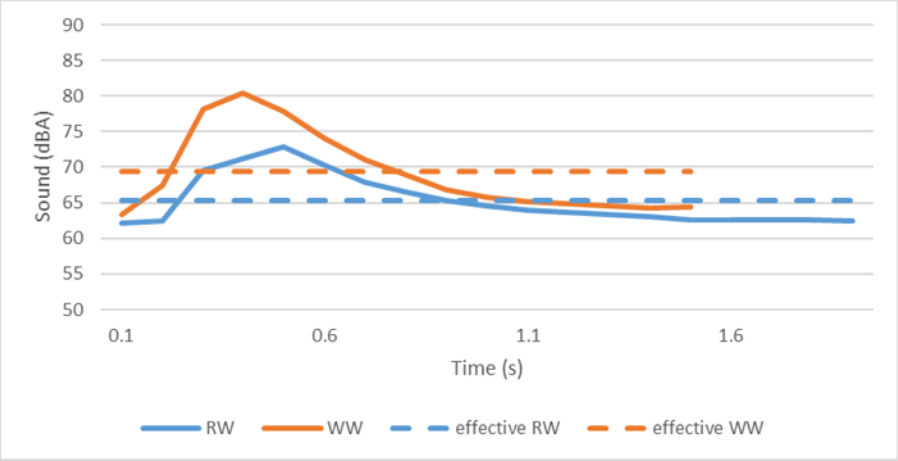

(a)

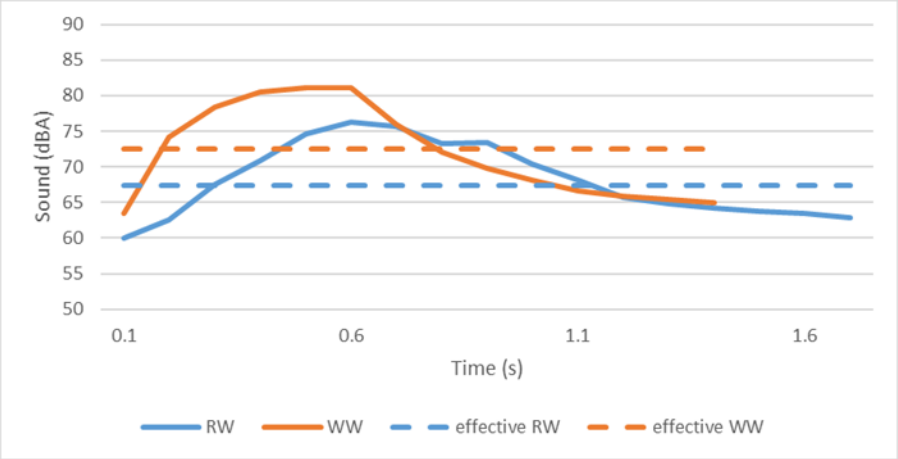

(b)

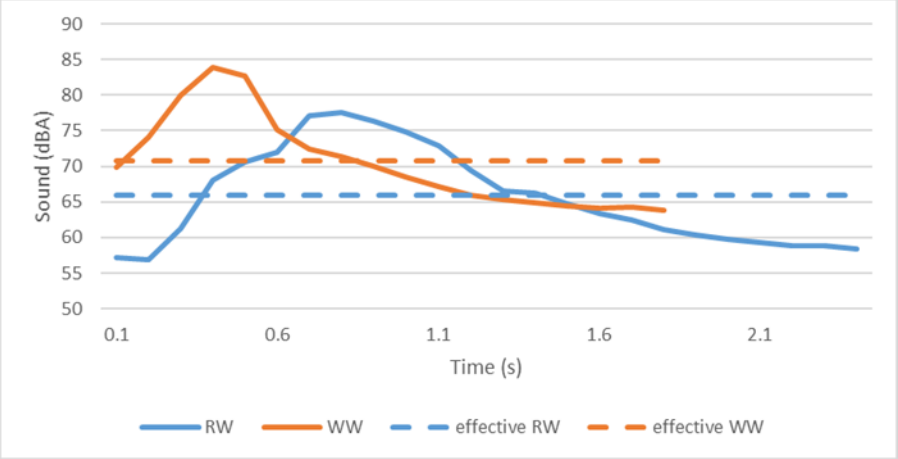

(c)

Figure 6.3 RW and WW sound of Pattern C: (a) 5 ft; (b) 2 ft; (c) 1 ft

6.1.3.3 Pattern D3

Figure 6.4 demonstrates the RW and WW sound levels when a vehicle passes Pattern D3. The RW speed was 10 mph and WW 25 mph. Compared with ambient circumstances, RW drivers were able to obtain a 13 dBA louder sound at most. While WW drivers would perceive 20 dBA more. Additionally, WW drivers can obtain 70.50 dBA sound in effect, which was 13 dBA more than the effective RW sound (57.5 dBA). The *t*-test result showed that the average RW and WW sound levels were significantly different by a *p*-value of 0.00.

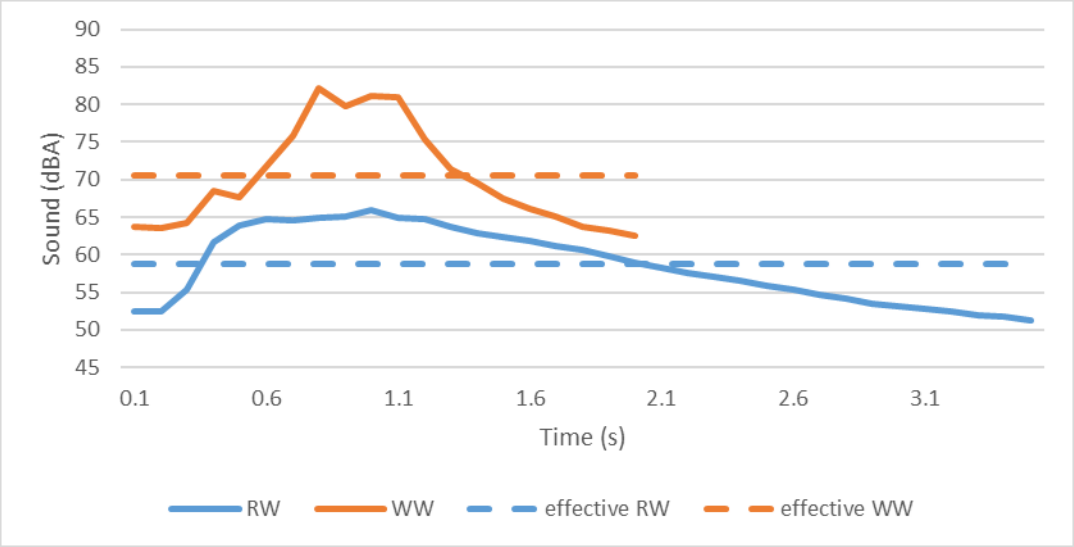

Figure 6.4 RW and WW sound of Pattern D3

6.2 EXTERIOR SOUND

This section inspects the exterior sound caused by the DRS, which is a source of disturbance and has been the cause of complaints from roadside residents. The findings could help to direct the usage of the DRS in consideration of noise disturbances at adjacent properties.

6.2.1 Data Description

As shown in Figure 6.5, a sound-level meter was positioned 25 ft from the center of the travel lane, according to a study on evaluating centerline rumble strip noises (Sexton 2014). The meter was also placed 5 ft above the lane surface, which helped to reduce the effects of ground surfaces on sound propagation (i.e., “ground effects”).

Figure 6.5 Data collection for exterior sound caused by the DRS

6.2.2 Methods

The exterior sound data was collected near the DRS under the ambient status (named “ambient”) and conditions when vehicles were passing the DRS (named “vehicle”). The ambient status was considered as long as no vehicle was on the off-ramp travel lane. For example, it was also counted as ambient status if other vehicles were using the nearby freeway mainline, on-ramp, or crossroad. To eliminate the overlapping sound effects, a total of 100 free-flow vehicles was sampled for each DRS pattern (Pattern E.1 and D3) or every strip group (Pattern C). To evaluate the average exterior sound increment caused by the DRS, the “ambient” data was collected for the same duration of acquiring the “vehicle” data.

6.2.3 Findings

Table 6.1 summarizes the exterior sound levels caused by the DRS. At Exit 208, the ambient condition at Pattern E.1 ranged from 55 to 75 dBA. Because it was close to the freeway mainline, the sound level was 75 dBA at a maximum when mainline vehicles passed by. The sound level was from 68 to 79 dBA when a vehicle passed Pattern E.1. By averaging the sound levels, it was found that Pattern E.1 generated an extra 8.9 dBA sound to the environment.

Pattern C was located on the segment between the off-ramp curve and terminal, which was close to neither the freeway mainlines nor the crossroad. Thus, the maximum ambient sound level was 65 dBA. The reduced spacings of strips led to the increasing sound levels generated by three strip groups. It also resulted in a sound increment. Therefore, the 5-ft-spacing strips generated an additional 3.2 dBA to the surroundings, with 5.1 and 9.7 dBA by the 2 and 1-ft strip groups, respectively.

Pattern D3 was placed at the ramp terminal, so that the ambient sound was a bit louder, compared with Pattern C. However, vehicles typically made complete stops at the stop bar and accelerated onto the crossroad. In this way, the exterior sound level was completely covered by and relied on the engine noise. Therefore, the sound increment caused by Pattern D3 was negligible.

Likewise, results were similar at Exit 284, except for the overall louder sound due to the larger traffic volumes. To summarize, Pattern E.1 can produce 9 dBA extra sound to the environment. Pattern C generated almost 10 dBA additional sound by the 5-ft-spacing strips, 5 dBA by the 2-ft ones, and 3 dBA by the 1-ft ones. The exterior sound impact of Pattern D3 was also negligible.

Table 6.1 Exterior sound levels caused by the DRS

Location	Pattern		Ambient (dBA)	Vehicle (dBA)	Mean Increment (dBA)
Exit 208 I-65, AL	E.1		55-75	68-79	8.9
	C	5-ft	55-65	58-68	3.2
		2-ft		60-70	5.1
		1-ft		65-74	9.7
	D3		55-67	engine noise	Negligible
Exit 284 I-65, AL	E.1		62-77	70-77	8.5
	C	5-ft	60-67	62-70	2.9
		2-ft		66-72	5.6
		1-ft		70-75	9.2
	D3		65-70	engine noise	negligible

6.3 INTERIOR VIBRATIONS

This section investigates the interior vibrations generated by the DRS for the purpose of understanding different vibration profiles perceived by RW and WW drivers.

6.3.1 Data Description

Interior vibration data was also acquired from field driving tests at Exit 208 on I-65, AL. Seven speed categories, i.e., 10, 15, 20, 25, 30, 35, and 40 mph, were tested for both RW and WW directions. The RW vibration data was collected from the deceleration lane to the off-ramp terminal on the closed ramp. The WW data was obtained from driving in the reverse direction. Figure 6.6 displays the sample RW vibration data along the off-ramp at a constant speed of 20 mph. There was a time lag between recording the sound data and triggering the vibration data collection. Hence, noises were caused by vehicle acceleration before 6 s. At 7 s, the vehicle started passing Pattern E.1, so that the first signal was generated. A second signal was created by passing the WW arrow at 15 s. As previously mentioned, the first lane-use WW arrow was not hit. Afterward, the vehicle passed the following WW and lane-use arrows at 27 and 32 s. Then, three signals were produced by Pattern C, followed by a consequential one from the dual WW arrows. Pattern D3 contributed to the last vibration signal.

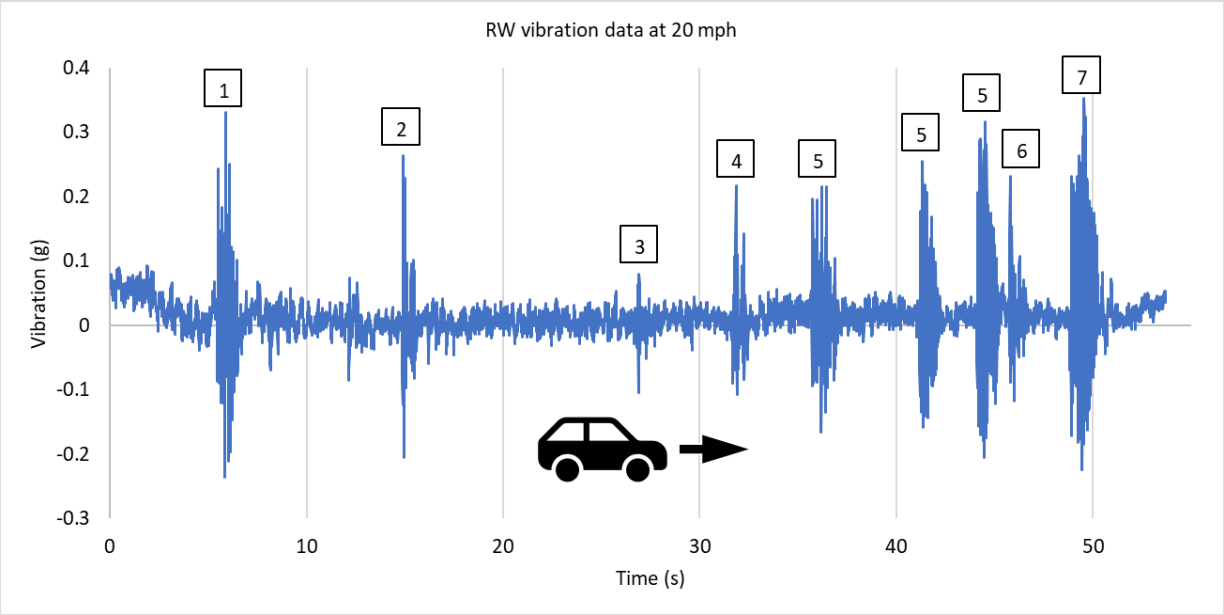

Note: 1 = Pattern E.1; 2 = WW arrow; 3 = WW arrow; 4 = lane-use arrow; 5 = Pattern C; 6 = dual WW arrows; 7 = Pattern D3.

Figure 6.6 Sample RW vibration data along the off-ramp at 20 mph

6.3.2 Methods

As with evaluating dynamic sound levels, RMS amplitudes of vibrations were also employed to present the equivalent constant values, which resulted in the same effect. Due to the different presentations of the sound and vibration data, it was close to zero by averaging the vibrations on the DRS. Thus, it was more meaningful to compare their variances between RW and WW directions. *F*-tests at the significance

level of 0.05 were then used to check whether there was a significant difference in variance between RW and WW vibrations.

In contrast with sound data, vibration required a spectrum analysis because different vibration patterns may be expressed similarly in the time series. Thus, fast Fourier transform (FFT) was employed to measure vibration amplitudes as a function of frequency. FFT converted the original vibration data from the time domain to the representation in the frequency domain. Nonstandard vibrations can be treated as a combination of various vibrations with different frequencies and amplitudes. The *X* axis in the FFT plot stands for frequencies ranging from low to high, while the *Y* axis shows the amplitude associated with each frequency. Equation 1 presents the procedure of dividing a nonstandard vibration signal into a list of standard vibration signals (i.e., sine and cosine signals). In this study, the vibration signals caused by the DRS can be presented as $f(x)$, which equals to the sum of various standard signals with different phases kx (i.e., $1/2\pi$, π, $3/2\pi$…) and the halved offset (a_0):

$$f(x) = \frac{a_0}{2} + \sum_{k=1}^{n} [a_k \cos(kx) + b_k \sin(kx)], \quad (1)$$

where

- $f(x)$ is the original signal;
- a_0 is the offset phase;
- a_k and b_k are the amplitudes of associated standard signals;
- kx is the multiple of $1/2\ \pi$ (e.g., $1/2\pi$, π, $3/2\pi$…).

Unlike the sound data in the presentation of the A-weighted decibel, the raw vibration data contained noises that may reduce the accuracy of the results. Thus, denoising was required before processing the data. Exponential smoothing was applied to filter potential noises caused by self-vibrations (e.g., vibrations from a car engine) during the field driving tests. Equation 2 presents the fundamental of the exponential smoothing:

$$S_t = \alpha y_{t-1} + (1-\alpha) S_{t-1} \quad (0 < \alpha \leq 1;\ t \geq 3), \quad (2)$$

where

- S_t is the smoothed value of time *t*;
- S_{t-1} is the smoothed value of time *t-1*;
- y_{t-1} stands for the original observation of time *t-1*;
- and α is the smoothing factor, which is 0.7 in this study.

In comparison with the simple moving average technique, which is another denoising method, the exponential smoothing places higher weighting on the recent data than on the older ones. Thus, it is more reactive to the latest value changes than the simple moving average, which makes the smoothed data timelier. Figure 6.7 demonstrates comparisons of the sample vibration data in the time domain. Both

smoothing techniques well illustrate the original data. However, the data after the simple moving average smoothing cannot reproduce the details at the inflection points, compared with the one by the exponential smoothing. Figure 6.8 manifests the data in the frequency domain. The data denoised by the simple moving average technique completely eliminated the higher frequencies over 25 Hz, which contradicts the original data. Nevertheless, the exponential smoothing method sufficiently reconstructed this feature without distorting the rest data. Therefore, data after the exponential smoothing was able to filter noises and well represented the original data.

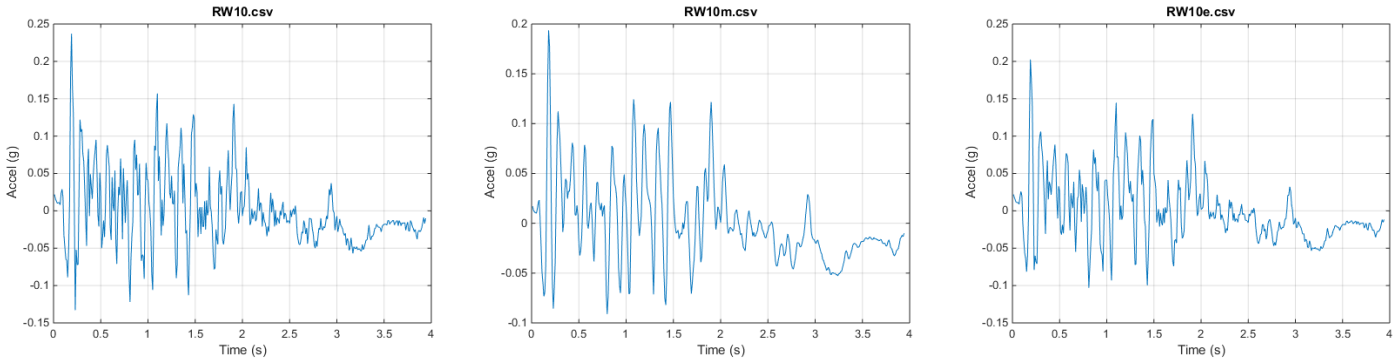

(a) original (b) simple moving average (c) exponential smoothing

Figure 6.7 Sample vibration data in the time domain (RW at 10 mph)

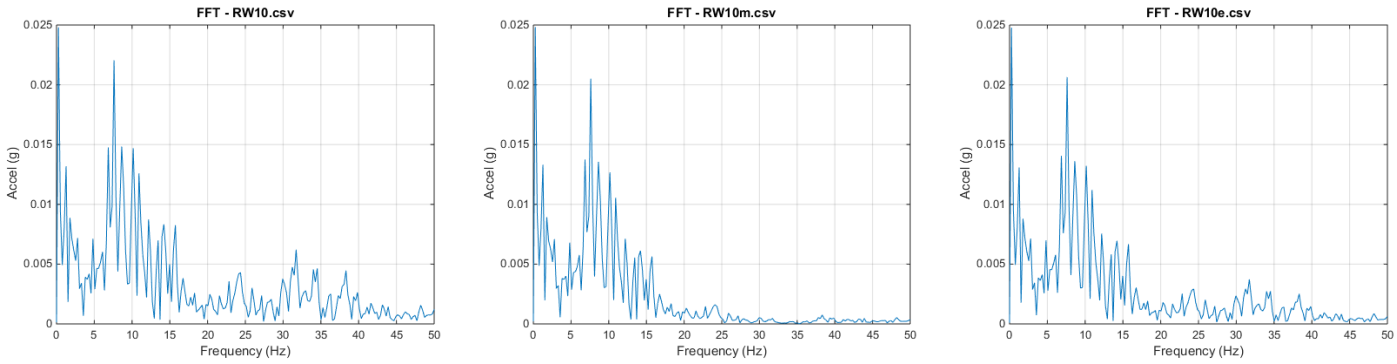

(a) original (b) simple moving average (c) exponential smoothing

Figure 6.8 Sample vibration data in the frequency domain (RW at 10 mph)

In this study, vertical acceleration values from the vibration data were not normally distributed. Compared with the other tests such as the paired *t*-test, the two-sample Kolmogorov–Smirnov (K-S) test did not specify what that common distribution was. Namely, these two samples can be either normal or not normal distributions. Accordingly, two-sample K-S tests were utilized to statistically check whether the

original and smoothed data came from the same distribution. Equations (3) and (4) illustrate the K-S statistic:

$$D_{n,m} = sup_x \left| F_{1,n}(x) - F_{2,m}(x) \right|, \tag{3}$$

where

- $F_{1,n}$ and $F_{2,m}$ are the empirical distribution functions of the two samples;
- sup_x is the supremum of the set of distances;
- n and m are the sizes of two samples.

The null hypothesis is rejected at significance level α if

$$D_{n,m} > c(\alpha) \sqrt{\frac{n+m}{nm}}, \tag{4}$$

where

- $c(\alpha) = \sqrt{-\frac{\ln \alpha}{2}}$ and $c(\alpha)$ equals to 1.224 when α is 0.05;
- n and m are the sizes of two samples.

For all seven speed categories, results from two-sample K-S tests at the significance level of 0.05 indicated that no significant difference existed between the original data and the denoised data after the exponential smoothing, regarding that *p*-values exceeded 0.05.

6.3.3 Findings

6.3.3.1 Pattern E.1

According to the NC-350 speed data, the average RW speed was 30 mph and WW 35 mph when vehicles passed Pattern E.1. The effective amplitude of WW vibrations was 0.106 *g*, which was 0.027 *g* higher than the RW direction (0.079 *g*). The *p*-value from the *f*-test at the significance level of 0.05 was 0.00, which showed that the variances of RW and WW vibrations were significantly different. Figure 6.9 presents the RW and WW spectrums of Pattern E.1. The RW vibrations had peaks of 2 and 13 Hz, while the WW direction had peak vibrations at 2, 16, 32, and 47 Hz. In short, WW drivers can perceive more severe vibrations of higher amplitudes and frequencies.

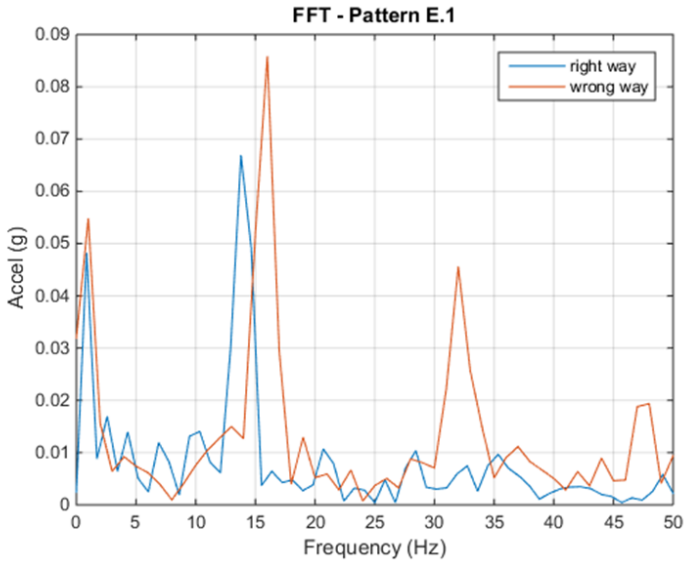

Figure 6.9 RW and WW spectrums of Pattern E.1

6.3.3.2 Pattern C

WW vehicles were recorded to have a constant speed of 35 mph while passing the segment where Pattern C was installed. However, RW drivers had decreased average speeds of 30, 25, and 20 mph at the strips of 5-ft, 2-ft, and 1-ft spacings, respectively.

Consequently, RW drivers were able to perceive vibrations equivalent to 0.041 *g* and WW 0.054 *g* when passing the strips of 5-ft spacings. The RW and WW vibrations were significantly different in variances according to the *p*-value of 0.00 from the *f*-test. As shown in Figure 6.10-a, vibrations for RW drivers had peaks of 3, 13, 21, and 35 Hz, while WW vibrations saw peaks of 2, 5, 13, 33, and 37 Hz. Visually, the peaks from RW and WW vibrations were alike due to the close speeds. However, WW vibration peaks had higher amplitudes.

The effective WW vibration was 0.117 *g*, which was 0.04 *g* more than the RW one (0.077 *g*) by the 2-ft-spacing strips. The *f*-test result also showed the significant difference between the variances of RW and WW vibrations. The spectrums of RW and WW vibrations produced by these strips are presented in Figure 6.10-b. RW vibrations had peaks of 13 and 35 Hz, while peaks occurred at 17 and 35 Hz in the WW direction. The amplitude of the 13 Hz RW peak was almost 0.02 *g* higher than the 17 Hz WW peak, while amplitudes of the 35 Hz WW peak were more than twice as high as the RW one.

For the 1-ft-spacing strips, RW drivers can get 0.098 *g* vibrations and WW 0.121 *g* in effect. A *p*-value of 0.02 from the *f*-test revealed a significant difference between RW and WW vibrations in variances. Figure 6.10-c exposed the spectrums of RW and WW vibrations. The RW vibration only had a peak of 14 Hz, while WW had two of 17 and 36 Hz.

To sum up, WW drivers can also perceive more severe vibrations by Pattern C regarding the larger amplitudes and higher frequencies.

(a)

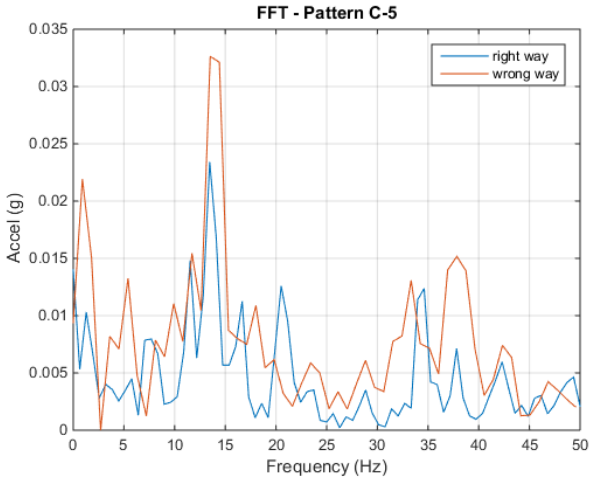

(b)

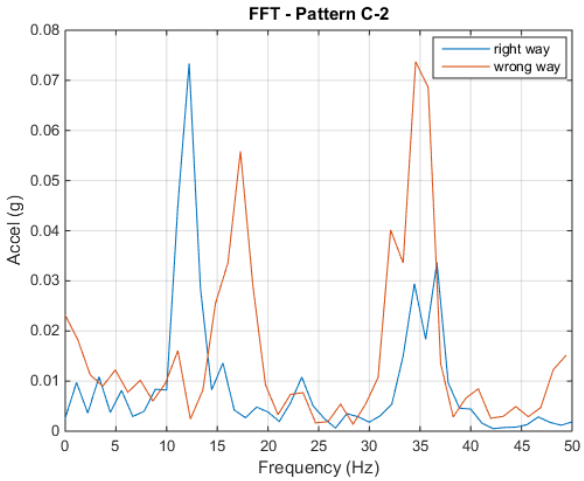

(c)

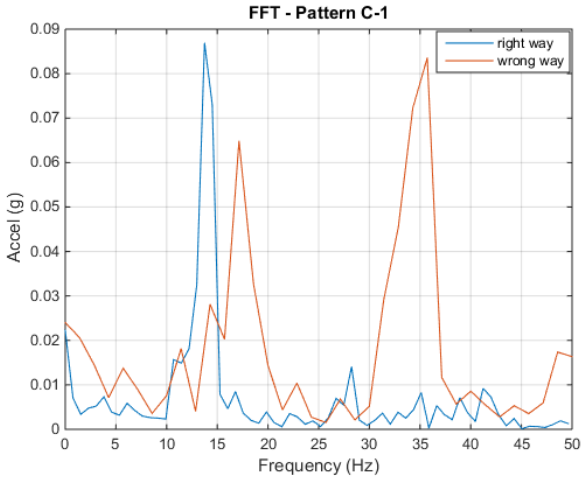

Figure 6.10 RW and WW spectrums of Pattern C: (a) 5 ft; (b) 2 ft; (c) 1 ft

6.3.3.3 Pattern D3

RW drivers further slowed down until making a complete stop at the stop bar. Thus, the average RW speed was about 10 mph at Pattern D3. In contrast, WW drivers considered the off-ramp terminal as the on-ramp entrance, which resulted in their entering speed being captured around 25 mph. Consequently, RW drivers can perceive vibrations equivalent to 0.044 *g* and WW 0.089 *g*. As shown in Figure 6.11, vibrations for RW drivers had peaks of 1 and 7 Hz, while WW drivers obtained peaks of 1, 12, and 35 Hz in vibration. Briefly, WW drivers would have twice as many RW vibrations in effects as well as peaks of higher frequencies.

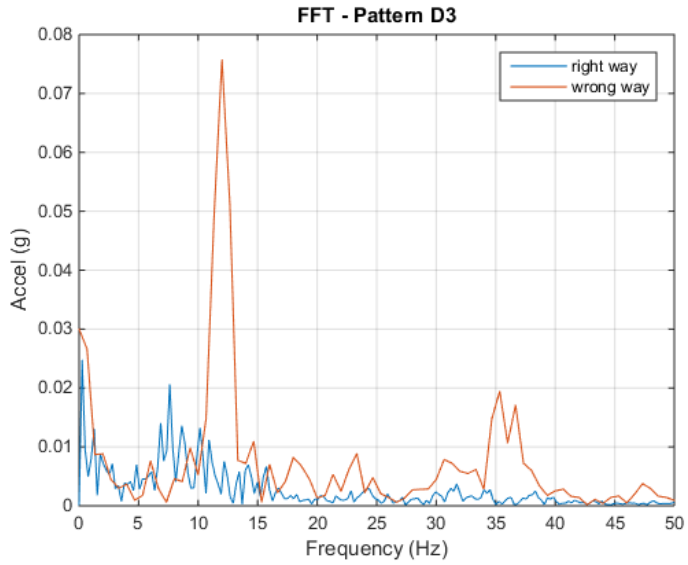

Figure 6.11 RW and WW spectrums of Pattern D3

6.4 CONSISTENCY WITH PHASE I RESULTS

To conclude, the above results are in line with those of the phase I project. Both RW and WW drivers would perceive sufficient sound and vibrations, compared with ambient conditions. WW drivers can hear a louder average sound and have more severe vibrations in terms of larger amplitudes and higher frequencies.

However, the results were not exactly the same in numbers because of the following potential reasons.

- Vehicle speeds were different. The phase I project used the RW on-ramp speeds as the WW off-ramp speeds in the assumption that WW drivers considered off-ramps as on-ramps. The speeds were collected by radar guns. In this project, the real RW and WW drivers' speeds were captured by the magnetic sensors and video cameras.
- Geometrics of test sites were dissimilar. The terrain and horizontal alignments of off-ramps in the field were different from the test site in the phase I project.

- Installation methods were dissimilar. Removeable rumble strips were placed by students for testing in the phase I project, while DRS patterns were installed by a professional striping company in this project.
- Test vehicles had a slight difference. A 2016 Nissan Altima was used in the phase I project, while a 2018 Nissan Maxima was employed in this project.

CHAPTER 7: OTHER FINDINGS

7.1 REDUCING LEFT-TURN CONFUSION

The video camera captured that the new channelization island can confuse left-turn drivers at the off-ramp terminal at Exit 208 on I-65, AL. As shown in Figure 7.1, an SUV driver entered a right-turn lane to turn left. The driver may mistakenly consider the new island as a right-in/right-out channelization design. Thus, there was concern that some drivers did not fully understand the purpose of the channelized island at the off-ramp terminal.

A hundred free-flow vehicles were sampled from videos that were recorded during random nonpeak hours on each weekend. Videos taken during daytime or nighttime were considered. Table 7.1 summarizes the changes in left-turn confusion (defined as left-turn maneuvers from the right-turn lane). Nearly 23% to 28% of left-turn vehicles were confused by the new channelization island before installation of Pattern D3. After implementation of Pattern D3, the percentage was roughly reduced by half. This indicated that the arrow shape of Pattern D3 can help to guide left-turning vehicles to stay in the correct lane.

Table 7.1 Change in the number of left-turn confusions

Time	Left-Turn Vehicles	Right-Turn Vehicles	Number of Left-Turn Confusion	Left-Turn Confusion%	Note
W0	35	65	8	23%	Pattern D3 wasn't installed
W1	40	60	11	28%	
W2	37	63	10	27%	
W3	33	67	4	12%	Pattern D3 was installed
W4	36	64	4	11%	

(a)

(b)

(c)

Figure 7.1 Example of left-turn confusion captured at Exit 208 on I-65, AL

7.2 UTILIZATION OF THE CENTER GAPS

Center gaps were tested at the removable TRS in a previous study (Meyer 2006). Considering the complaints from motorcyclists on TRS, the 2-ft gap in Patterns E.1 and C allowed motorcycles to pass the strips without hitting them. As shown in Figure 7.2, a motorcycle is utilizing the center gap to pass Pattern C. Additionally, no complaints were heard from road users thus far based on the feedback from the division offices.

Other than serving motorcycles, the center gap has the potential to help emergency vehicles passing DRS patterns without receiving additional sound and vibrations.

Figure 7.2 A motorcycle using the center gaps to pass the DRS Pattern C

CHAPTER 8: GUIDELINES FOR DRS IMPLEMENTATION

The DRS is a relatively new traffic control device for drivers to distinguish between the on and off-ramps. Currently, there is no standard or guideline for implementing this device. This study found that DRS has advantages in alerting WW drivers and reducing WWD incidents by providing WW drivers with elevated interior sound and vibrations. Given the reduction in frequencies and travel distances of WWD incidents, DRS proved to be a low-cost countermeasure to deter WW freeway entries. The following includes recommended guidelines from DRS implementation based on the results of this study.

8.1 RECOMMENDATIONS FOR IMPLEMENTING PATTERN E.1

Pattern E.1 is recommended to be installed ahead of the advisory ramp speed sign in advance of the sharp horizontal ramp curve. The distance between Pattern E.1 and the advisory ramp speed sign shall be considered based on the sight distance study and engineering judgment. For example, 30 ft was employed in this study that can provide a good sight distance for drivers to see the advisory ramp speed limit signs and the horizontal curve when passing the DRS.

The yellow and white strip colors are in conformance with MUTCD Section 3A.05. The use of yellow strips should be permitted to Pattern E.1. Based on the results of this study, Pattern E.1 with one-side yellow strips were more effective in reducing the speed SDs. Thus, it is recommended to have yellow strips of Pattern E.1 on the left side of the travel lane.

8.2 RECOMMENDATIONS FOR IMPLEMENTING PATTERN C

Pattern C is recommended to be installed at the long straight off-ramp segment between the ramp gore area and terminal. It can alert RW drivers of a need to slow down or stop or to other upcoming changes. It will also alert WW drivers via sound and vibrations to pay attention to WW signs on the roadside. Therefore, it is recommended to have WW signs placed ahead of Pattern C. Lower-mounted WW signs could be an option per MUTCD Section 2B.41.

Furthermore, the placement of Pattern C should not be overlapping with other pavement markings. Base on this study, it can be placed between two sets of WW arrows.

8.3 RECOMMENDATIONS FOR IMPLEMENTING PATTERN D3

It is recommended to deploy Pattern D3 at the off-ramp terminals. This pattern is effective in terms of reducing WW entries by alerting WW drivers with louder sound and more severe vibrations and a clear visual cue. It can work in collaboration with DNE signs. An optional lower mounting height for DNE signs can also be considered, according to MUTCD Section 2B.41. The strips should not be attached to other pavement markings such as stop bars or yield lines. In this study, the 1-ft strip of this pattern was installed 1 ft behind the stop bars and the yield line. As described in MUTCD Section 3B.13, retroreflective markers may be used to supplement wide lateral line markings (e.g., stop bar) and wrong-way arrows. Similarly, red retroreflective paint can be applied onto the WW side of Pattern D3, as shown in Figure 8.1.

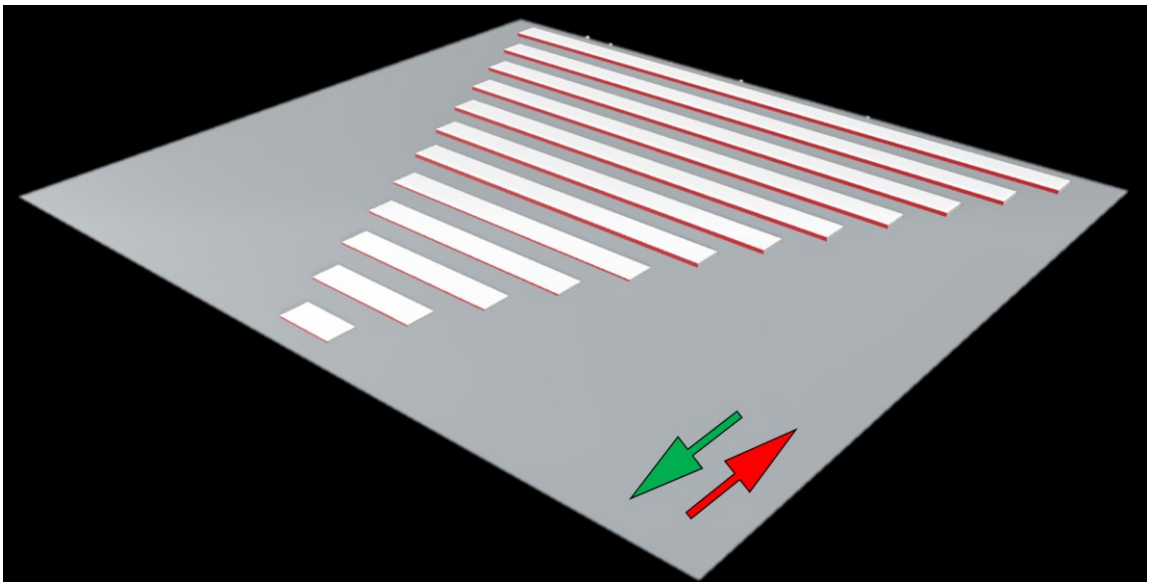

Note: Green arrow = RW direction; red arrow = WW direction

Figure 8.1 Pattern D3 with red retroreflective paint

CHAPTER 9: CONCLUSIONS AND DISCUSSIONS

WW Drivers on freeways pose a serious risk to the safety of other RW motorists. This project implemented three DRS patterns (D3, C, and E.1) at two exit ramps in Alabama. The results showed that these DRSs patterns can not only reduce WWD incident frequencies but also RW traffic speed and speed SDs. The elevated sound and vibrations generated by these DRS can alert WW drivers and improve the effectiveness of other standard low-cost WW-related traffic control devices as shown by the reduced driving distances per WWD incident after implementing the DRS.

Pattern D3 is similar to the advance warning markings for speed humps, which has a triangle appearance, as the length of the strip gradually increases from 1 to 12 ft. The thickness of the strip for Pattern D3 ranges from 0.25 to 0.5 (0.25 in. for strips from 1 to 5 ft and 0.5 in. for strips from 6 to 12 ft). Pattern C is similar to the traditional TRS but has different spacings. Three groups of strips with spacings of 1, 2, and 5 ft, respectively, were placed apart with 100- and 50-ft spacing. All of the strips had the same thickness of 0.25 in. Pattern E.1 had double strips on the driver side in the WW direction to ensure that WW drivers received elevated sound and vibrations. The width of the strips was 6 in., and the thickness was about 0.25 in.

Southbound off-ramps at Exits 208 and 284 on I-65 in Alabama were selected for implementation based on model prediction results and number of recurring WWD incidents observed in the field. Speed and video data were collected using cameras and magnetic sensors. Field driving tests were conducted to collect sound and vibration data at various speed categories for both RW and WW drivers. Time-series were applied to analyze sound, while spectrum analysis was used in analyzing vibrations. For these two off-ramps, Pattern D3, which was shaped like an arrow to indicate the right direction, was installed at the off-ramp terminal near the stop bar/yield lines. Pattern C was implemented at the segment between the terminal and the ramp curve. WW drivers were alerted by the increasing sound and vibrations from three strip groups, so that they could pay attention to the standard WW-related signs and pavement arrows. Pattern E.1 was installed on the tangent part before the ramp curve, which can alert a WW driver before entering the freeway mainline and reduce aggressive driving speeds for vehicles exiting the freeway before entering the oncoming curve.

Before and after studies were conducted to evaluate the effectiveness of these patterns based on WWD incidents, drivers' speeds, and drivers' behavior changes. Both numbers of WWD incidents and WWD distances significantly dropped toward zero after implementing the DRS patterns. Though a critical event was rare (e.g., WW vehicle drove all the way to the freeway), one WW vehicle was stopped on the ramp curve by Pattern E.1. Further evaluation will be required to test its effectiveness in countering WW incidents. After deploying Pattern C, WWD frequencies and average WWD traveling distances were reduced by almost by half. According to changes in time frames when most WW incidents occurred, Pattern C significantly reduced the number of WW incidents around afternoon peaks. Pattern D3 was considered the most effective, as it prevented vehicles from entering the off-ramps from crossroads. After implementing Pattern D3, WWD frequencies and distances were reduced to near zero. To conclude, no WWD vehicles traveled farther than the latest implemented DRS pattern in this study.

The before and after speed analysis suggested that Pattern E.1 can reduce average speed by 2.3 to 6.5 mph depending on the difference between the speed limit and operational speeds. For the location at Exit 208, when the operational average speed was about 10 mph over the speed limit, Pattern E.1 could also reduce speed SD by 2.5 mph. For the location at Exit 284, where the operational speed is close to the speed limit, adding Pattern E.1 accurately increased the speed SD by 1.4 mph. The results from both locations showed that the average speeds and speed SDs decreased by 2.7 and 0.5 mph, respectively, due to the implementation of Pattern C. Pattern D3 helped lower the speed SDs by 0.5 and 1.0 mph at the stopped and yield-controlled terminals, respectively. The trends of changes in speed SDs indicated that two to three days were needed for drivers to become familiar with these new traffic control devices. Speed comparisons between daytime and nighttime illustrated that Pattern C could reduce the speed SD 5% more during the nighttime than the daytime.

While all the DRS patterns generated enough interior sound to alert drivers, WW drivers could perceive louder sound from all three patterns (12 dBA by D3, 5 dBA by Patterns C and E.1). The exterior sound increasements caused by the DRS suggested that Pattern C could produce a maximum of 10 dBA additional noises and Pattern E.1 could produce 9 dBA. However, extra noises caused by Pattern D3 were negligible. After denoising the vibration data, all of the patterns generated higher frequencies of vibrations for WW drivers. Pattern D3 produced 0.045 *g* more vibrations for WW drivers, while Pattern C generated at least 0.011 *g* more and Pattern E.1 0.027 *g* more.

In addition to the above findings, Pattern D3 showed that it can provide additional guidance for RW left-turn drivers. Confused left-turns at the channelized island were reduced by nearly 50% after installing Pattern D3. Moreover, the center gaps at Patterns C and E.1 provided convenience to motorcyclists.

REFERENCES

Atiquzzaman, M., & H. Zhou. (2018). Modeling the risk of wrong-way driving entry at the exit ramp terminals of full diamond interchanges. *Transportation Research Record*, *2762(17), 35–47*.

Cain, B., D. Riley, & P.-J. McKelvey. (2018). Summary and Initial Findings of the Arizona Department of Transportation Wrong-way Driver Pilot System. The Intelligent Transportation Society of America Annual Meeting. Detroit, MI.

Cooner, S. A., A. S. Cothron, & S. Ranft. (2004). *Countermeasures for Wrong-Way Movement on Freeways: Overview of Project Activities and Findings (*FHWA/TX-04/4128-1). Austin, TX: Texas Department of Transportation.

Garber, N. J., & R. Gadiraju. (1989). Factors affecting speed variance and its influence on accidents. *Transportation Research Record*, *1213,* 64-71.

Lin, P.S., C. Chen, & S. Ozkul. (2018). Testing and evaluation of freeway wrong-way detection systems. Florida Department of Transportation. Retrieved from https://ftp.fdot.gov/file/d/FTP/FDOT%20LTS/CO/research/Completed_Proj/Summary_TE/FDOT-BDV25-977-40-rpt.pdf. Accessed 04/23/2019

Meyer, E. (2006). *Guidelines for the application of removable rumble strips* (No. K-TRAN: KU-02-3). Lawrence, KS: Kansas. Dept. of Transportation.

Pour-Rouholamin, M., H. Zhou, J. Shaw, & P. Tobias. (2015). "Current practices of safety countermeasures for wrong-way driving crashes." *TRB 94th Annual Meeting Compendium of Papers*. DOI: 10.13140/2.1.1050.6564.

Reference. (2019). "What Is the average length of a car?" *Reference*, IAC Publishing, Retrieved from www.reference.com/vehicles/average-length-car-2e853812726d079d

Rose, D. (2011). Wrong-way vehicular detection proof of concept. Paper presented at the 18th World Congress on Intelligent Transport Systems. Orlando, FL.

Sexton, T. V. (2014). *Evaluation of current centerline rumble strip design (s) to reduce roadside noise and promote safety* (No. WA-RD 835.1). Olympia, WA: Washington Dept. of Transportation.

TransCore. (2008). *White paper: Wrong-way detection system procurement.* Houston, Texas: Harris County Toll Authority.

Zhou, H., C.Xue, L. Yang, & A. Luo. (2018). Directional rumble strips for reducing wrong-way-driving freeway entries (CTS 18-04). Minneapolis, MN: Roadway Safety Institute, University of Minnesota.

Zhou, H., & M. P. Rouholamin. (2014a). Guidelines for reducing wrong-way crashes on freeways (FHWA-ICT-14-010). Urbana, IL: Illinois Center for Transportation/Illinois Department of Transportation.

Zhou, H., & P. P. Rouholamin. (2014b). Proceedings of the 2013 National Wrong-Way Driving Summit. *Illinois Center for Transportation Series No. 14-009*. Urbana, IL: Illinois Center for Transportation/Illinois Department of Transportation.

Zhou, H., & M. Atiquzzaman. (2019). Logistic regression models to predict wrong-way driving risk at freeway off-ramp terminals. Alabama Department of Transportation. Retrieved from http://eng.auburn.edu/files/centers/hrc/aldot-wwd-predictive.pdf

APPENDIX A

SUMMARY OF WW INCIDENTS

Table A.1 WW incidents during W0 weekend at Exit 208 on I-65, AL

Exit 208	Speed from Sensors (mph)				Distance traveled (ft)	Note	Classification	Potential Countermeasure
	96/ 97	98	99	100				
2018/11/2 18:56	23	11	-	-	55	just passed dual large WW arrows	pickup truck (with trailer)	dual large WW arrows
2018/11/3 4:09	24	-	-	-	50	in front of dual large WW arrows	pickup truck	dual large WW arrows
2018/11/3 22:38	25	-	-	-	50	in front of dual large WW arrows	SUV	dual large WW arrows
2018/11/3 22:44	23	35	-	-	270	around concrete barrier	pickup truck	single small WW arrow
2018/11/4 7:03	26	10	-	-	55	just passed dual large WW arrows	SUV	dual large WW arrows
2018/11/4 8:25	25	33	-	-	240	before concrete barrier	RV	off-ramp traffic
2018/11/4 19:27	25	-	-	-	35	just passed channelized island	semitrailer truck	dual large WW arrows
2018/11/5 5:19	27	36	30	-	650	middle of ramp curve	passenger car	on-ramp traffic

Table A.2 WW incidents during W0 weekend at Exit 284 on I-65, AL

Exit 284	Speed from Sensors (mph)				Distance Traveled (ft)	Note	Classification	Potential Countermeasure
	101	102	103	104				
2018/11/2 19:00	22	-	-	-	15	just passed stop bar	passenger car	DNE sign
2018/11/2 19:23	21	25	29	33	800	all the way to the freeway	passenger car	N/A
2018/11/3 1:08	-	-	-	-	-	hesitated before yield line	pickup truck	DNE sign
2018/11/3 5:28	23	-	-	-	55	in front of WW arrow	passenger car	WW sign; dual WW arrows
2018/11/3 11:58	32	-	-	-	65	in front of WW arrow	pickup truck	WW sign; dual WW arrows
2018/11/3 15:41	-	-	-	-	40	hesitated in front of WW arrow	SUV	WW sign; dual WW arrows
2018/11/4 4:21	-	-	-	-	-	hesitated before yield line	pickup truck	DNE sign
2018/11/4 19:14	-	-	-	-	-	hesitated before stop bar	pickup truck	Divided roadway sign
2018/11/4 20:10	22	-	-	-	30	just passed stop bar	passenger car	Divided roadway sign
2018/11/5 2:01	27	-	-	-	100	at WW arrow	passenger car	WW sign; dual WW arrows
2018/11/5 13:30	25	-	-	-	15	just passed channelized island	pickup truck	WW sign; dual WW arrows

Table A.3 WW incidents during W1 weekend at Exit 208 on I-65, AL

Exit 208	Speed from Sensors (mph)				Distance Traveled (ft)	Note	Classification	Potential Countermeasure
	96/97	98	99	100				
2018/12/14 10:09	23	10	-	-	50	in front of dual large WW arrows	passenger car	dual large WW arrows
2018/12/14 13:23	26	33	29	-	650	middle of ramp curve	semitrailer truck	Pattern E.1

Table A.4 WW incidents during W1 weekend at Exit 284 on I-65, AL

Exit 284	Speed from Sensors (mph)				Distance Traveled (ft)	Note		Classification	Potential Countermeasure
	101	102	103	104					
2018/12/14 17:14	23	-	-	-	65	in front of dual WW arrows	group of 3	passenger car	off-ramp traffic
2018/12/14 17:14	23	-	-	-	55	in front of dual WW arrows		pickup truck	off-ramp traffic
2018/12/14 17:14	20	-	-	-	15	just passed channelized island		passenger car	off-ramp traffic
2018/12/14 18:51	20	16	-	-	205	at 2nd WW sign		passenger car	WW sign
2018/12/14 20:31	20	-	-	-	15	just passed channelized island	group of 2	passenger car	WW sign; dual WW arrows
2018/12/14 20:31	15	-	-	-	10	just passed channelized island		SUV	WW sign; dual WW arrows
2018/12/14 21:15	-	-	-	-	-	hesitated before stop bar		pickup truck	WW sign; dual WW arrows
2018/12/15 15:04	15	-	-	-	15	just passed channelized island		SUV	DNE sign
2018/12/15 17:34	25	-	-	-	15	just passed stop bar		passenger car	WW sign; dual WW arrows
2018/12/15 17:35	24	-	-	-	55	in front of dual WW arrows		van	WW sign; dual WW arrows
2018/12/15 18:21	26	-	-	-	20	just passed channelized island		pickup truck	DNE sign
2018/12/15 19:12	-	-	-	-	-	hesitated before stop bar		pickup truck	WW sign; dual WW arrows
2018/12/16 15:23	23	-	-	-	15	just passed channelized island		pickup truck	DNE sign

2018/12/16 18:16	27	26	-	-	155	middle of WW signs	passenger car	WW sign; dual WW arrows

Table A.5 WW incidents during W2 weekend at Exit 208 on I-65, AL

Exit 208	Speed from Sensors (mph)				Distance Traveled (ft)	Note	Classification	Potential Countermeasure
	96/97	98	99	100				
2018/12/21 11:42	23	15	-	-	95	before 2nd set of Pattern C	passenger car	Pattern C; WW sign
2018/12/22 23:10	17	-	-	-	35	just passed channelized island	semitrailer truck	DNE sign
2018/12/23 11:26	24	-	-	-	50	in front of dual large WW arrows	SUV	dual large WW arrows
2018/12/24 6:44	25	-	-	-	50	in front of dual large WW arrows	passenger car	dual large WW arrows
2018/12/24 8:23	20	26	-	-	110	just passed 2nd set of Pattern C	semitrailer truck	Pattern C; WW sign

Table A.6 WW incidents during W2 weekend at Exit 284 on I-65, AL

Exit 284	Speed from Sensors (mph)				Distance Traveled (ft)	Note	Classification	Potential Countermeasure
	101	102	103	104				
2018/12/21 12:09	15	-	-	-	10	just passed yield markings	minivan	DNE sign
2018/12/21 20:06	19	22	-	-	130	just passed 1st set of Pattern C	SUV	Pattern C; WW sign
2018/12/22 13:32	14	-	-	-	10	just passed yield markings	pickup truck	off-ramp traffic
2018/12/22 21:32	18	25	-	-	170	at 2nd set of Pattern C	passenger car	Pattern C; WW sign; off-ramp traffic
2018/12/22 22:55	21	32	23	-	280	at 3nd set of Pattern C	passenger car	Pattern C; off-ramp traffic
2018/12/22 22:57	15	-	-	-	10	just passed yield markings	passenger car (police)	Divided roadway sign
2018/12/23 15:50	-	-	-	-	-	hesitated at the entrance	passenger car	Divided roadway sign

Table A.7 WW incidents during W3 weekend at Exit 208 on I-65, AL

Exit 208	Speed from Sensors (mph)				Distance Traveled (ft)	Note	Classification	Potential Countermeasure
	96/97	98	99	100				
2019/1/13 2:48	21	-	-	-	13	at Pattern D	SUV	Pattern D; DNE sign; off-ramp traffic

Table A.8 WW incidents during W3 weekend at Exit 284 on I-65, AL

Exit 284	Speed from Sensors (mph)				Distance Traveled (ft)	Note	Classification	Potential Countermeasure
	101	102	103	104				
2019/1/13 21:56	25	-	-	-	30	just passed Pattern D	passenger car	Pattern D; WW sign

APPENDIX B

SPEED DISTRIBUTIONS AND CHARACTERISTICS

Speed Distribution

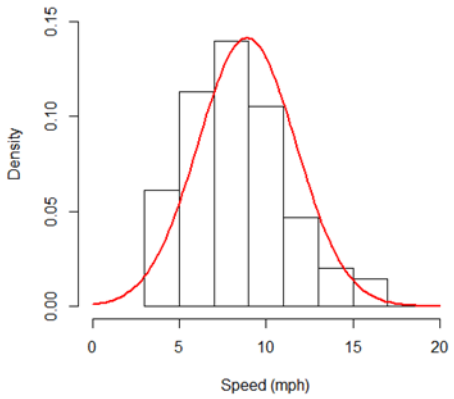

(a) W0

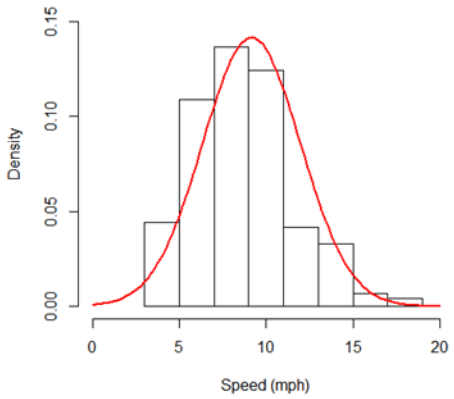

(b) W1

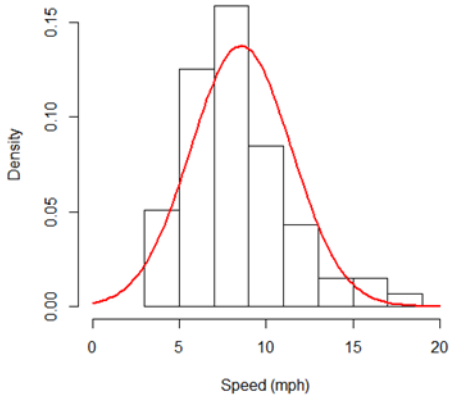

(c) W2

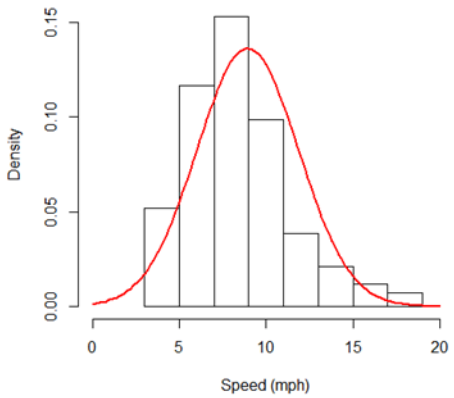

(d) W3

Note: bar - observed distribution; curve - fitted normal distribution

Figure B.1 Speed Distributions at sensor #96

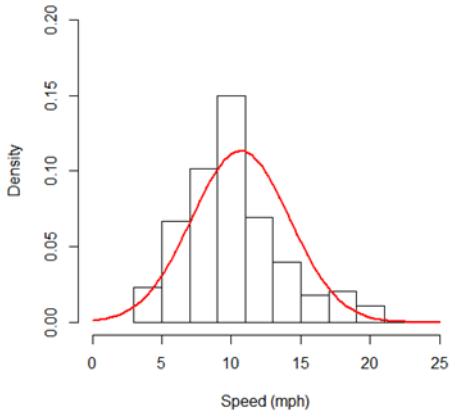

(a) W0

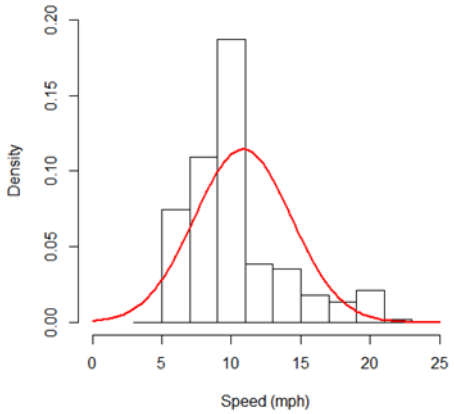

(b) W1

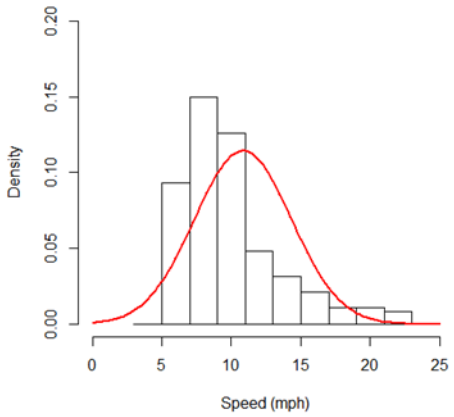

(c) W2

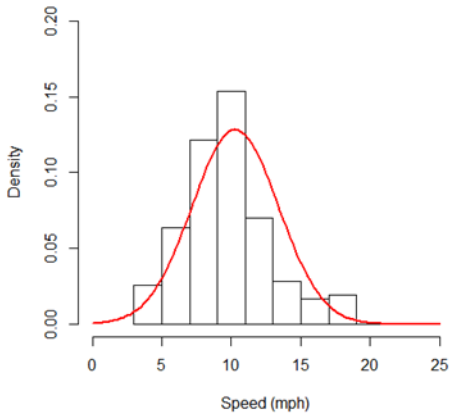

(d) W3

Note: bar - observed distribution; curve - fitted normal distribution

Figure B.2 Speed Distributions at sensor #97

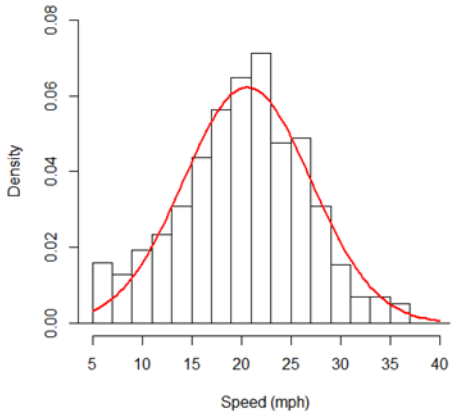

(a) W0

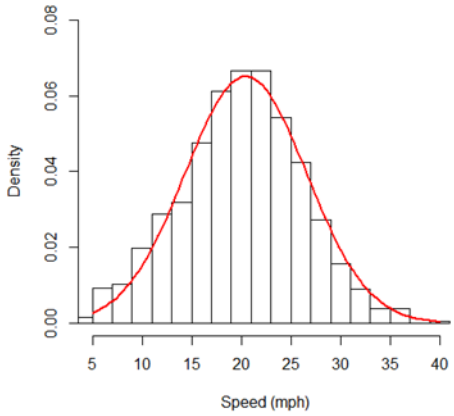

(b) W1

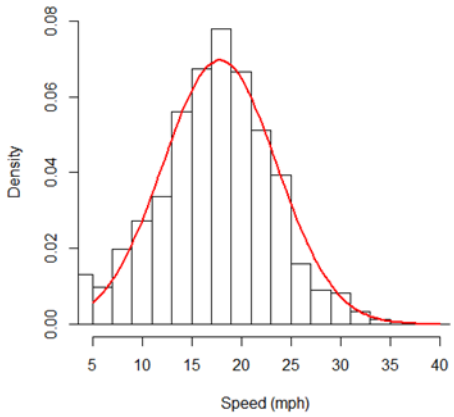

(c) W2

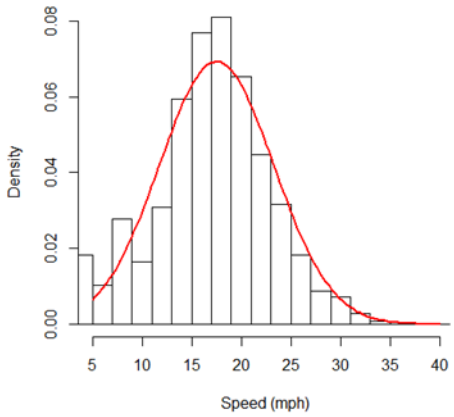

(d) W3

Note: bar - observed distribution; curve - fitted normal distribution

Figure B.3 Speed Distributions at sensor #98

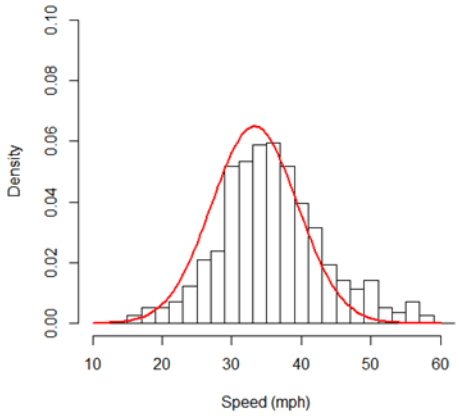

(a) W0

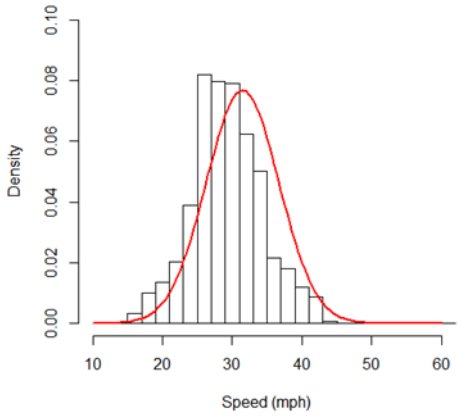

(b) W1

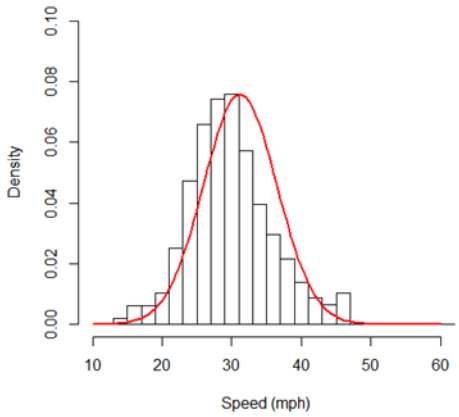

(c) W2

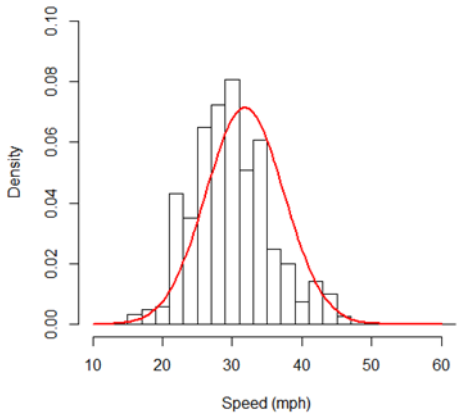

(d) W3

Note: bar - observed distribution; curve - fitted normal distribution

Figure B.4 Speed Distributions at sensor #99

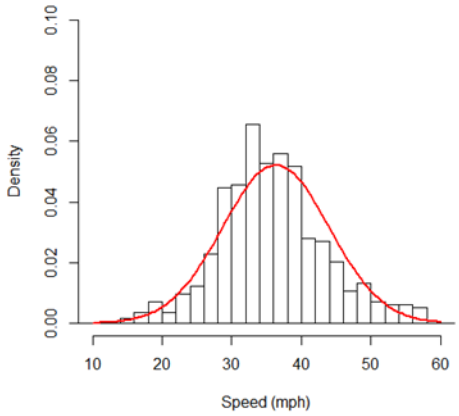

(a) W0

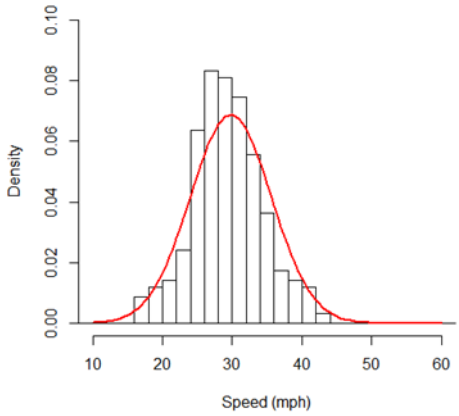

(b) W1

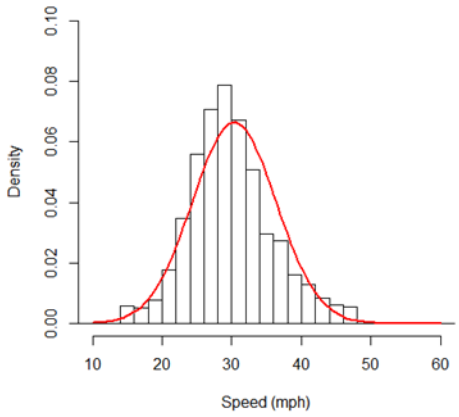

(c) W2

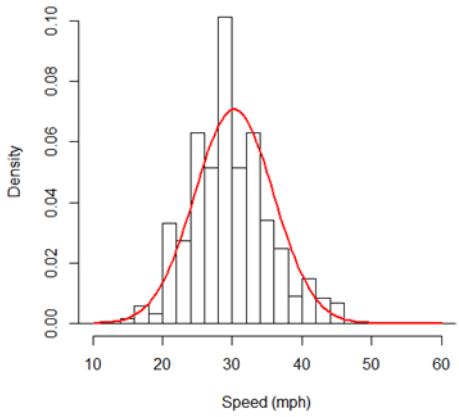

(d) W3

Note: bar - observed distribution; curve - fitted normal distribution

Figure B.5 Speed Distributions at sensor #100

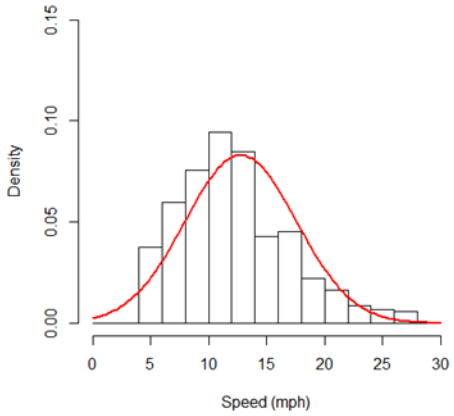

(a) W0

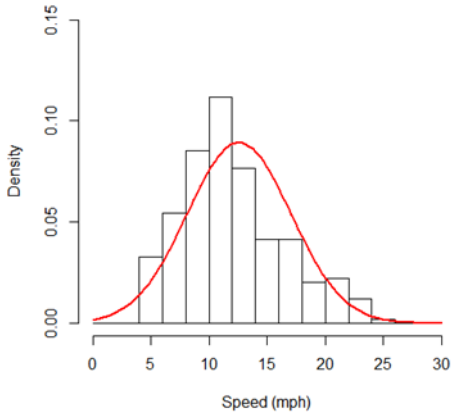

(b) W1

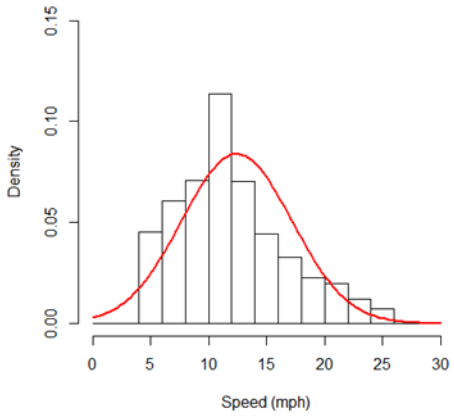

(c) W2

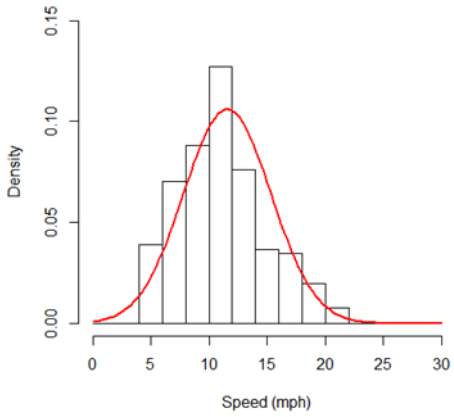

(d) W3

Note: bar - observed distribution; curve - fitted normal distribution

Figure B.6 Speed Distributions at sensor #101

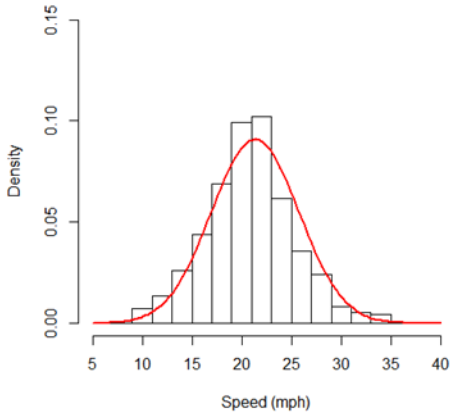

(a) W0

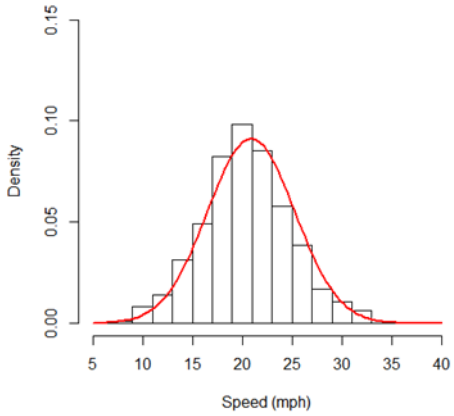

(b) W1

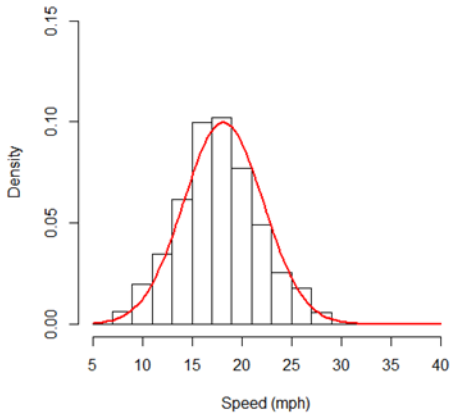

(c) W2

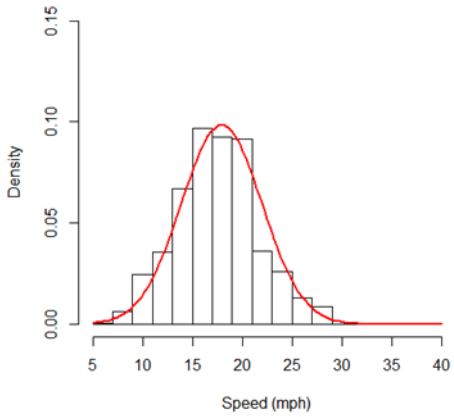

(d) W3

Note: bar - observed distribution; curve - fitted normal distribution

Figure B.7 Speed Distributions at sensor #102

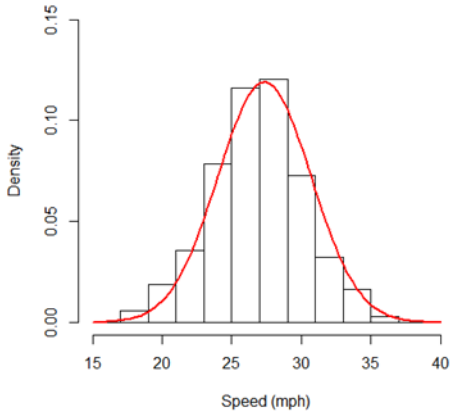

(a) W0

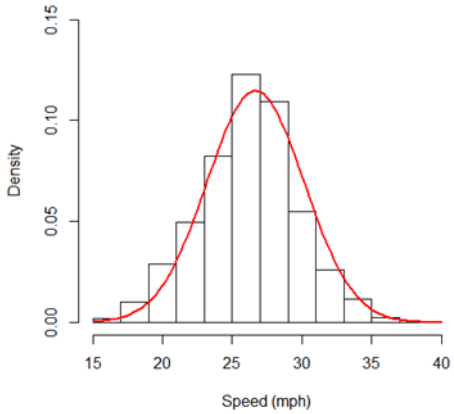

(b) W1

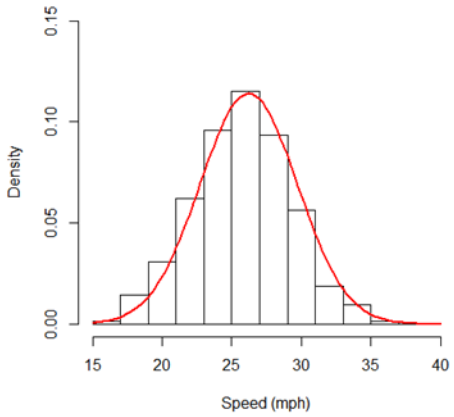

(c) W2

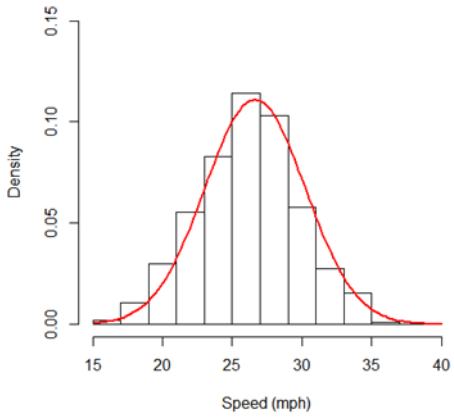

(d) W3

Note: bar - observed distribution; curve - fitted normal distribution

Figure B.8 Speed Distributions at sensor #103

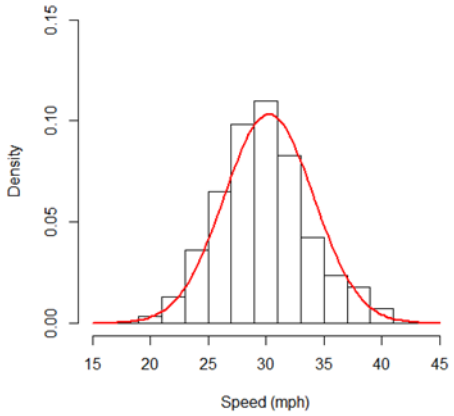

(a) W0

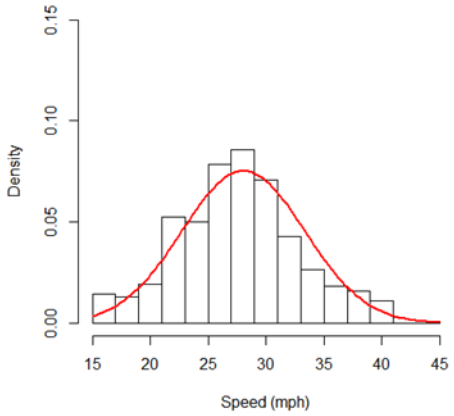

(b) W1

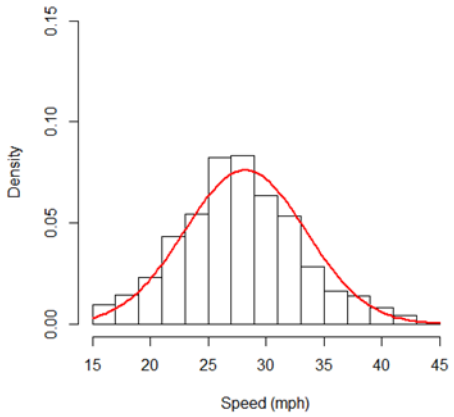

(c) W2

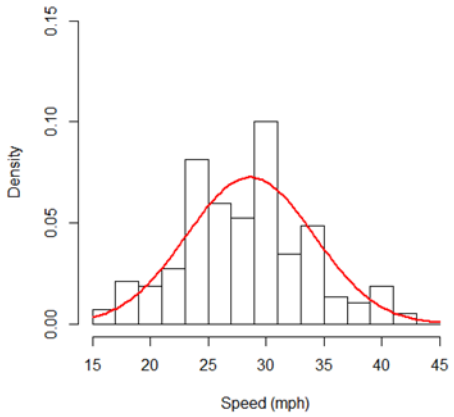

(d) W3

Note: bar - observed distribution; curve - fitted normal distribution

Figure B.9 Speed Distributions at sensor #104

Speed Characteristics

Table B.1 Speed characteristics at W0 (unit: mph)

Sensor	Mean	85th	Max	Min	Variance	Standard Deviation
#96	8.9	12.0	17.0	5.0	7.9	2.8
#97	10.7	14.0	21.0	5.0	12.4	3.5
#98	20.6	27.0	37.0	6.0	41.1	6.4
#99	33.3	39.0	51.0	16.0	37.8	6.2
#100	36.3	44.0	58.0	16.0	58.5	7.6
#101	12.8	18.0	27.0	5.0	23.1	4.8
#102	21.4	26.0	34.0	10.0	19.3	4.4
#103	27.3	31.0	37.0	18.0	11.2	3.3
#104	30.3	34.0	40.0	21.0	14.9	3.9

Table B.2 Speed characteristics at W1 (unit: mph)

Sensor	Mean	85th	Max	Min	Variance	Standard Deviation
#96	9.2	12.0	19.0	5.0	7.9	2.8
#97	10.8	14.0	22.0	6.0	12.2	3.5
#98	20.6	26.0	37.0	6.0	36.4	6.0
#99	31.5	37.0	45.0	18.0	27.1	5.2
#100	29.8	35.0	44.0	17.0	25.8	5.1
#101	12.6	17.0	25.0	5.0	20.0	4.5
#102	20.9	25.0	33.0	9.0	19.1	4.4
#103	26.7	30.0	36.0	17.0	12.1	3.5
#104	28.0	33.0	41.0	15.0	28.0	5.3

Table B.3 Speed characteristics at W2 (unit: mph)

Sensor	Mean	85th	Max	Min	Variance	Standard Deviation
#96	8.9	12.0	19.0	5.0	8.4	2.9
#97	10.5	14.0	22.0	6.0	12.7	3.6
#98	17.9	24.0	34.0	5.0	32.8	5.7
#99	31.2	36.0	45.0	18.0	27.8	5.3
#100	30.4	37.0	47.0	15.0	36.1	6.0
#101	12.4	18.0	26.0	5.0	22.6	4.8
#102	18.2	22.0	28.0	9.0	16.0	4.0
#103	26.2	30.0	36.0	17.0	12.3	3.5
#104	28.2	33.0	42.0	15.0	27.3	5.2

Table B.4 Speed characteristics at W3 (unit: mph)

Sensor	Mean	85th	Max	Min	Variance	Standard Deviation
#96	8.9	12.0	19.0	5.0	8.6	2.9
#97	11.8	13.0	19.0	5.0	9.7	3.1
#98	17.5	23.0	34.0	5.0	33.1	5.8
#99	31.8	37.0	48.0	16.0	31.3	5.6
#100	30.3	36.0	46.0	16.0	31.8	5.6
#101	11.6	16.0	21.0	5.0	14.2	3.8
#102	17.9	22.0	29.0	7.0	16.4	4.0
#103	26.2	30.0	36.0	17.0	12.3	3.5
#104	28.6	34.0	43.0	15.0	30.2	5.5

APPENDIX C

SOUND AND VIBRATION FIELD DRIVING RESULTS

Sound Profile

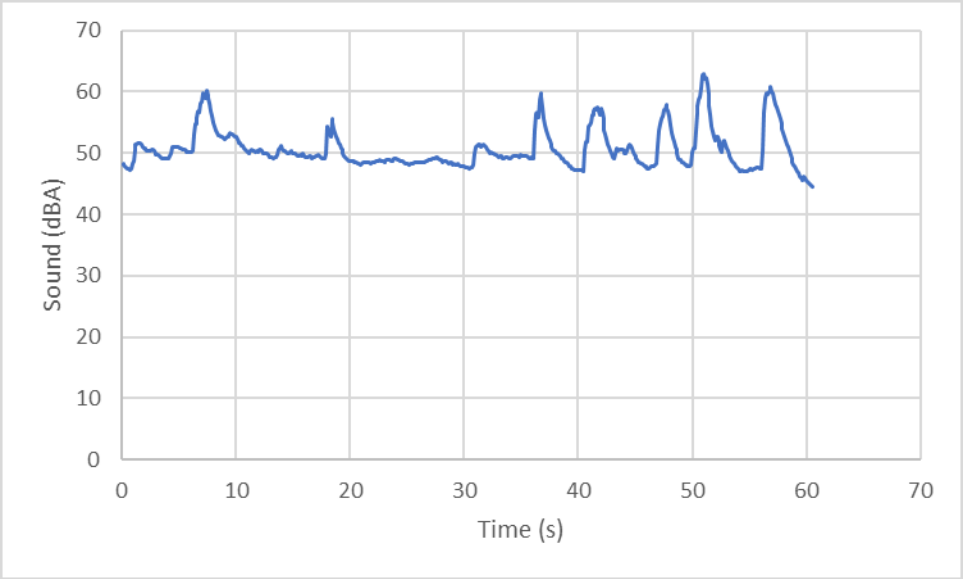

(a)

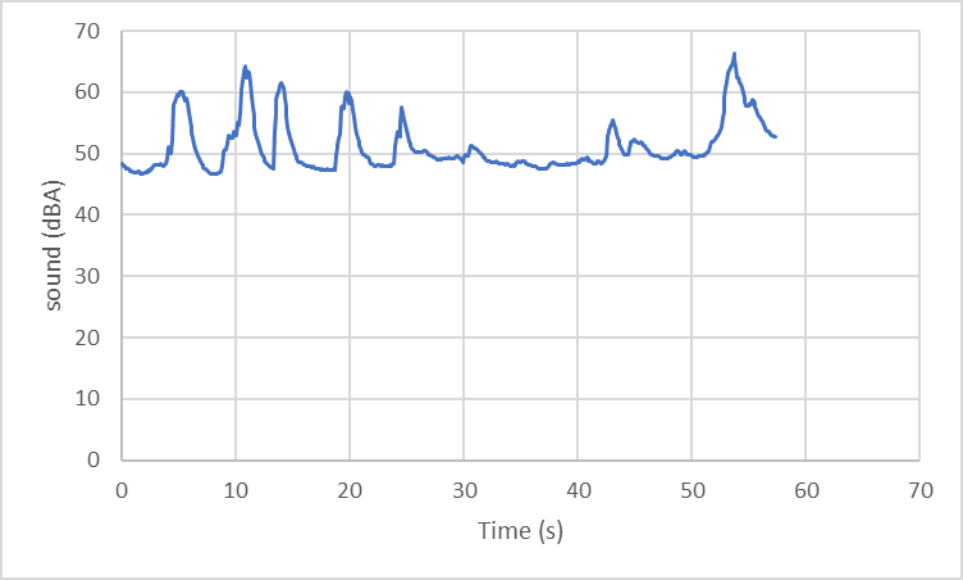

(b)

Figure C.1 Sound profile at 10 mph (a: RW; b: WW)

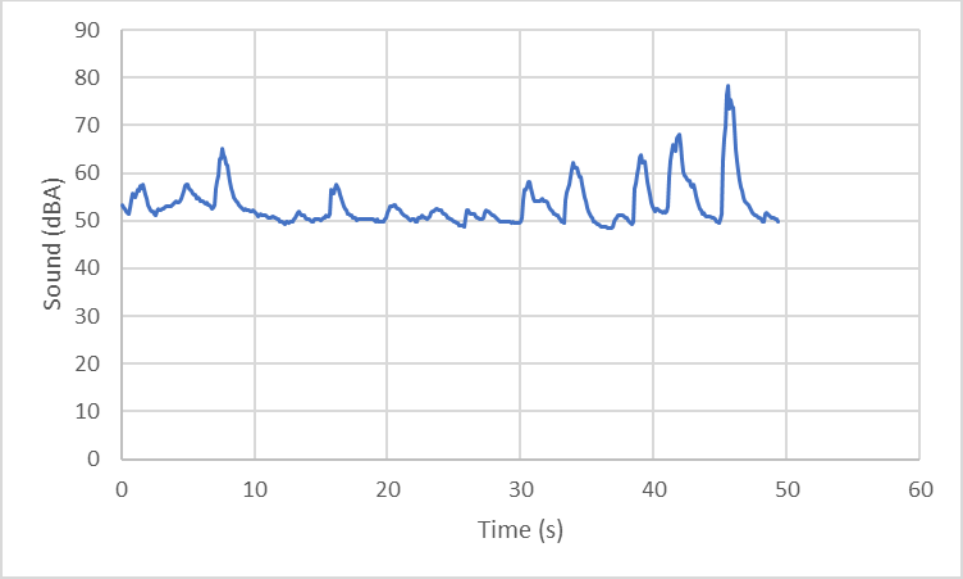

(a)

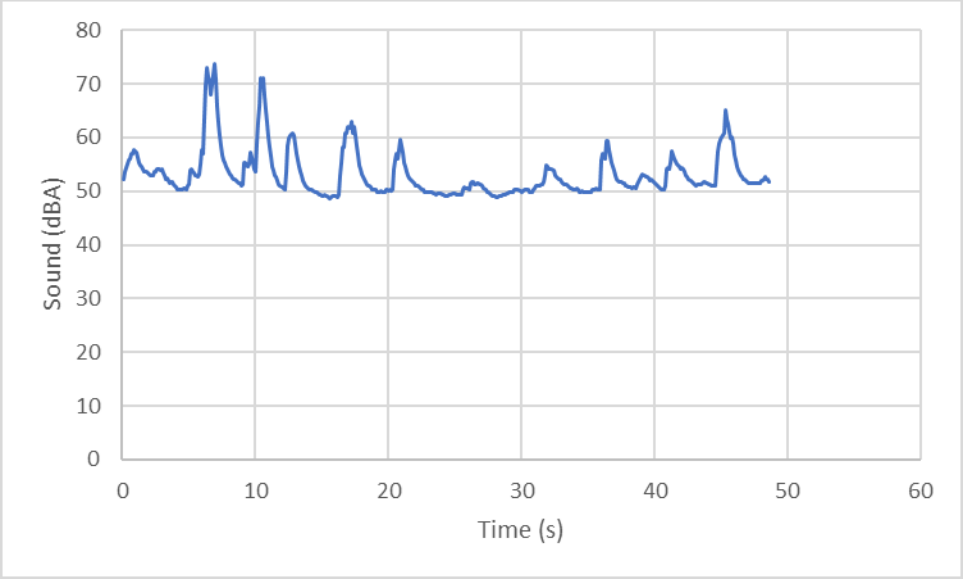

(b)

Figure C.2 Sound profile at 15 mph (a: RW; b: WW)

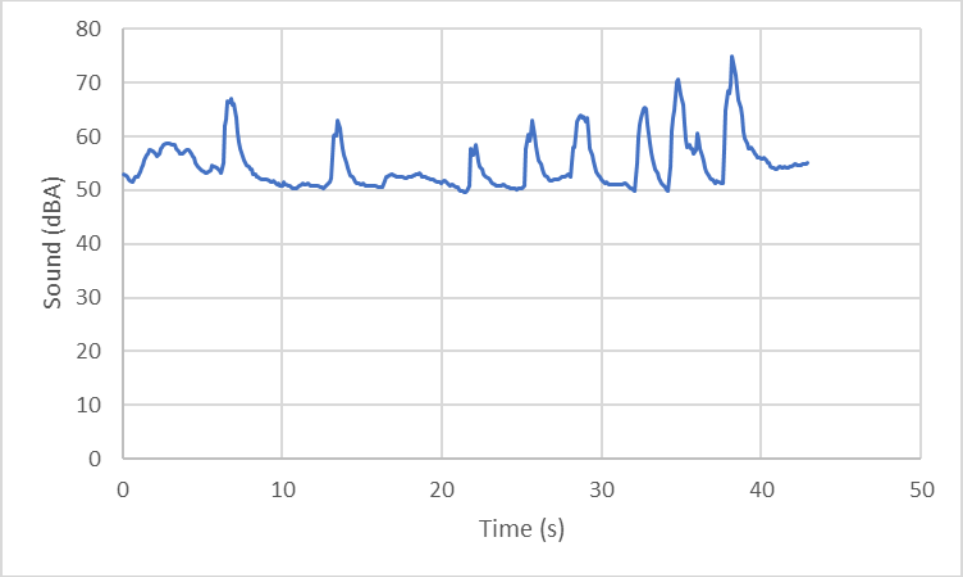

(a)

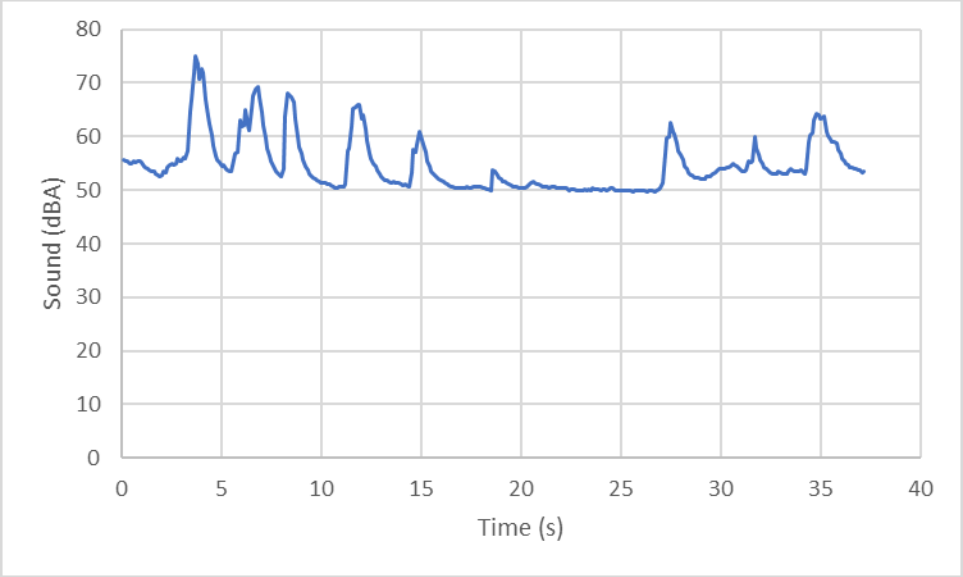

(b)

Figure C.3 Sound profile at 20 mph (a: RW; b: WW)

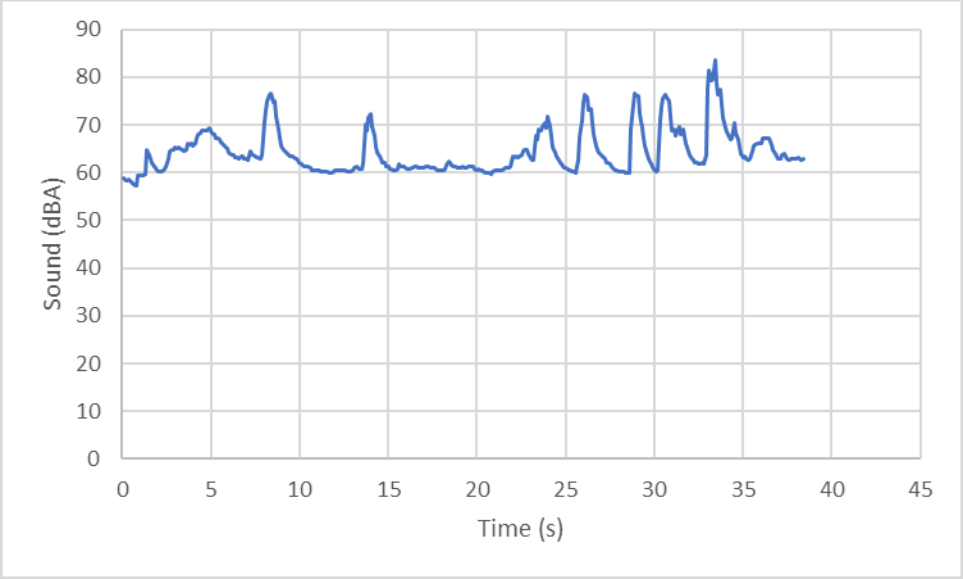

(a)

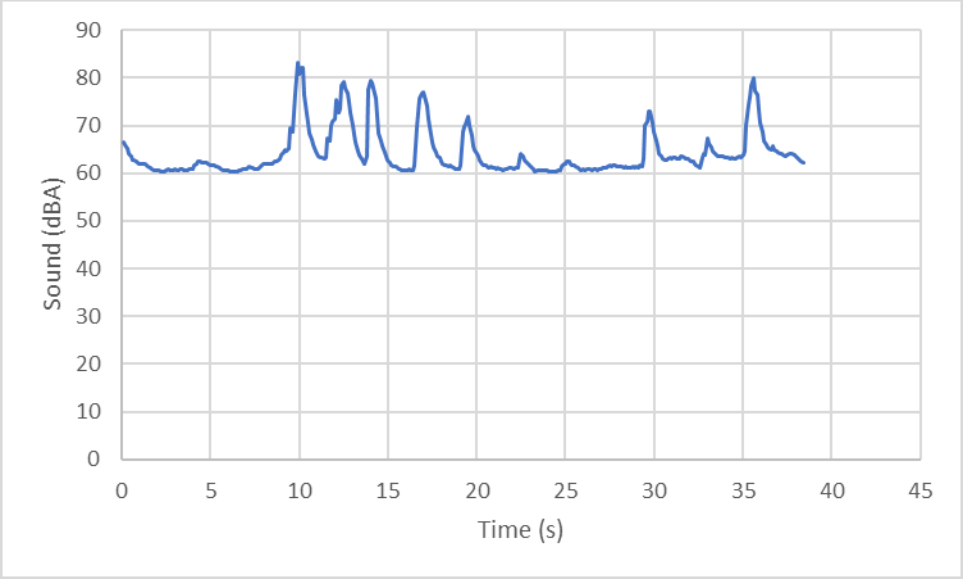

(b)

Figure C.4 Sound profile at 25 mph (a: RW; b: WW)

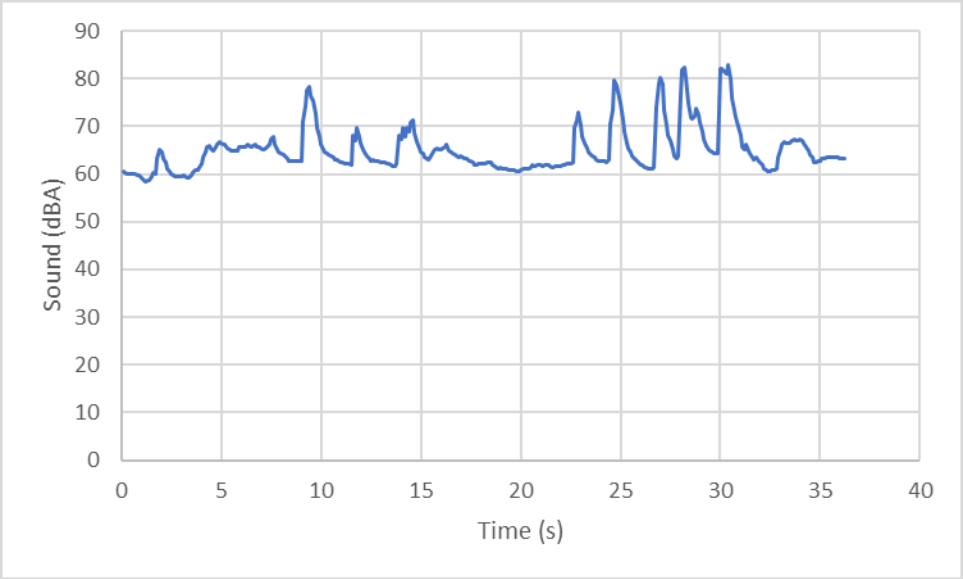

(a)

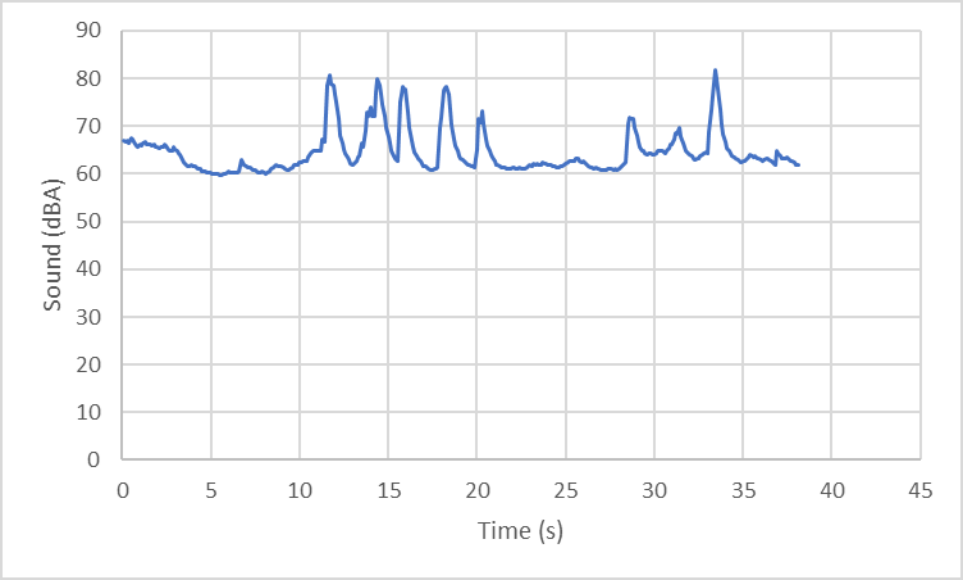

(b)

Figure C.5 Sound profile at 30 mph (a: RW; b: WW)

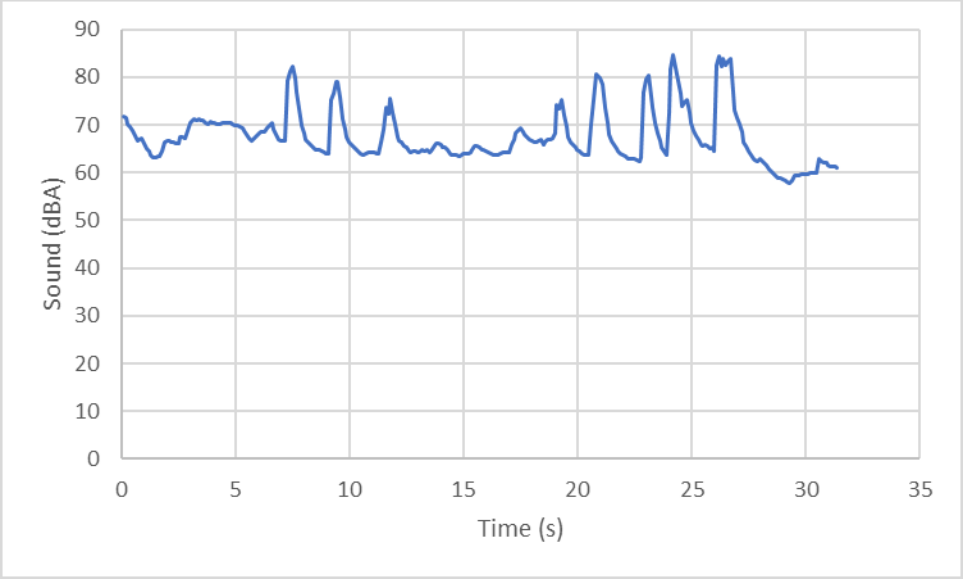

(a)

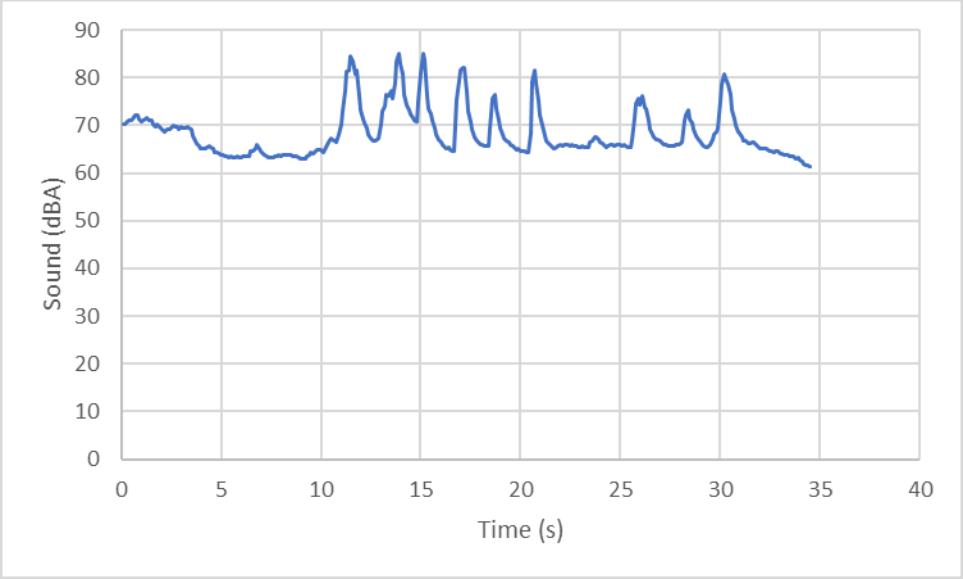

(b)

Figure C.6 Sound profile at 35 mph (a: RW; b: WW)

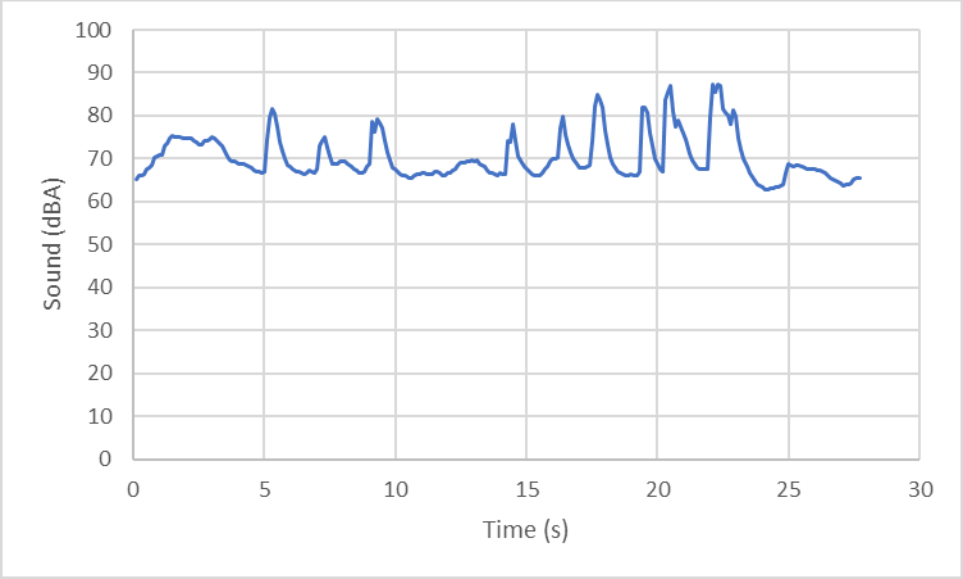

(a)

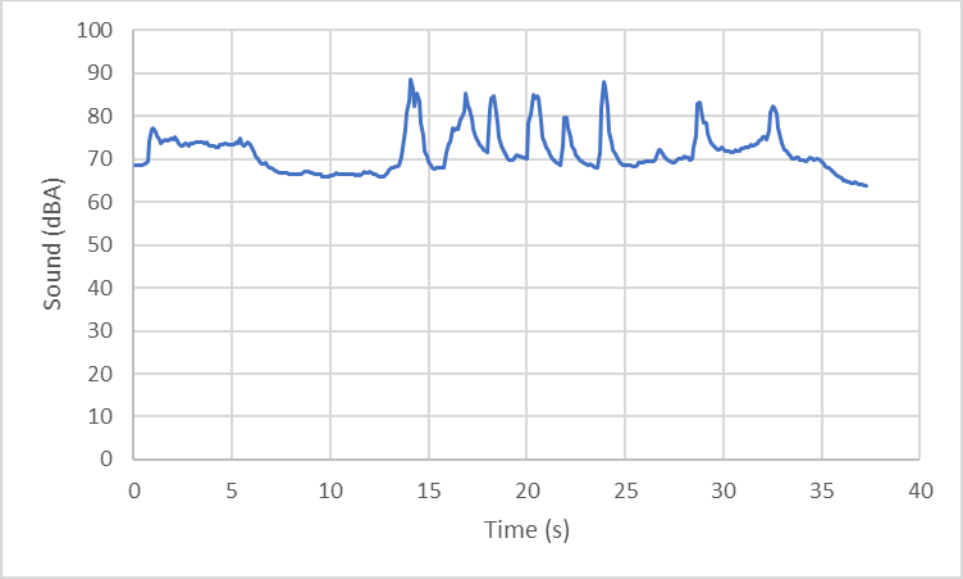

(b)

Figure C.7 Sound profile at 40 mph (a: RW; b: WW)

Vibration Profile

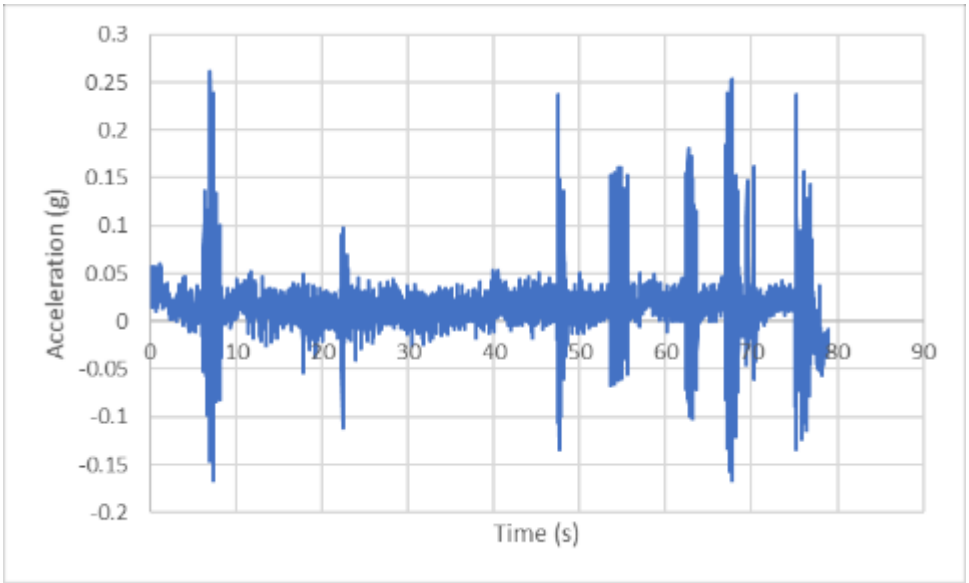

(a)

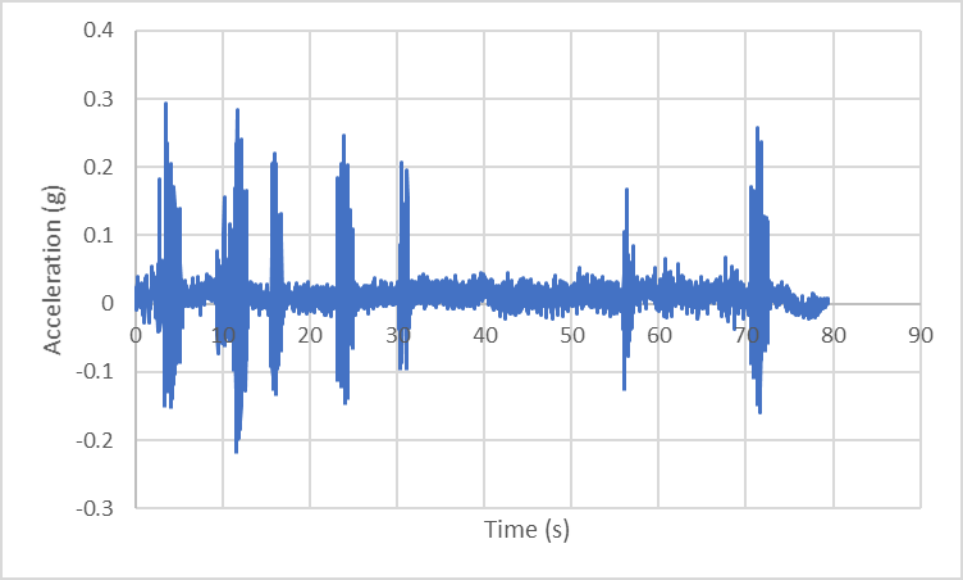

(b)

Figure C.8 Vibration profile at 10 mph (a: RW; b: WW)

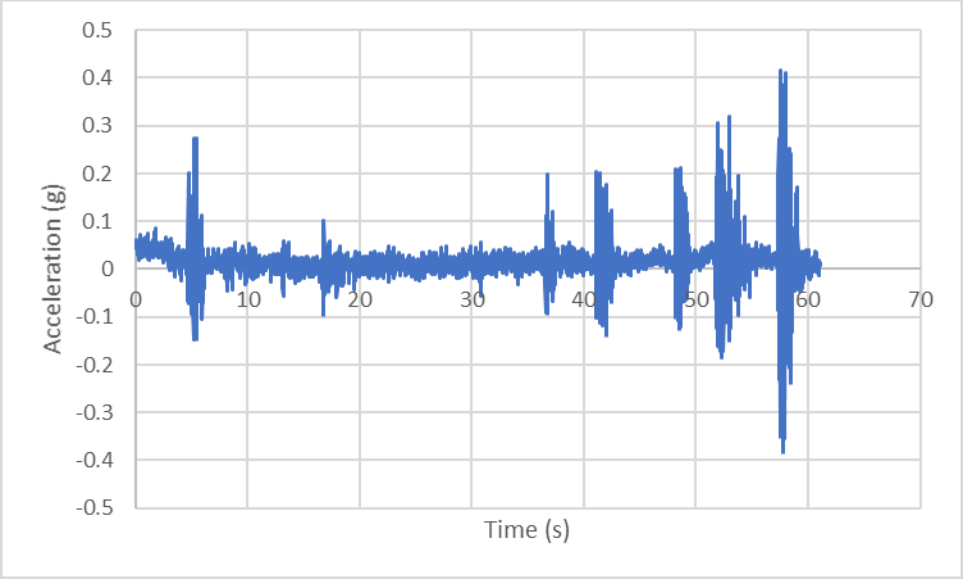

(a)

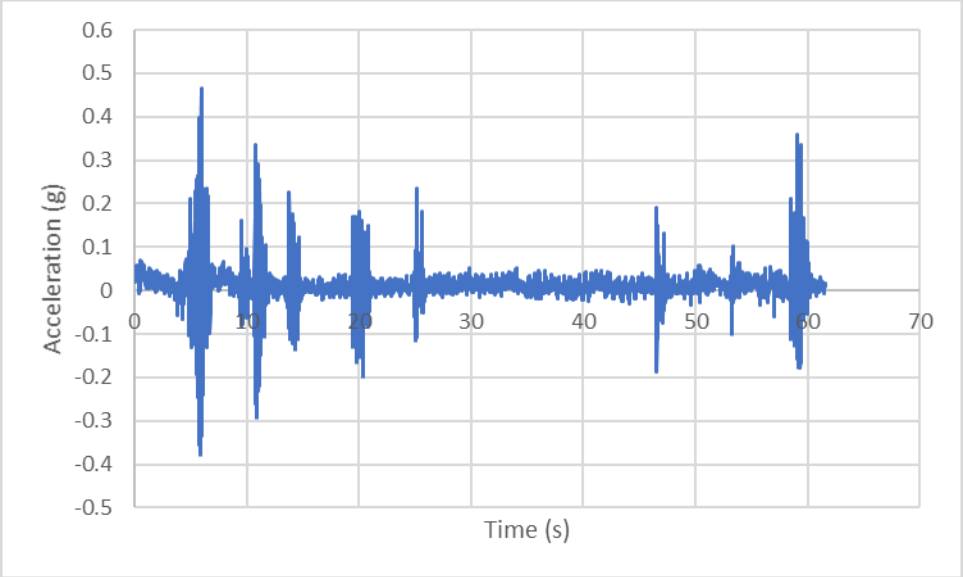

(b)

Figure C.9 Vibration profile at 15 mph (a: RW; b: WW)

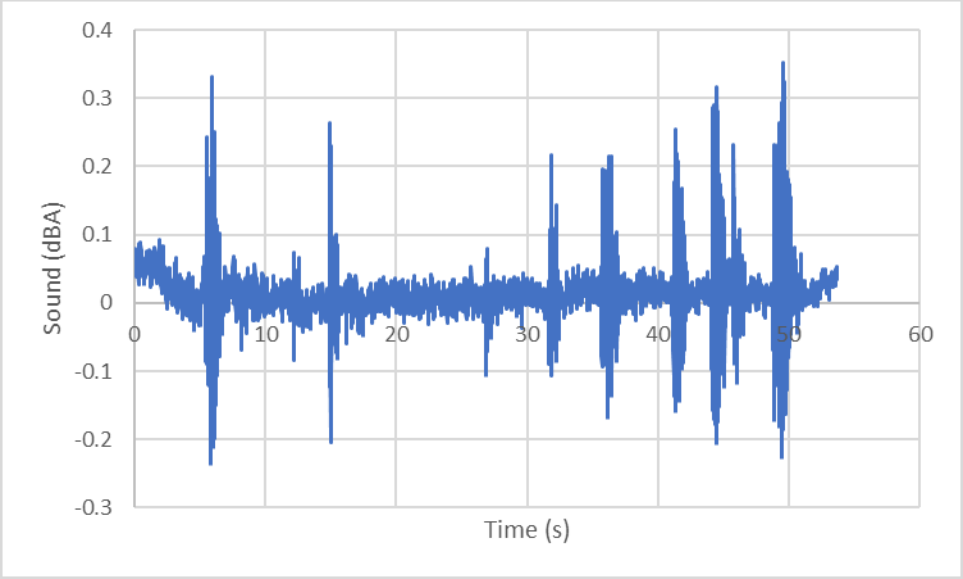

(a)

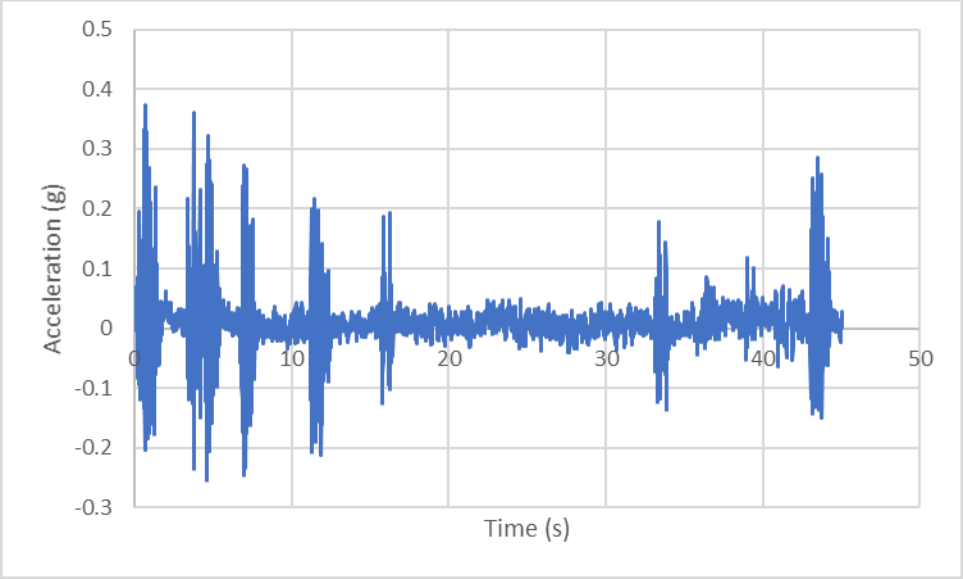

(b)

Figure C.10 Vibration profile at 20 mph (a: RW; b: WW)

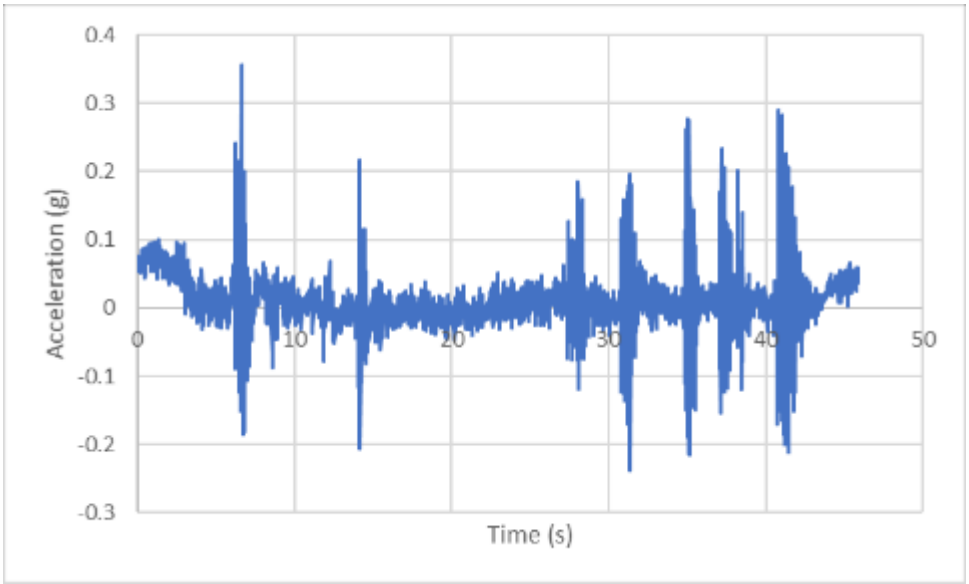

(a)

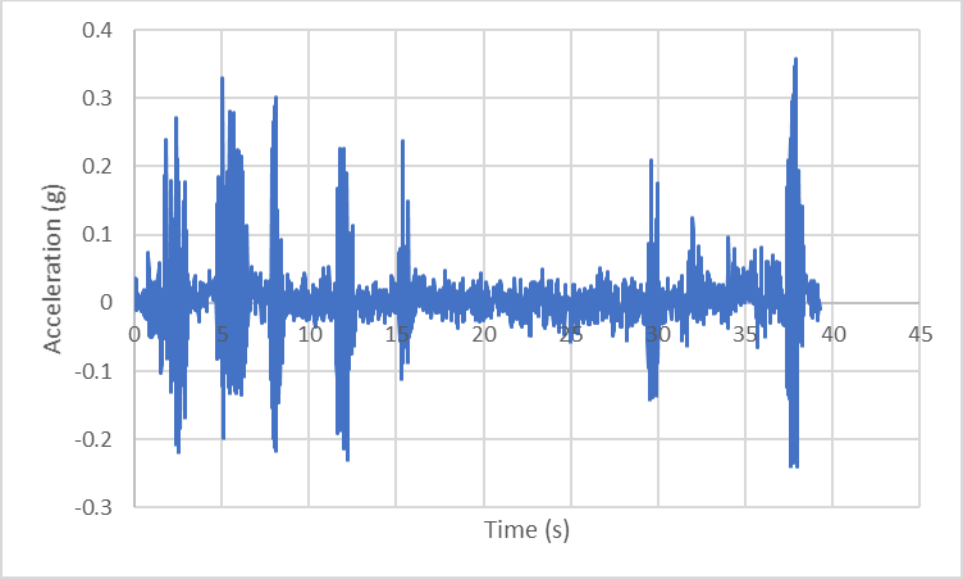

(b)

Figure C.11 Vibration profile at 25 mph (a: RW; b: WW)

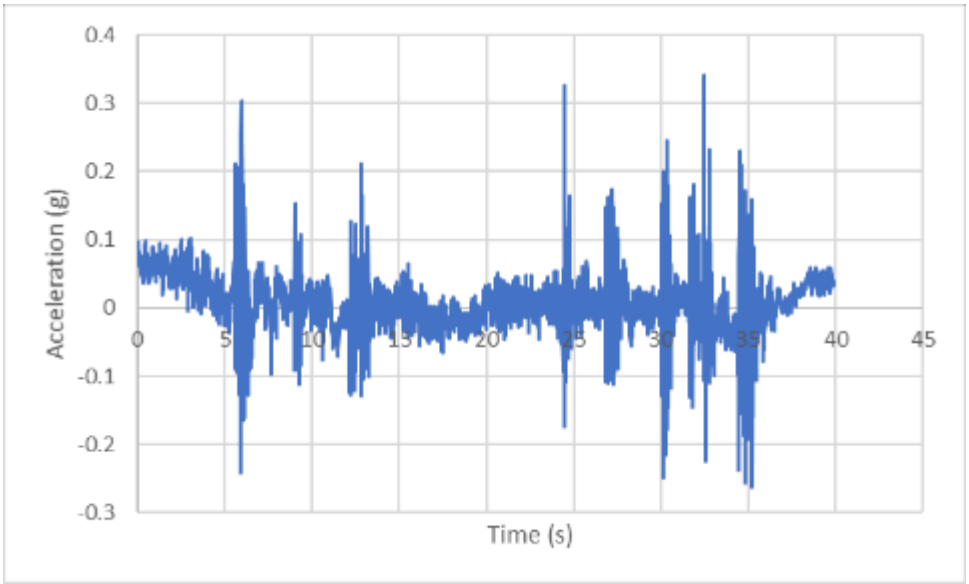

(a)

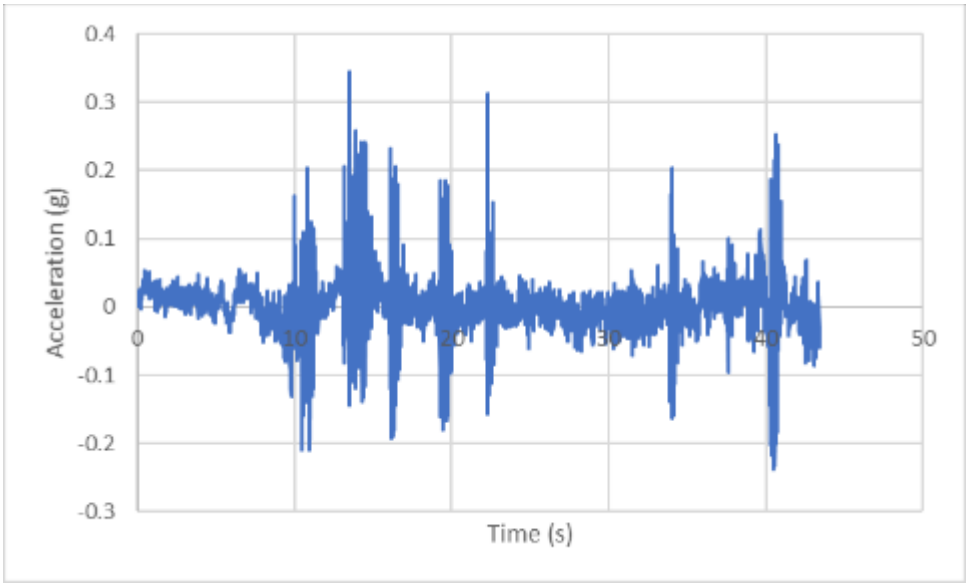

(b)

Figure C.12 Vibration profile at 30 mph (a: RW; b: WW)

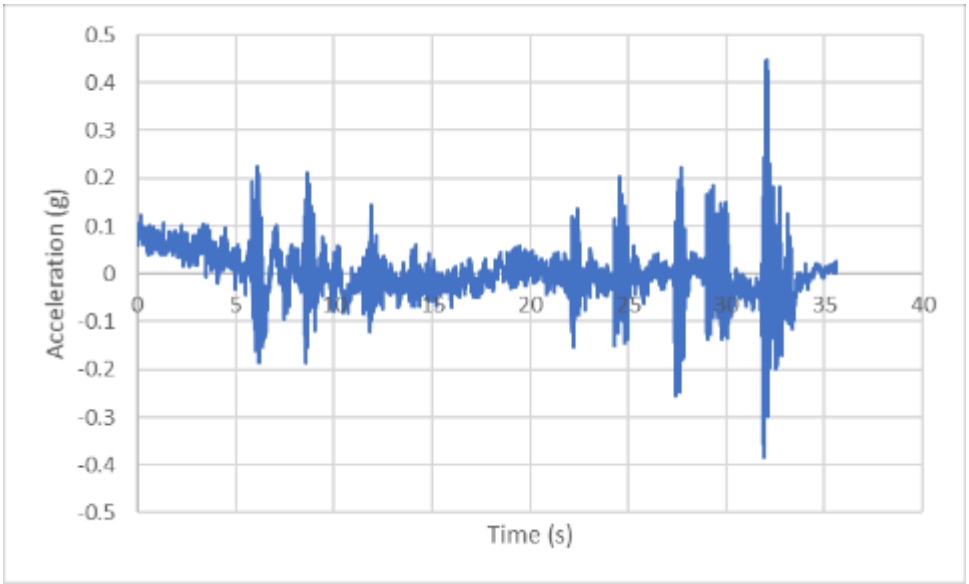

(a)

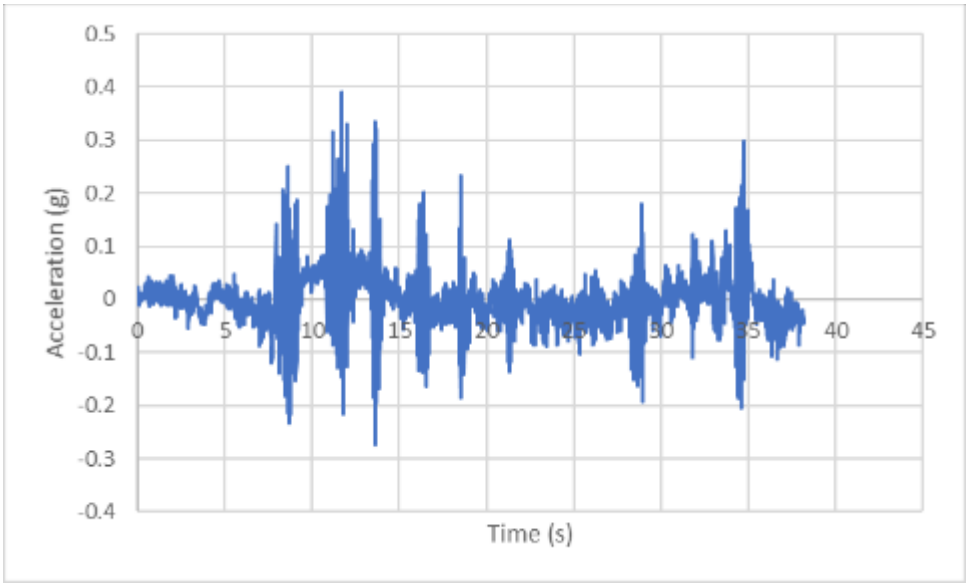

(b)

Figure C.13 Vibration profile at 35 mph (a: RW; b: WW)

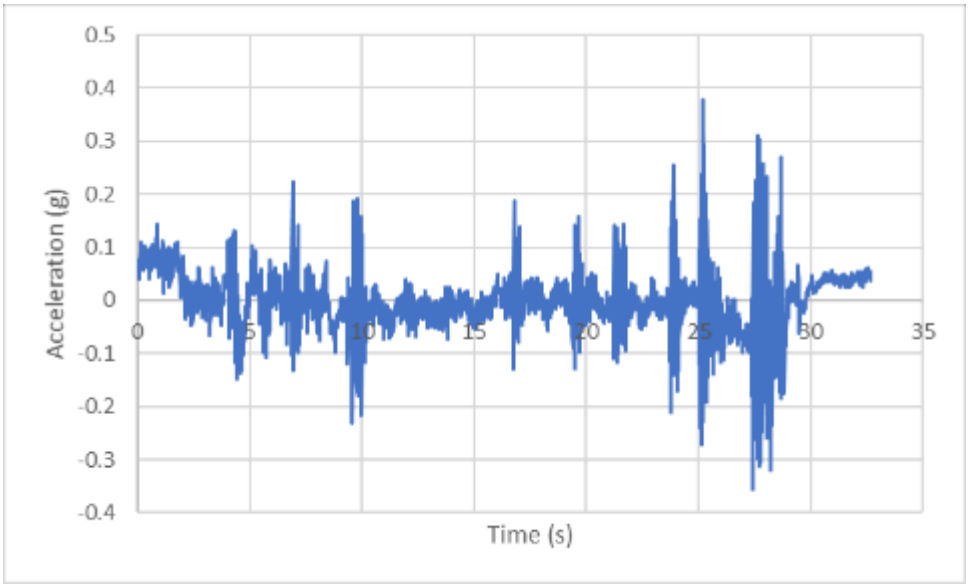

(a)

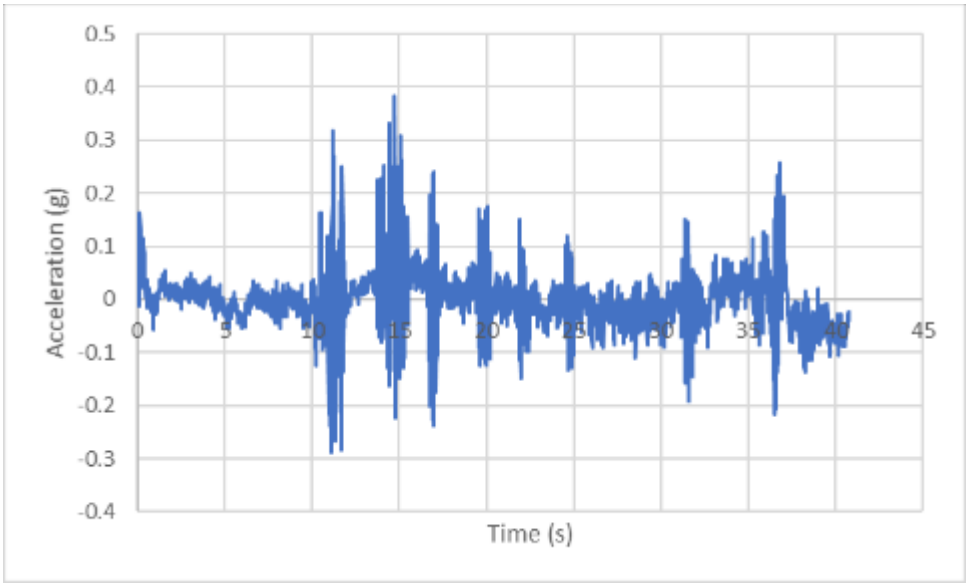

(b)

Figure C.14 Vibration profile at 40 mph (a: RW; b: WW)

APPENDIX D

TYPICAL A-WEIGHTED SOUND LEVEL

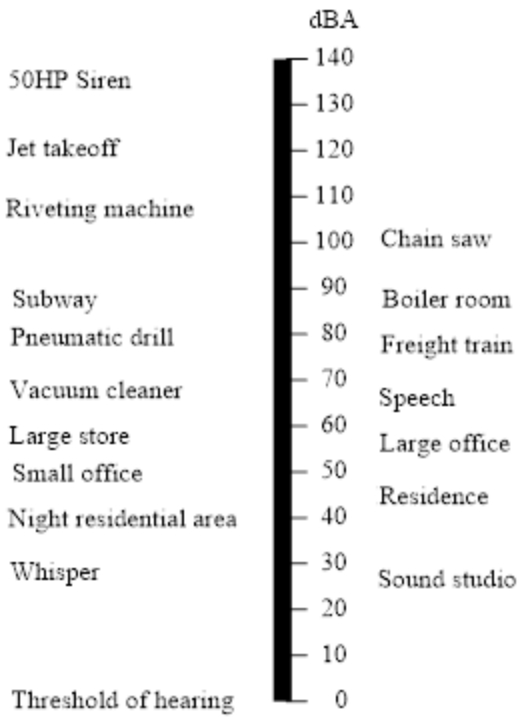

Figure D.1 Typical A-weighted sound level